UNIVERSITY OF COPENHAGEN
FACULTY OF HEALTH AND MEDICAL SCIENCES

Intrinsic resistance mechanisms and CRISPR-Cas immunity of the opportunistic pathogen, *Staphylococcus aureus*

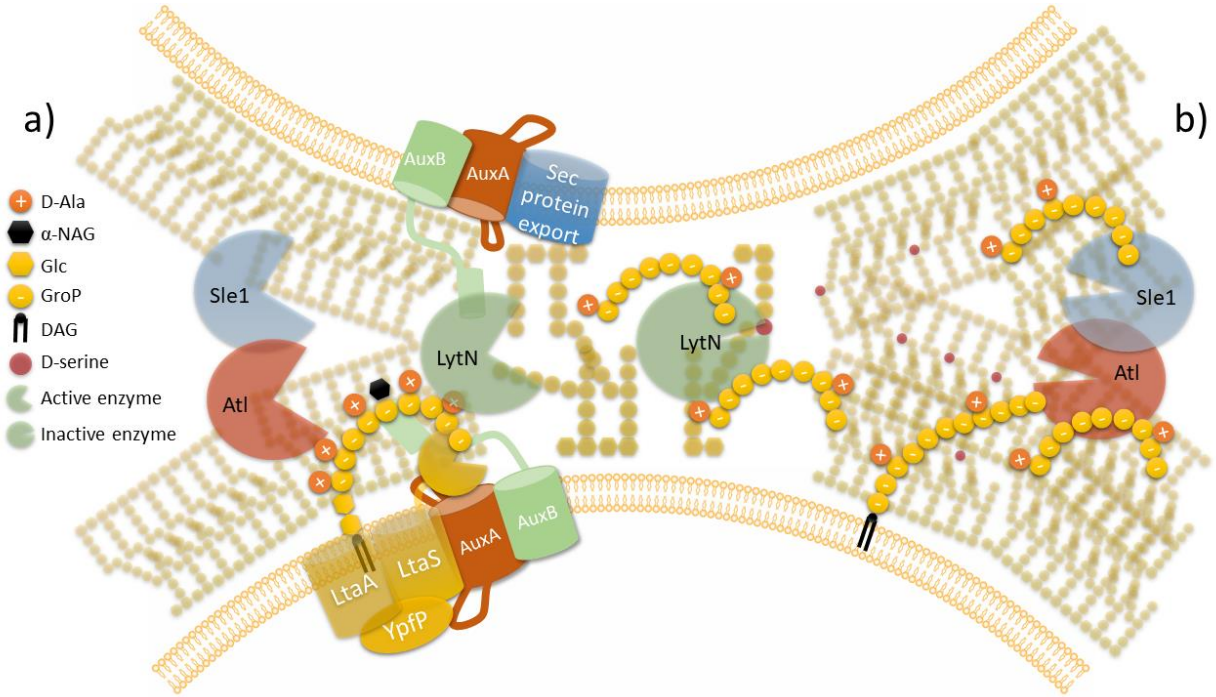

PhD thesis by Kasper Mikkelsen

Supervisor: Professor Hanne Ingmer

This thesis has been submitted to the Graduate School of Health and Medical Sciences, University of Copenhagen 14th of January, 2021

Intrinsic resistance mechanisms and CRISPR-Cas immunity of the opportunistic pathogen, *Staphylococcus aureus*

This thesis has been submitted to the Graduate School of Health and Medical Sciences, University of Copenhagen 14th of January, 2021 by

Kasper Mikkelsen

Department of Veterinary and Animal Sciences University of Copenhagen, Denmark

Principal supervisor:

Professor Hanne Ingmer

Department of Veterinary and Animal Sciences

University of Copenhagen, Denmark

Co-supervisor:

Adjunct Professor Paal Skytt Andersen

Department of Bacteria, Parasites and Fungi

Statens Serum Institut, Denmark

Assessment committee:

Associate Professor Dorte Frees

Department of Veterinary and Animal Sciences

University of Copenhagen, Denmark

Associate Professor Jan Martinussen

Department of Biotechnology and Biomedicine

Technical University of Denmark, Denmark

Professor Angelika Gründling

Section of Microbiology & MRC Center for Bacteriology and Infection

Imperial College London, United Kingdom

Acknowledgements

First and foremost, I would like to thank my primary supervisor Hanne Ingmer. Thank you for your invaluable guidance and enthusiasm. You have been a supreme support through my entire PhD and always happy to help with an eternal positive mind. I always leave your office with a boost and a lot of positive energy. We've had a lot of ideas along the way, and you are always eager to test these new ideas, even when it's a long shot – it could be cool if… I'm very thankful for you to accept me into your group, and I'm really looking forward to hang around for a while longer.

A deep thank you to my co-supervisor Paal Skytt Andersen. You know what I don't know (and much more) and that really helps to push things along and put them in perspective. But most of all, you're the nicest guy and I wish you the best on Bornholm. People from islands are not the worst kind you know.

Thank you Martin Vestergaard and Nina Molin Høyland-Kroghsbo for all the "non-official" supervision and help going through parts of the thesis. Thank you Martin Bojer, my whistling companion, for the great help with any lab issues. If you have problems with molecular biology, just ask Martin. And thank you to Katrine Nøhr-Meldgaard for your initial contributions to the Aux story.

A deep thank you to Professor Waldemar Vollmer and Associate Professor Rikke Louise Meyer for letting me into your labs, and to Waldemars wife Daniela Vollmer for the great help during my stay in Newcastle. I would very much like to thank Professor Guoqing Xia and Ohood Alharbi for the great collaboration in the hard quest of finding the mechanism for what these hypothetical proteins do. Thank you for the great discussions and the sharing of data.

A HUGE thank you goes to all my wonderful colleagues and for creating the best working environment. For all the nice beers, the petanque games, the trips, you name it. Thank you Ahlam (you know how it's pronounced) for the laughs and company in our "own" little lab. Thank you Janine and Bolette for all the office fun, and Janine as well for the great collaborations on CRISPR. Thank you Helena for the openhearted and cake baking spirit. And thank you Anaëlle for the pastries, the coffees, the beers, the podcast suggestions, Idéfix &

rosé, for criticizing my sad lunch, and for laughing at my jokes and taking them way too far. Merci.

Thanks to Gitte and Vi who have always been there to help me if I needed anything. Thank you for all your help.

A big thank you goes to all my friends and family! Even though it might not be everything that you have understood regarding my work, you have always been very supportive! Thank you! And a special thanks to my mom and Erik, who provided me with food and shelter during parts of the thesis writing, so I only needed to leave the computer for the daily meals. What a luxury!

Last but not least I would like to thank my girlfriend, Lise. Thank you so much for taking the trip to Copenhagen with me. I know I don't say it enough, but I am truly grateful! I know it has not always been easy, so thank you for standing by my side and being as supportive as you always are. Thank you for just being you and I can't wait for the times to come together with you and for our new exciting adventure.

Table of Contents

Abstract

Staphylococcus aureus is a serious human pathogen with a remarkable ability to adapt to challenging conditions and cause life-threatening infections. The most important class of antimicrobials for the treatment of *S. aureus* infections is the β-lactams. By the acquisition of the staphylococcal chromosome cassette (SCC*mec*), some *S. aureus* isolates have evolved methicillin-resistance (MRSAs) that are resistant to nearly every β-lactam antibiotic, why additional measures are needed to combat this pathogen.

In this presented work, we identify and characterize two novel auxiliary factors, AuxA and AuxB, which are essential for MRSA to withstand β-lactam antimicrobials. AuxA and AuxB are membrane-associated proteins that interact with one another to form a hetero-multimeric complex, which further interacts with members of the peptidoglycan synthesis machinery, the divisome, and lipoteichoic acid and D-alanylation pathways. Mutants lacking either of the Aux proteins show attenuated autolytic activity and release wild type-length lipoteichoic acid polymers into the growth medium. This suggest that the Aux proteins carry a stabilizing role of the lipoteichoic acid polymer and might carry additional roles in division and peptidoglycan synthesis of the staphylococcal cell.

Another factor of β-lactam resistance could be the SCC*mec* type IVh that is carried by several highly β-lactam-resistant clonal complex 22 isolates. Clonal complex 22 is a superior clone to cause human bloodstream infections, which might be caused by the SCC*mec* type IVh combined with integrated prophages to provide β-lactam resistance and virulence, respectively.

The SCC*mec* may not only be important for β-lactam resistance, but is likely to be involved in the spread of anti-phage immunity. The emerging Danish clone ST630 carry the SCC*mec* type V(5C2&5) in which the *S. aureus* CRISPR-Cas type III-A adaptive immune system is located. The *S. aureus* CRISPR-Cas system is active against phage attack and excise at high rates together with the type V(5C2&5) SCC*mec*, which could serve to spread antimicrobial and phage resistance simultaneously, endangering both antibiotic and phage therapy approaches.

Resumé

Staphylococcus aureus er en alvorlig human patogen bakterie, der kan forårsage livstruende infektioner og har en bemærkelsesværdig tilpasningsevne. Den vigtigste type af antibiotika til behandling af infektioner med *S. aureus* er β-lactamer. Ved erhvervelse af stafylokokkromosom-kassetten (SCC*mec*) har nogle *S. aureus*-isolater udviklet methicillin-resistens (MRSA'er), der er resistente over for stort set samtlige β-lactam antibiotika, hvorfor der er behov for nye tiltag for at bekæmpe denne patogene bakterie.

I denne afhandling identificerer og karakteriserer vi to nye faktorer, AuxA og AuxB, der er essentielle for at opretholde MRSA'ernes modstandsdygtighed over β-lactam antibiotika. AuxA og AuxB er forankrede i membranen, hvori de interagerer med hinanden og danner et hetero-multimert kompleks. Endvidere interagerer de med aktive medlemmer af peptidoglykan-syntese og celledeling, samt til medlemmer involveret i syntesen af glycerol-fosfat polymeren lipo-teichoesyre og dennes modifikationer. Celler der mangler Aux-proteinerne, viser svækket autolytisk aktivitet og frigiver lipo-teichoesyre-polymerer, af samme længde som vildtype-celler, til vækstmediet. Dette indikerer, at Aux-proteinerne bærer en stabiliserende rolle for lipo-teichoesyre-polymeren og kan have en tilstødende rolle i celledeling of peptidoglykan syntese i stafylokok bakterier.

En anden faktor med indflydelse på β-lactamresistens kunne være SCC*mec* type IVh, der bæres af flere stærkt β-lactamresistente isolater tilhørende klonal kompleks 22. Klonal kompleks 22 er en overlegen klon til at inficere blodbanen. Denne evne kan være forårsaget af tilstedeværelsen af SCC*mec* type IVh der, kombineret med kromosomalt integrerede profager, kunne bidrage til henholdsvis β-lactamresistens og virulens af denne klon.

SCC*mec* er ikke kun vigtig for β-lactamresistens, men er sandsynligvis også involveret i spredning af anti-fag-immunitet. Den nye danske *S. aureus* klon, ST630, bærer en SCC*mec* type V(5C2&5), hvori det bakterielle adaptive immunsystem CRISPR-Cas type III-A er placeret. *S. aureus* CRISPR-Cas-systemet er aktivt mod fagangreb og kan frigøre sig fra kromosomet sammen med type V(5C2&5) SCC*mec*-kassetten, som kan medvirke til parallelt at sprede antibiotika- og fag-resistens og bringe både antibiotika- og fagbehandling i fare.

Objectives

Staphylococcus aureus is well-known for its ability to acquire antibiotic resistance, which threaten undermine the efficacy of current antimicrobial solutions. With the work present here we wanted to contribute to the fight against methicillin-resistant *Staphylococcus aureus* by

- Finding novel targets suitable for future antimicrobial solutions
- Gain insight into unknown resistance mechanisms
- Discover novel acquired resistance determinants assisting high resistance levels
- Examine the prevalence and possible transfer mechanisms of CRISPR-Cas immunity in *S. aureus*

Abbreviations

HGT	Horizontal gene transfer
SNP	Single-nucleotide polymorphism
ST	Sequence type
CC	Clonal complex
MRSA	Methicillin-resistant *Staphylococcus aureus*
SCC*mec*	Staphylococcal chromosome cassette *mec*
PG	Peptidoglycan
IWZ	Inner wall zone
OWZ	Outer wall zone
NAG	N-acetylglucosamine
NAM	N-acetylmuramic acid
UndP	Undecaprenyl phosphate
TG	Transglycosylase
TP	Transpeptidase
PBP	Penicillin-binding protein
SEDS	Sporulation, elongation, division, and septation
WTA	Wall teichoic acid
LTA	Lipoteichoic acid
LCP	LytR-CpsA-Psr
GroP	Glycerolphosphate
CRISPR	Clustered regularly interspaced short palindromic repeats
c-oligoA	Cyclic oligoadenylate
PAM	Protospacer adjacent motif
LAS	Leader anchoring sequence
MGE	Mobile genetic element

Introduction

Staphylococcus aureus – an ever adaptive opportunistic pathogen

Staphylococcus aureus (*S. aureus*) is a gram-positive bacterium forming "grape-like" clusters with a spherical cell shape. It is part of the commensal flora of the human skin and nasal cavity, with about one-third of the population being constant carriers [1]. Besides being a commensal, *S. aureus* is a well-known opportunistic pathogen able to colonize skin breach sites and cause superficial, deep skin, and soft tissue infections, along with life-threatening infections such as endocarditis and osteomyelitis [2].

The success of *S. aureus* as a colonizer is mainly due to its high ability to adapt to changing environments by acquisition of new DNA by horizontal gene transfer (HGT) or to gain occasional beneficial mutations of to its chromosomal DNA [2, 3]. The ability of *S. aureus* to spread in both hospital and community settings has made it necessary to develop tools to distinguish isolates to track epidemiological spread. Previous typing methods include pulsed-field gel electrophoresis, staphylococcal protein A typing and multilocus sequencing typing (MLST) where 7 house-keeping genes are sequenced and grouped into sequence types (ST). Related STs can then be grouped into larger clusters designated as clonal complexes (CC) [3]. However, due to the still decreasing costs of whole genome sequencing this has become the new method of choice when it comes to typing [3]. Since the 1960s, the vast majority of *S. aureus* isolates belong to 11 CCs of which 5 (CC5, 8, 22, 30, and 45) are the most common CCs of methicillin-resistant *S. aureus* (MRSA) [4].

Almost immediately after the introduction of methicillin (a modified penicillinase-resistant β-lactam antibiotic) the first MRSA strain was isolated, which had acquired the staphylococcal chromosome cassette *mec* (SCC*mec*) I [4]. The SCC*mec* is a genomic island that carries methicillin resistance through the expression of the *mec* gene, encoding a penicillin-binding protein (PBP2a) with low affinity for β-lactams [5]. Besides carrying the *mec* gene, all SCCmec elements share several characteristics: (i) the cassette chromosome recombinase (*ccr*) gene complex, responsible for integration and excision of the SCC*mec* from the bacterial genome; (ii) direct repeats flanking the SCC*mec* at both ends and (iii) integration of the cassette into

the 3'-end of the *orfX* gene with integration of additional elements (e.g. plasmids or transposons) happening in the non-essential joining regions (J region) in the middle and extremities of the SCC [6, 7].

The acquisition of the SCC*mec* combined with the adaptability of the *S. aureus* genome has made treatment of *S. aureus* infections increasingly hard. Until the mid-1990s, MRSA isolates were largely confined to healthcare environments (HA-MRSA) particularly causing infections after surgical procedures or of devices contained within the human body. With the occurrence of MRSA infections originating outside the hospital setting (community-acquired MRSA (CA-MRSA)), and among livestock (LA-MRSA), the threat from MRSA continues to grow [8]. As the MRSAs are resistant towards nearly all β-lactam antimicrobials, the glycopeptide vancomycin is the most common drug used to treat severe MRSA infections [8]. However, vancomycin intermediate susceptibility *S. aureus* (VISA) caused by differences in cell wall related expression patterns [9], and vancomycin-resistant *S. aureus* (VRSA) caused by acquisition of the *vanA* cluster from vancomycin-resistant enterococci, have started to emerge [10]. Additional last-resort antibiotics exist including linezolid and daptomycin, and a few possible future drugs are in the pipeline with teixobactin so far reported to be *"without detectable resistance"* [3, 11]. A new approach to find markers of antimicrobial resistance via MRSA genome profiles will be addressed in manuscript 1.

Even though resistance against β-lactams, the common name for antimicrobials sharing a β-lactam ring structure, arose with MRSA, they continue to be the preferred drug to treat methicillin-susceptible *S. aureus* (MSSA) infections [8]. This is due to their wide spectrum of activity (target both gram-positive and gram-negative bacteria), superior efficacy, and safety profile combined with a powerful target; the bacterial cell wall [12].

The staphylococcal cell wall

In contrast to gram-negative bacteria like *Escherichia coli* that carries a cytoplasmic and an outer membrane, gram-positive species including *S. aureus*, only contain a cytoplasmic membrane. To protect the *S. aureus* cell membrane from bursting due to internal turgor pressure, the cell is covered by a multilayered cell wall named the sacculus [13]. The sacculus is made up of linear chains of peptidoglycan (PG) consisting of repeating disaccharide units

cross-linked by short peptide side chains (Figure 1a) [14]. The glycan chains are made up of alternating N-acetylglucosamine (NAG) and N-acetylmuramic acid (NAM) sugar residues with a peptide stem connected to the NAM molecules. The glycan chains have an average chain length of 6 disaccharide units, with a predominant length between 3 and 10 units but with 10-15 % being longer than 26 disaccharides [15, 16]. This is much shorter than what is reported in e.g. *Bacillus subtilis* (up to 5,000 disaccharide units long), which is caused by the spherical shape of *S. aureus* compared to the elongated rod-shaped *B. subtilis* [17].

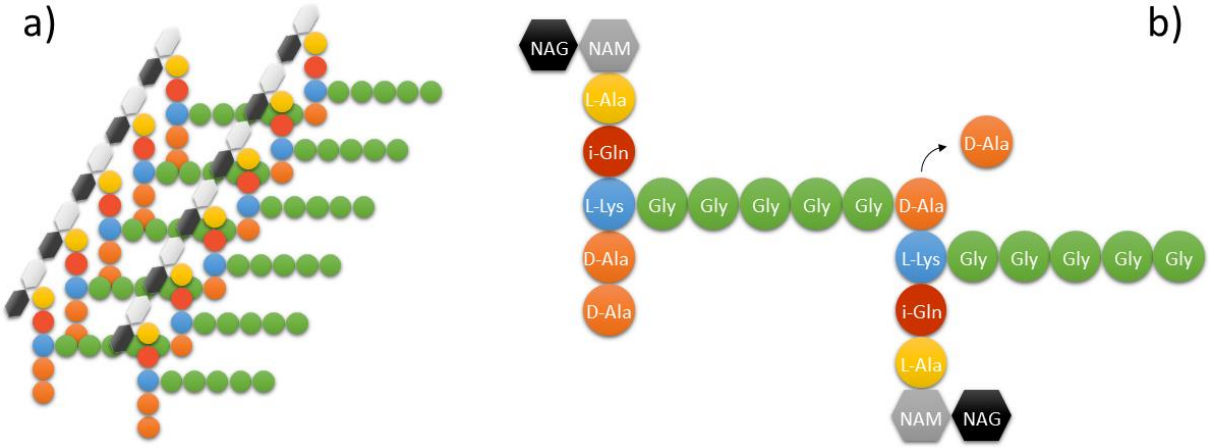

Figure 1. Peptidoglycan structure. (a) *The PG glycan chains are cross-linked to neighboring glycan chains via a peptide stem.* ***(b)*** *Cross-linking occur between the position 3 L-Lys residue of one chain and the position 4 D-Ala of the neighboring chain through a pentaglycine bridge. The cross-linking reaction release the terminal D-ala to the environment.*

The NAM molecule contains a lactate group to which an L-Ala-D-isoGlu-L-Lys-D-Ala-D-Ala peptide stem is connected. Peptide stems of neighboring glycan chains are cross-linked via a penta-glycine bridge, connecting the position three L-Lys residue on one chain and the position 4 D-Ala of another, which loses the terminal D-ala residue in the process (Figure 1b) [18].

Peptidoglycan biosynthesis

The biosynthesis of PG begins in the cytosol with the synthesis of the PG precursor lipid II (Figure 2). Initially, uridine diphosphate (UDP)-linked NAG is converted to UDP-NAM by the activities of MurA and MurB [19, 20]. Next, the L-Ala-D-Glu-L-Lys stem is added to UDP-NAM in a stepwise manner by MurC, MurD, and MurE, respectively. The terminal stem peptide D-Ala-D-Ala is prepared by the conversion of L-Ala to D-Ala by alanine racemases (Alr) followed by the ligation of two D-Ala residues by the D-Ala-D-Ala ligase (Ddl) [21]. MurF adds D-Ala-D-

Ala to the peptide stem with MraY subsequently attaching the NAM sugar of the PG precursor to the lipid carrier undecaprenyl phosphate (UndP) on the inside of the membrane (known as lipid I). When attached to the lipid membrane, the D-iso-glutamate residue in position two of the peptide stem is amidated to D-iso-Gln. This step is done by the murein ligase MurT and glutamine amidotransferase GatD [22] before MurG links a NAG sugar to the position 1 carbon of the NAM sugar (known as lipid II) (Figure 2). The pentaglycine bridge is added by FemX, FemA and FemB which adds one, two and two glycines to the L-Lys residue of the peptide stem before this final PG precursor is flipped by MurJ to the outside of the membrane [23, 24].

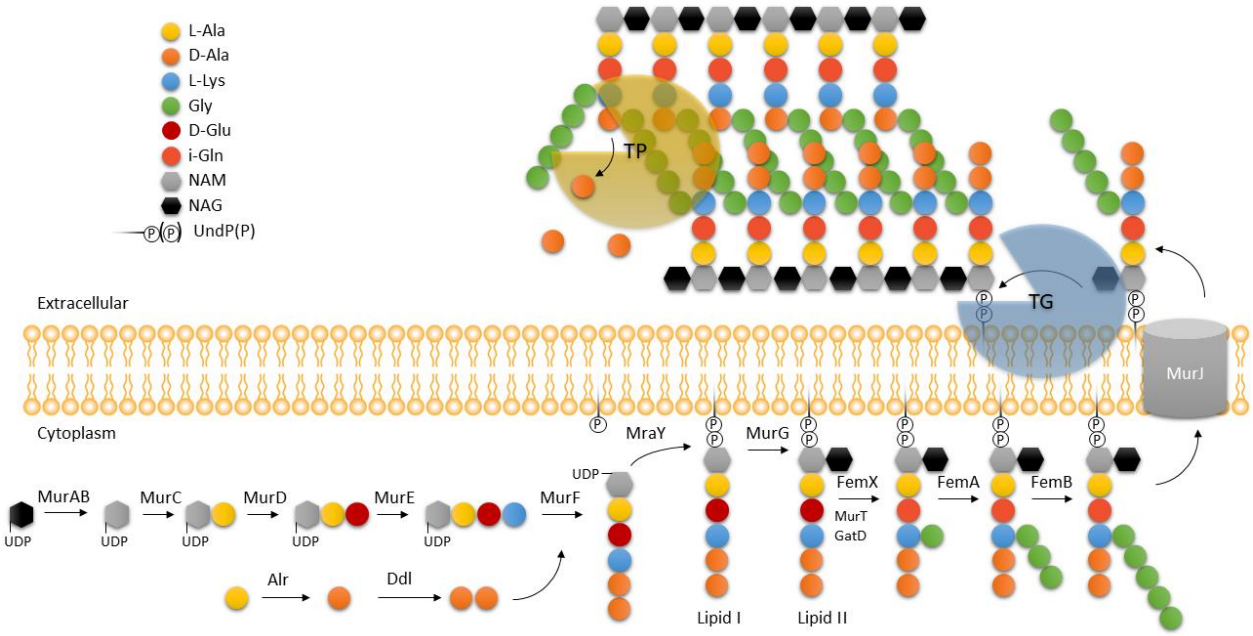

Figure 2. Peptidoglycan biosynthesis. *The initial steps of peptidoglycan biosynthesis take place in the cytoplasm, where MurABCDEF are responsible for the assembly of the peptide stem on UDP-NAM. The PG precursor is then attached to the membrane via UndPP where the peptaglycine bridge is added before being flipped across the membrane by MurJ. Extracellularly the PG monomer is polymerized by TGs and linked to neighbouring glycan strands by TPs.*

Once in the outer leaflet of the membrane, the lipid II-pentaglycine is polymerized and integrated into the existing PG network by transglycosylases (TGs) and transpeptidases (TPs) [18]. The initial polymerization of the growing glycan polymer chain is carried out by either class A penicillin-binding proteins (aPBPs) carrying TG activity (PBP2 in *S. aureus*), monoglycosyltransferases (e.g. SgtB) or TGs belonging to the sporulation, elongation, division, and septation (SEDS) family [14, 25]. These SEDS proteins are only active when in complex with their cognate class B PBP (bPBP) [26]. *S. aureus* carries two pairs of SEDS-bPBP, with

FtsW-PBP1 mainly active at the septum and RodA-PBP3 working at the sidewall [27]. The growing glycan polymer is integrated into the PG network by the TP activity of the PBPs to cross-link the polymers via their pentaglycine bridge. Finally, the nascent, cross-linked glycan polymer is cleaved in defined lengths by release factor complexes (e.g. SagB-SpcD complex) that release the polymer from the membrane as a fully integrated part of the cell wall [28]. The resulting cell wall network is approximately 35 nm thick, consisting of a 16 nm low-density inner wall zone (IWZ) surrounded by a 19 nm high-density outer wall zone (OWZ) [29].

Cell wall synthesis machinery during *S. aureus* cell division

Cell division in *S. aureus* involves spatial and temporal coordination of multiple cell division proteins - the divisome. Assembly of the divisome is initiated by the polymerization of FtsZ, a cytoskeletal homologue of the eukaryotic tubulin [30, 31]. Polymerization and movement of FtsZ is dependent on its GTPase activity and treadmilling ability, respectively. FtsZ treadmilling, being the directional movement of a polymer by adding monomers to one end and remove them from the other [32], mediates a condensation of the FtsZ polymers to form a loosely organized ring structure (the Z-ring) at mid-cell, the site of future division (Figure 3b) [33, 34]. The Z-ring is stabilized and tethered to the cell membrane by the conserved FtsA protein [35] and tightly regulated by several division proteins. EzrA is generally considered a negative regulator of Z-ring formation and depletion of EzrA leads to increased Z-ring formation rates in *Bacillus subtilis* [36] and can *in vitro* bind FtsZ to inhibit polymerization and bundling [37]. However, in *S. aureus,* EzrA carries additional essential roles of involvement in peptidoglycan biosynthesis and thought to be required for recruitment of 'late' divisional proteins together with FtsA and FtsZ, to gather the entire divisome [38-40]. This recruitment include DivIB, DivIC, FtsL, PBP1, PBP2 and GpsB, which again can be regulated by SepF [38, 41]. Entry of the GpsB protein at the division site stimulate the GTPase activity of FtsZ and form bundels in combination with FtsZ to form a tight Z-ring [42]. This bundling triggers FtsZ treadmilling to initiate membrane constriction and begin septal peptidoglycan synthesis (Figure 3c) [34, 40].

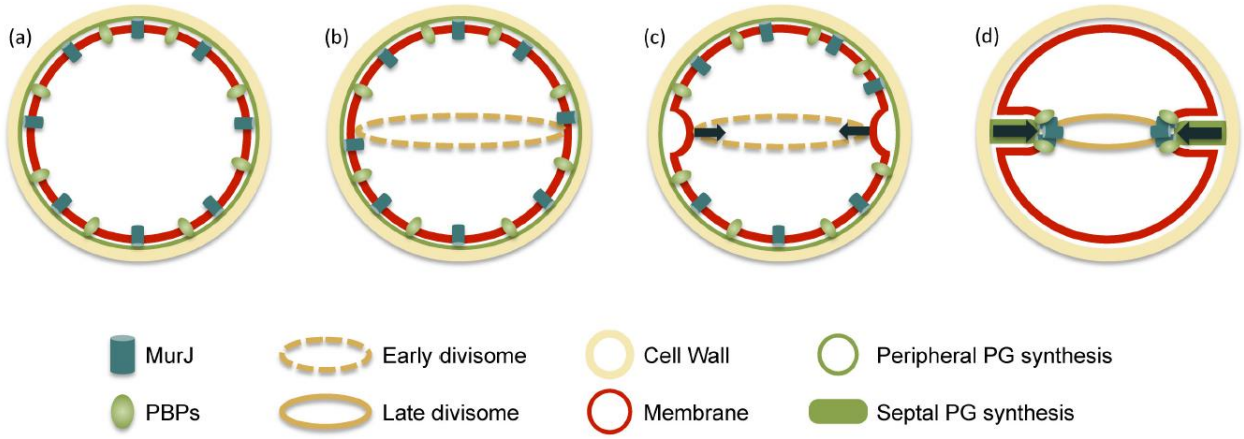

***Figure 3. Overview of cell division in* Staphylococcus aureus.** *The newly split cell **(a)** starts another round of division by the assembly of the early divisome, orchestrated by the treadmilling activity of FtsZ **(b)**. Bundling of FtsZ polymers triggers FtsZ treadmilling to start constriction **(c)** and recruit late division proteins and PBPs to initiate septal PG synthesis **(d)**. Figure from [43].*

Peptidoglycan synthesis at septum is dependent on the presence of PBPs, their cognate SEDS and the availability of the PG precursor Lipid II-pentaglycine. PBP1, its cognate SEDS, FtsW, and the DivIB protein all arrive concurrently to the division site, where DivIB form a complex with DivIC and FtsL to recruit the lipid II flippase MurJ [43]. This ensure that translocation of Lipid II-pentaglycine exclusively occur at midcell, which recruits PBP2 via substrate affinity to the free PG precursor [44, 45]. Once lipid II-pentaglycine translocation initiates, PBP1-FtsW and PBP2 begins to synthesize the septal PG in a process redundantly guided by FtsZ treadmilling (Figure 3d) [27, 34, 43]. Finally, PBP4 is guided to the septum by a newly synthesized cell wall polymer (wall teichoic acid intermediates), to create highly cross-linked PG ready for the autolytic splitting into two separate daughter cells [46-50].

Daughter cell segregation

Cell segregation after ended cell division is taken on by three cell wall hydrolases, also known as autolysins. The major autolysin Atl preprotein holds both amidase (NAM-L-Ala cleavage) and glucosaminidase (NAG-NAM cleavage) domains that are processed to two separate hydrolases [51]. These hydrolases are excreted and guided to the exterior division plane by repeat units that are repelled by wall teichoic acids (WTA) on the cell surface [52] to direct them to lipoteichoic acid polymers (LTA, see next section) at the surface exposed cell division site [53]. Sle1 is another amidase that is guided to the exterior division plane by three consecutive LysM domains that, like Atl repeat units, are repelled by WTA to associate with

NAM-NAG repeating disaccharides of PG at the cell division site [54, 55]. The activities of Atl and Sle1 introduce perforation holes along the outer edge of the division site [56, 57]. Unlike Atl and Sle1, LysN is directed to the septum by a YSIRK/GS signal peptide, where it cleaves cross-links and stem peptides via Gly-D-Ala endopeptidase and amidase activities between the two coming daughter cells [58]. Intra-septal LytN processing of the complete septum, combined with Atl/Sle1 exterior processing of division plane cell wall, will finally result in a less than 2 millisecond mechanical splitting of the septum, resulting in two separate daughter cells [57, 59].

Lipoteichoic acid synthesis, modifications and contributions to cell division

As described above, many different players are contributing to proper cell division. Additional key role players are teichoic acids and their synthesis pathway members. Teichoic acids (TA) are gram-positive bacterial polymers that comes in two classes: wall teichoic acids (WTAs) and lipoteichoic acids (LTAs) [60]. Even though cells deficient in both TAs are non-viable [61] suggesting that these polymers carry overlapping functions [62], they have several distinct differences. WTA is a cell surface exposed ribitolphosphate polymer that, as peptidoglycan, is synthesized in the cytoplasm on UndP and flipped across the membrane, where it is attached to the cell wall by LCP (LytR-CpsA-Psr) family enzymes [63, 64]. Contrarily, LTA is a membrane-linked, septum located, glycerolphosphate (GroP) polymer synthesized outside the cell on a glycolipid anchor [60, 65]. The two polymers differ in stereochemistry, enabling stereospecific differentiation between the two, utilized for e.g. degradation purposes [66].

The synthesis of LTA starts by the production of the glycolipid anchor in the cytoplasm (Figure 4a). UDP-linked glucose (UDP-Glc) is built from glucose-6-phosphate by the actions of PgcA and GtaB, before two glucose moieties from two UDP-Glc molecules are connected to membrane diacylglycerol (DAG) by YpfP to constitute the final Glc_2DAG LTA anchor [67]. This Glc_2DAG anchor is flipped across the membrane by LtaA [68, 69], ready for attachment of up to 50 consecutive GroP molecules. The GroP units are derived from the membrane lipid phosphatidylglycerol and polymerized by LtaS at the distal end of the growing polymer [69-72]. When LTA production is no longer favored, the LtaS synthase is processed between its

membrane and extracellular domain by the type I signal peptidase SpsB, leaving the synthase inactive [73]. Inactivation of the genes responsible for anchor assembly (*pgcA, gtaB* or *ypfP*) or LTA flipping (*ltaA*) result in polymers with extended length assembled on phosphatidylglycerol [68, 72].

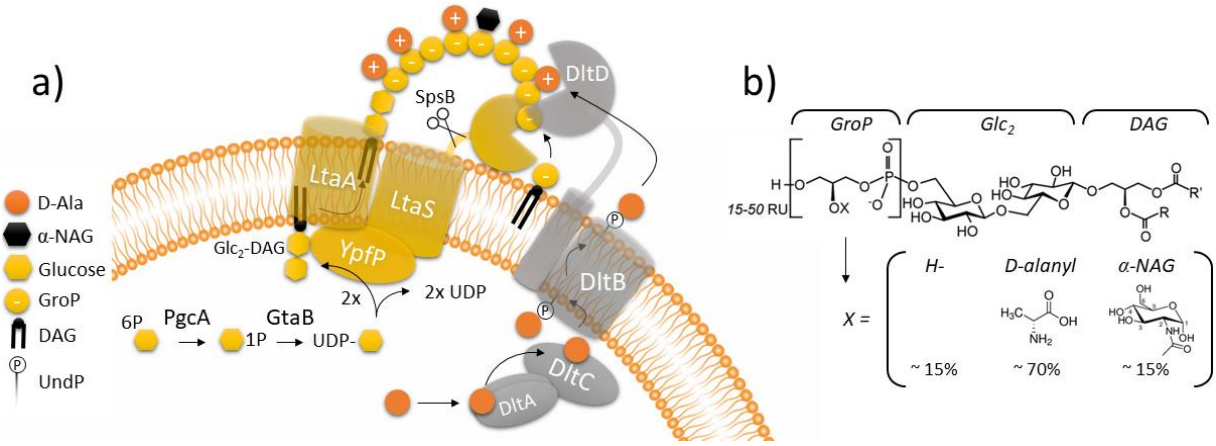

Figure 4. Lipoteichoic acid synthesis and modification pathways. (a, yellow) *Two UDP-Glc molecules are formed from glucose-6-phosphate in the cytoplasm by PgcA and GtaB and attached to DAG in the inner membrane leaflet by YpfP. LtaA flips the anchor across the membrane, where LtaS synthesize the nascent polymer from GroP units of membrane phosphatidyl glycerol.* ***(a, grey)*** *D-alanylation of LTA starts by activation of D-alanine by DltA, which through DltC is attached to UndP in the membrane by DltB. DltB flips UndP-D-Ala across the membrane where DltD attach the D-alanyl groups to the C2 position of the LTA GroP units.* ***(b)*** *LTA structure and modifications of the GroP C2 position.*

The phosphate groups introduce a negative charge for every GroP unit added to the nascent LTA polymer (Figure 4b). To modulate the level of negative charge outside the cell, LTA is frequently decorated with D-alanine moieties that introduce a neutralizing positive charge to the otherwise negative polymer. D-alanylation of LTA is taken on by the *dlt* operon (Figure 4a, grey) and starts with DltA activating D-alanine in an ATP-dependent reaction and transferring it to the D-alanyl carrier protein DltC. DltC is then thought to transfer D-alanine to UndP in the membrane by an acetyltransferase activity of DltB [74]. DltB belongs to the membrane-bound O-acetyltransferase (MBOAT) family of proteins and acts to both transfer D-alanine to UndP and to transport UndP-D-Ala across the membrane [75]. From here, DltD is responsible for the final catalytic transfer of D-alanine to the C2 position of GroP (Figure 4a and b) [76]. D-ala-LTA is thought to be the D-alanine donor for D-alanylation of WTA [77, 78] and D-alanylation of WTA have shown to be diminished but not abolished in an LTA-negative strain [75].

Another modification of LTA is the addition of a NAG molecule to the C2 position, which recently was shown to be added to LTA in a manner similar as D-alanine. NAG is attached to UndP, transported across the membrane and attached to LTA by CsbB, GtcA and YfhO, respectively [79, 80]. The C2 GroP positions are suggested to be 70 % D-alanylated and 15 % α-NAG glycosylated with the remainder left unmodified [78].

The LTA polymer is essential for bacterial growth and cell division, as cells lacking the LtaS synthase rely on compensatory mutations to preserve proliferation [81-83]. The synthesis of the LTA polymer on a Glc_2DAG anchor is not essential for cell growth, but inactivating mutations of *pgcA, gtaB* or *ypfP* show severe cell division defects [72, 84, 85]. LtaA flippase mutants as well show division defects, however, to a lesser extent than mutants of *ypfP* [69, 72]. Cell divison phenotypes of mutants of LTA pathway members include multiple division septa, placing new septa at angles non-orthogonal to former septa and impairment of separation after ended division cycle [69, 70, 72, 84, 85]. In *B. subtilis*, UgtP (YpfP) has been identified as a glucose-sensitive inhibitor of Z-ring formation able to delay cell division of rapid growing cells. Nutrient rich conditions are thought to increase the amount of UDP-glucose and localize UgtP to the Z-ring to stall cell division until cells reach a sufficient length to allow for proper chromosome segregation [86]. However, no binding of *S. aureus* LtaS, LtaA or YpfP was observed to FtsZ in a bacterial two-hybrid setup, but interactions with early stage cell division proteins EzrA and FtsA, late stage DivIB, DivIC and FtsL and all four PBPs point to a direct link to cell divison [65].

Intrinsic resistance and auxiliary factors

The natural ability of the bacterial cell to withstand foreign attack (e.g. antimicrobials or bacterial viruses) or stress (e.g. high salt concentrations or temperature) independently of previous pressure and acquired foreign DNA is referred to as intrinsic resistance [87]. The endogenous genes required for MRSA to withstand β-lactam antimicrobial pressure, known as auxiliary factors, include members of the divisome, teichoic acids, and genes required for cell envelope integrity [88, 89].

The cell envelope is vital for the bacterial cell, and perturbations of its structure can have immense effects on its ability to withstand β-lactam pressure. The *fem* (factor essential for

the expression of methicillin resistance) factors responsible for the addition of the pentaglycine bridge to lipid II, was some of the early identified auxiliary factors shown to increase sensitivity to β-lactams after inactivation [24, 90]. Lipid II biosynthesis [91], amidation of the lipid II stem D-iso-glutamate [22, 92], and peptidoglycan cross-linking and polymerization [91, 93, 94] are crucial activities to build, modify and maintain the cell wall. Genes responsible for these actions are critical to maintain β-lactam resistance and are obvious targets for potentiating β-lactam antibiotics against MRSA.

Members of the divisome are likewise crucial for β-lactam resistance as they ensure proper cell division and coordination of the cell wall machinery. This is exemplified by the synergistic effects between the FtsZ inhibitor PC190723 and imipenem (a carbapenem β-lactam), where addition of PC190723 e.g. prompt PBP2 mislocalization [95]. Besides correct localization, transport and folding is critical, as deletion of the PBP2a chaperone PrsA ease resistance levels by a decrease in PBP2a levels in the membrane, possibly combined with a lack of proper PBP2a folding [96]. The successful combination of daptomycin (DAP) together with β-lactams (the so-called "seesaw effect") is due to DAP-induced compensatory mutations in *mprF* that among others cause delocalization of PrsA [97].

Transport of cell wall associated proteins across the membrane is another area important for β-lactam intrinsic resistance, as inhibitors of the essential surface-located signal peptidase SpsB re-sensitize MRSA [98]. SpsB cleaves the N-terminal secretory signal sequence as the excreted proteins pass through the Sec secretory protein complex [99]. The synergistic effect was proposed to be due to the lack of SpsB-mediated secretion of proteins required for β-lactam resistance [98]. Alternatively, as SpsB regulate LTA synthase activity [73] and suppression of SpsB inhibitor fatality can arise by limiting LtaS expression [100], the SpsB inhibition will leave the LTA synthase unregulated, which could result in perturbations of LTA and thereby cell wall homeostasis and leave the cell susceptible to PBP inhibitors.

Teichoic acid polymers as well as their modifications are important for β-lactam resistance. Disruption of both the addition (via *dlt* operon mutations or the DltB inhibitor amsacrine [101, 102]) and release (by FmtA [103, 104]) of D-alanine moieties and WTA β-O-GlcNAc decorations [105] will leave the cells susceptible to β-lactams. The same effect has the entire WTA polymer, as the WTA polymer is important for PBP2a function (via the β-O-GlcNAc

residues [105]) and acts as a temporal and spatial regulator of PBP4 localization at the septum for the final cross-linking step before daughter cell splitting [46].

Recently, different studies using either genome-wide screening of a *S. aureus* transposon-library or transposon sequencing show that additional factors modulate β-lactam susceptibility [106, 107]. This is the topic of manuscripts 2 and 3, where we characterize two novel auxiliary factors.

CRISPR-Cas immunity

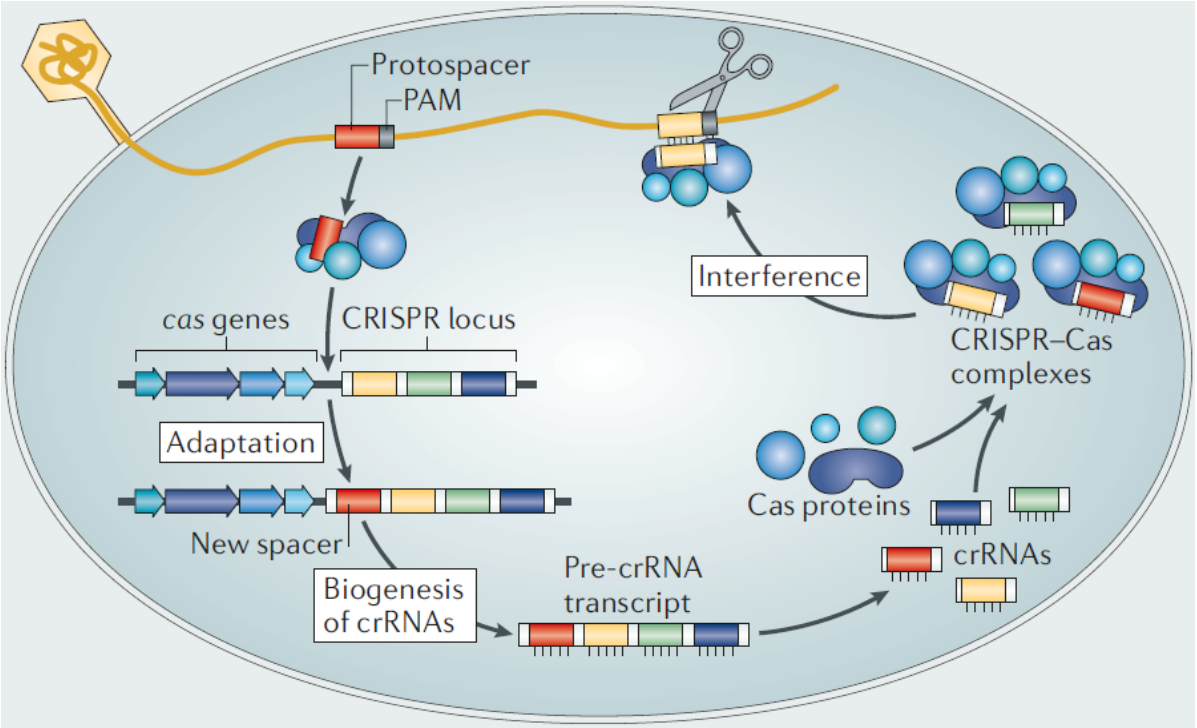

Figure 5. Steps in CRISPR-Cas immunity. *During adaptation, DNA from the foreign invader is selected, processed and integrated into the CRISPR locus. This is then transcribed into a long pre-crRNA that is processed into mature crRNAs, ready to guide the Cas interference machinery to its foreign target for DNA (or RNA) cleavage. Figure from [108].*

Besides antimicrobials, there are many other threats a bacterial cell can encounter – one is bacterial viruses (bacteriophages or just phages). Innate defense mechanisms against these foreign invaders include blockage of bacteriophage adsorption, cleavage of the incoming foreign DNA by restriction-modification enzymes, and abortive infection systems that shuts down and sacrifice the infected cell [109-111]. In addition to innate immunity, around 40 % of bacterial genomes additionally carry an adaptive immune system [112], known as the clustered regularly interspaced short palindromic repeats (CRISPR) system [113].

In 1987, alternating identical repeats with 32 nucleotide spacings (subsequently termed spacers) were found in the genome of *Escherichia coli* [114] and later shown to be homologous to foreign plasmids and bacteriophages [115, 116]. A phage-sensitive strain with acquired resistance after phage-exposure had adopted spacers matching the genome of the challenging phage, demonstrating the role of CRISPR as an adaptive immune system [117]. The CRISPR spacers rely on CRISPR-associated (Cas) genes located adjacent to the CRISPR locus, and transcription and processing of the CRISPR array into RNA (crRNA) to mediate immunity [113]. This is done in three steps; adaptation, crRNA biogenesis and interference (Figure 5). During adaptation, DNA from the invader (e.g. a phage, plasmid, or transposon) is selected, processed, and integrated into the CRISPR locus. This is transcribed, directed from an upstream leader sequence, to produce a long precursor crRNA containing both repeat and spacer sequences. Precursor crRNA is processed within the repeat sequences, and individual spacers are delivered to an interference protein or complex to guide it to a foreign target sequence complementary to the crRNA (protospacer) [118, 119].

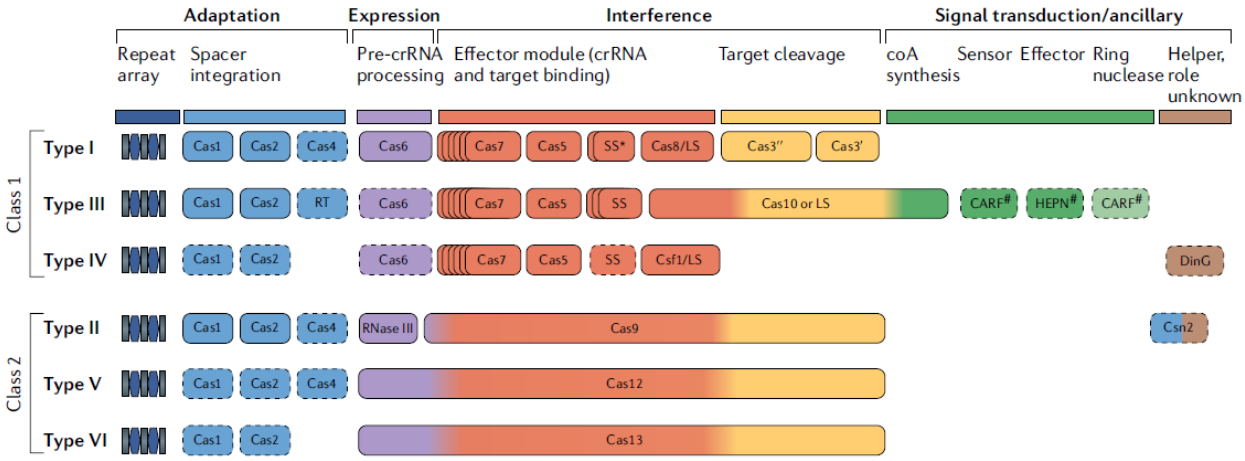

Figure 6. Overview of CRISPR-Cas systems. *CRISPR-Cas systems are divided into two classes. Class 1 systems contain multi-membered effector modules, whereas class systems 2 rely on one large interference protein. Class 1 is further divided into type I, III, and IV systems where class 2 contain type II, V and VI. Common for all types of CRISPR systems is the presence of the Cas1 and Cas2 genes involved in adaptation of new spacers into the CRISPR array. Figure from [112].*

CRISPR-Cas systems are divided in two classes based on their Cas content and mode of action. Class 1 CRISPR-Cas systems consist of multiple Cas proteins to form an interference complex, whereas class 2 systems rely on a single large effector protein. The two classes are further

divided into six different types: I, III and IV belong to class 1, and II, V and VI belong to class 2 (Figure 6) [112].

The type III-A CRISPR system

In staphylococci, described CRISPR systems belong to the type III-A, and have been reported with low currency in isolated strains [120, 121]. Unlike other types of CRISPR-cas systems that bind DNA targets, the type III systems bind RNA sequences, making it transcription dependent. The interference machinery is a multi-subunit complex containing five different Cas proteins, and holds both RNase and DNAse activity (Figure 7) [119]. Immunity via the type III-A system start with the transcription of the CRISPR locus, which fold up into hairpin structures due to the palindromic repeats. The Cas6 endonuclease cleaves the spacers 8 nucleotides upstream into the repeat sequences immediately prior to an RNA loop structure [122]. Cas6 is believed to deliver the intermediate crRNAs to the interference complex, which maturates the crRNA by a shortening of the 3' repeat sequence in 6 bp intervals mediated by Csm2 and the Cas7-family proteins Csm3 and Csm5 [123]. The mature crRNA is bound in the 5' repeat handle by the Cas protein Csm4 along with the Cas10 protein that hold DNase (HD domain) and cyclic oligoadenylate (c-oligoA) synthase (Palm domain) activity [124]. Upon binding of the interference complex to the target RNA, the Cas10 protein activates and the HD domain cleaves the non-template DNA strand [125], while the Palm domain start to synthesize c-oligoA from ATP, which activates the final member of the type III-A system, Csm6 [124]. Csm6 resembles an abortive infection (Abi) module through an unspecific RNAase activity that shuts down the host, leading to its growth arrest [112, 126].

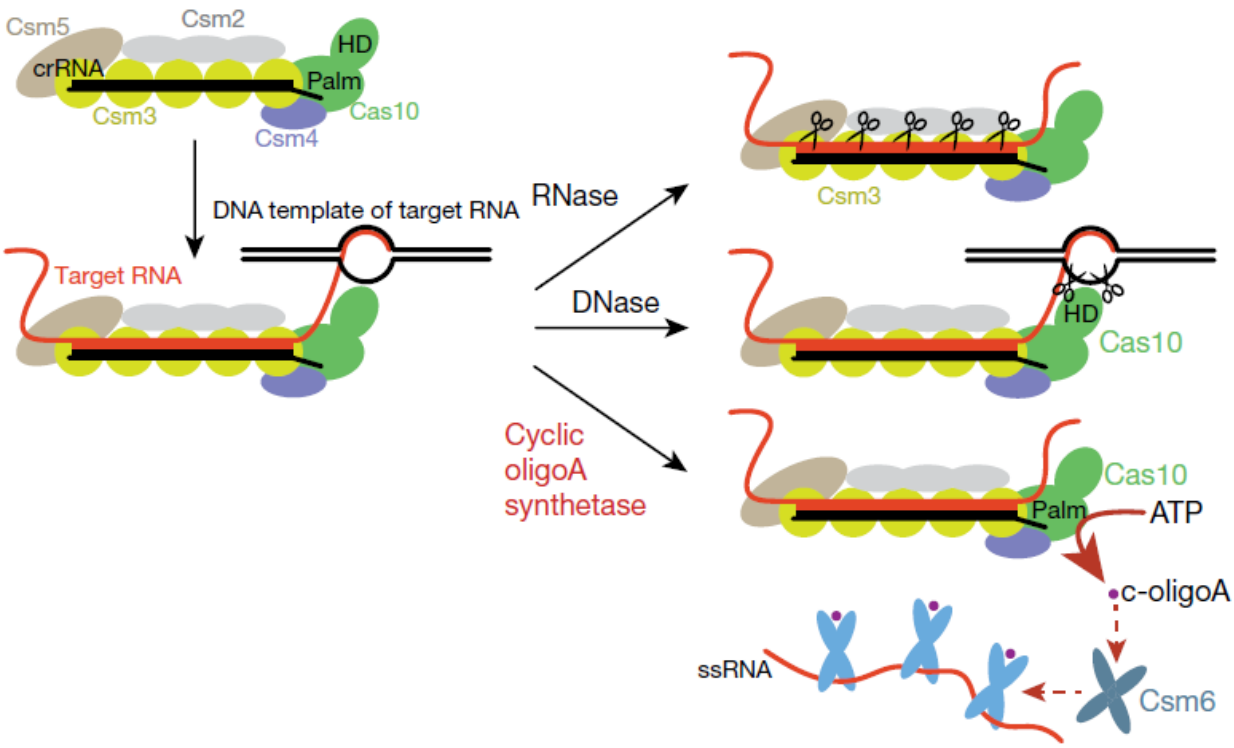

Figure 7. Interference mechanisms of the CRISPR-Cas type III-A system. *Upon binding and maturation of the crRNA, the interference complex binds to crRNA-complementary protospacer transcript RNA, where Csm3 proteins cleaves the RNA target. Binding of the protospacer transcript activates the two domains of Cas10. The HD domain cuts the coding-strand, accessible via the RNA polymerase transcription bubble, and the Palm domain synthesize c-oligoA from ATP. Binding of c-oligoA activates Csm6 that holds unspecific RNAse activity which shuts down the host cell leading to growth arrest. Figure from [124].*

Spacer adaptation

When a bacterial cell encounters an unknown foreign enemy, it can adapt to this enemy by acquiring new spacers to the CRISPR locus, complementary to parts of the invaders genetic code. This is orchestrated by the Cas1-Cas2 complex consisting of two Cas1 dimer molecules bridged by a Cas2 dimer, where Cas1 carries catalytic activity and Cas2 serves a structural function [127]. To limit the risk of auto-immunity, it is important to be able to distinguish self from non-self. In type I and II CRISPR-Cas systems, foreign protospacers are distinguished from genomic CRISPR array spacers by the location of a protospacer adjacent motif (PAM) immediately upstream of the protospacer, and recognized by the Cas1-Cas2 complex [128]. The type III-A system, however, does not use a PAM sequence. Instead, it distinguishes self from non-self via the -5 to -2 positions of the 5'-terminal repeat sequence of the crRNAs [129, 130]. The Cas1-Cas2 complex selects and processes the protospacer and integrates it as the first spacer in the 5' end of the CRISPR array, via interaction with the last part of the upstream

leader sequence, known as the leader anchoring sequence (LAS) [128, 131]. Mutations of the LAS can result in ectopic spacer integration to the middle of the array [131].

The *cas1* and *cas2* genes are present in nearly all CRISPR systems (Figure 6) [112, 132], but have never experimentally shown to expand the type III-A CRISPR locus [119]. In the *Streptococcus thermophilus* type II-A system, overexpression of the Cas1, Cas2, and Csn2 genes are necessary for adaptation, demonstrating that acquisition of new spacers is a rare event across different classes of CRISPR [133].

For both classes of CRISPR-Cas systems, phage escape mutations are typically located within the PAM or seed region (6-8 nucleotides of the protospacer immediately adjacent to the PAM) of the protospacer. However, the type III-A system does not rely on either PAM or seed sequences, which makes it more tolerant to protospacer and adjacent mutations. In fact, complete escape from type III-A immunity was shown to require complete deletions of the targeted phage protospacer [134].

The *S. aureus* type III-A CRISPR system and SCC*mec* type V (5C2&5)

The *S. aureus* CRISPR-Cas type III-A system has shown to be active against both plasmid [120] and viral infections [Li, Y, Mikkelsen, K *et al.*, submitted manuscript], with spacers at the leader end being heavier transcribed and providing greater immunity than distal spacers [Li, Y, Mikkelsen, K *et al.*, submitted manuscript]. The type III-A system is dependent on all *cas*/*csm* genes except Cas1 and Cas2 for interference of invading foreign DNA [120, 135].

The first *S. aureus* isolate reported to contain CRISPR-Cas type III-A was the Canadian 08BA02176 ST398 LA-MRSA strain [136]. Emerging clones of the ST630, closely related to CC8 CA-MRSAs, have recently been reported in China and Denmark, which contain the type III-A system and shares spacers with the Canadian 08BA02176 isolate [120, 137]. Spacers are highly conserved both within and between clonal complexes, implying that the CRISPR system can be acquired via HGT. CC45 isolates, however, does not share spacers with other clonal complexes, and spacer content diverges within the CC45 group as to whether the CRISPR system is present within the SCC*mec* type IV or V, or the isolate is SCC*mec* negative (Figure 8) [Li, Y, Mikkelsen, K *et al.*, submitted manuscript].

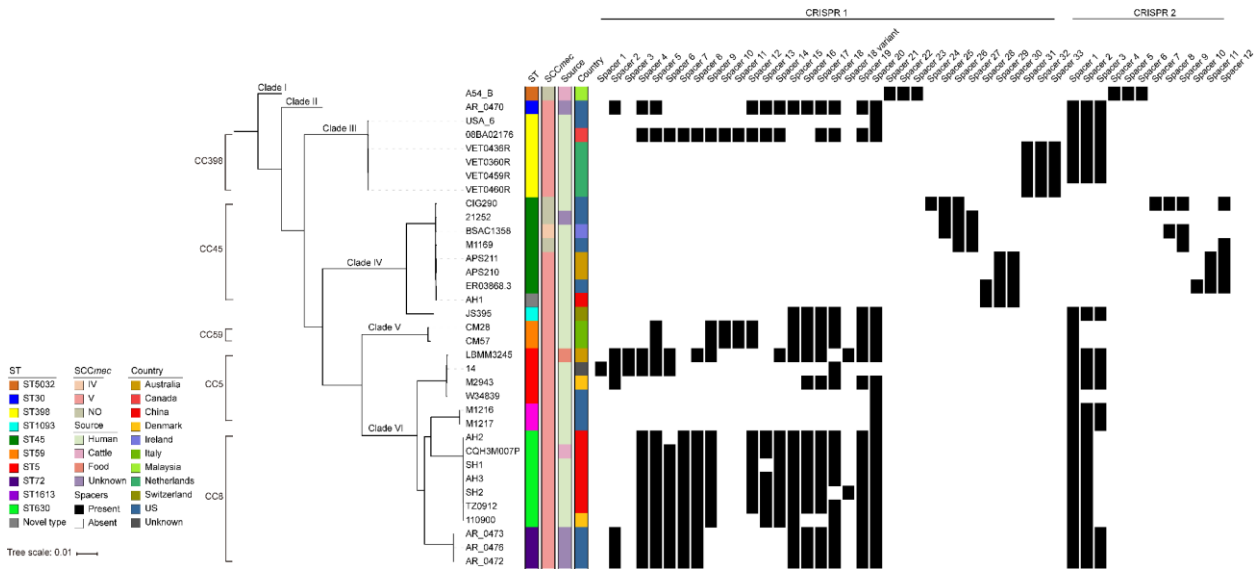

Figure 8. *Single nucleotide polymorphism (SNP) phylogenetic tree of CRISPR-Cas positive* S. aureus *genomes, available from the National Center for Biotechnology Information (NCBI) database. Spacer content of the isolates are shown with CRISPR1 and CRISPR2 being upstream and downstream CRISPR loci, respectively. Figure from [Li, Y, Mikkelsen, K et al., submitted manuscript].*

Interestingly, the majority of CRISPR positive isolates carries the type III-A system within the SCC*mec* type V (5C2&5) [120, 136-138]. As mentioned earlier, the SCC*mec* is a mobile genetic element able to excise from the chromosome, possibly replicate [139, 140] and transfer between strains and species [141]. The presence of CRISPR within the SCC*mec* cassette might help the spread of CRISPR-Cas systems and adds additional gain to the SCC*mec* recipient: β-lactam resistance and adaptive immunity. CRISPR-Cas prevalence within the SCC*mec* of MRSA isolates and the possible dissemination of the CRISPR system will be further characterized in manuscript 4.

References

1. Kluytmans, J., A. van Belkum, and H. Verbrugh, *Nasal carriage of Staphylococcus aureus: epidemiology, underlying mechanisms, and associated risks.* Clin Microbiol Rev, 1997. **10**(3): p. 505-20.
2. Aryee, A. and J.D. Edgeworth, *Carriage, Clinical Microbiology and Transmission of Staphylococcus aureus.* Curr Top Microbiol Immunol, 2017. **409**: p. 1-19.
3. Monaco, M., et al., *Worldwide Epidemiology and Antibiotic Resistance of Staphylococcus aureus.* Curr Top Microbiol Immunol, 2017. **409**: p. 21-56.
4. Chambers, H.F. and F.R. Deleo, *Waves of resistance: Staphylococcus aureus in the antibiotic era.* Nat Rev Microbiol, 2009. **7**(9): p. 629-41.
5. Lim, D. and N.C. Strynadka, *Structural basis for the beta lactam resistance of PBP2a from methicillin-resistant Staphylococcus aureus.* Nat Struct Biol, 2002. **9**(11): p. 870-6.
6. Ito, T., et al., *Staphylococcal Cassette Chromosome mec (SCCmec) analysis of MRSA.* Methods Mol Biol, 2014. **1085**: p. 131-48.
7. International Working Group on the Classification of Staphylococcal Cassette Chromosome, E., *Classification of staphylococcal cassette chromosome mec (SCCmec): guidelines for reporting novel SCCmec elements.* Antimicrob Agents Chemother, 2009. **53**(12): p. 4961-7.
8. David, M.Z. and R.S. Daum, *Treatment of Staphylococcus aureus Infections.* Curr Top Microbiol Immunol, 2017. **409**: p. 325-383.
9. Howden, B.P., et al., *Reduced vancomycin susceptibility in Staphylococcus aureus, including vancomycin-intermediate and heterogeneous vancomycin-intermediate strains: resistance mechanisms, laboratory detection, and clinical implications.* Clin Microbiol Rev, 2010. **23**(1): p. 99-139.
10. Courvalin, P., *Vancomycin resistance in gram-positive cocci.* Clin Infect Dis, 2006. **42 Suppl 1**: p. S25-34.
11. Ling, L.L., et al., *A new antibiotic kills pathogens without detectable resistance.* Nature, 2015. **517**(7535): p. 455-9.
12. Llarrull, L.I., et al., *The future of the beta-lactams.* Curr Opin Microbiol, 2010. **13**(5): p. 551-7.
13. Egan, A.J.F., J. Errington, and W. Vollmer, *Regulation of peptidoglycan synthesis and remodelling.* Nat Rev Microbiol, 2020. **18**(8): p. 446-460.
14. Rajagopal, M. and S. Walker, *Envelope Structures of Gram-Positive Bacteria.* Curr Top Microbiol Immunol, 2017. **404**: p. 1-44.
15. Boneca, I.G., et al., *Characterization of Staphylococcus aureus cell wall glycan strands, evidence for a new beta-N-acetylglucosaminidase activity.* J Biol Chem, 2000. **275**(14): p. 9910-8.
16. Ward, J.B., *The chain length of the glycans in bacterial cell walls.* Biochem J, 1973. **133**(2): p. 395-8.
17. Hayhurst, E.J., et al., *Cell wall peptidoglycan architecture in Bacillus subtilis.* Proc Natl Acad Sci U S A, 2008. **105**(38): p. 14603-8.
18. Vollmer, W., D. Blanot, and M.A. de Pedro, *Peptidoglycan structure and architecture.* FEMS Microbiol Rev, 2008. **32**(2): p. 149-67.
19. Benson, T.E., et al., *Overexpression, purification, and mechanistic study of UDP-N-acetylenolpyruvylglucosamine reductase.* Biochemistry, 1993. **32**(8): p. 2024-30.
20. Blake, K.L., et al., *The nature of Staphylococcus aureus MurA and MurZ and approaches for detection of peptidoglycan biosynthesis inhibitors.* Mol Microbiol, 2009. **72**(2): p. 335-43.
21. Walsh, C.T., *Enzymes in the D-alanine branch of bacterial cell wall peptidoglycan assembly.* J Biol Chem, 1989. **264**(5): p. 2393-6.

22. Figueiredo, T.A., et al., *Identification of genetic determinants and enzymes involved with the amidation of glutamic acid residues in the peptidoglycan of Staphylococcus aureus.* PLoS Pathog, 2012. **8**(1): p. e1002508.
23. Ruiz, N., *Bioinformatics identification of MurJ (MviN) as the peptidoglycan lipid II flippase in Escherichia coli.* Proc Natl Acad Sci U S A, 2008. **105**(40): p. 15553-7.
24. Berger-Bachi, B. and M. Tschierske, *Role of fem factors in methicillin resistance.* Drug Resist Updat, 1998. **1**(5): p. 325-35.
25. Taguchi, A., D. Kahne, and S. Walker, *Chemical tools to characterize peptidoglycan synthases.* Curr Opin Chem Biol, 2019. **53**: p. 44-50.
26. Taguchi, A., et al., *FtsW is a peptidoglycan polymerase that is functional only in complex with its cognate penicillin-binding protein.* Nat Microbiol, 2019. **4**(4): p. 587-594.
27. Reichmann, N.T., et al., *SEDS-bPBP pairs direct lateral and septal peptidoglycan synthesis in Staphylococcus aureus.* Nat Microbiol, 2019. **4**(8): p. 1368-1377.
28. Schaefer, K., et al., *Structure and reconstitution of a hydrolase complex that may release peptidoglycan from the membrane after polymerization.* Nat Microbiol, 2020.
29. Matias, V.R. and T.J. Beveridge, *Native cell wall organization shown by cryo-electron microscopy confirms the existence of a periplasmic space in Staphylococcus aureus.* J Bacteriol, 2006. **188**(3): p. 1011-21.
30. Lowe, J. and L.A. Amos, *Crystal structure of the bacterial cell-division protein FtsZ.* Nature, 1998. **391**(6663): p. 203-6.
31. Nogales, E., et al., *Tubulin and FtsZ form a distinct family of GTPases.* Nat Struct Biol, 1998. **5**(6): p. 451-8.
32. Schoenemann, K.M. and W. Margolin, *Bacterial Division: FtsZ Treadmills to Build a Beautiful Wall.* Curr Biol, 2017. **27**(8): p. R301-R303.
33. Lutkenhaus, J., S. Pichoff, and S. Du, *Bacterial cytokinesis: From Z ring to divisome.* Cytoskeleton (Hoboken), 2012. **69**(10): p. 778-90.
34. Whitley, K.D., et al., *FtsZ treadmilling is essential for Z-ring condensation and septal constriction initiation in Bacillus subtilis cell division.* bioRxiv, 2020: p. 2020.07.01.182006.
35. Pinho, M.G., M. Kjos, and J.W. Veening, *How to get (a)round: mechanisms controlling growth and division of coccoid bacteria.* Nat Rev Microbiol, 2013. **11**(9): p. 601-14.
36. Levin, P.A., I.G. Kurtser, and A.D. Grossman, *Identification and characterization of a negative regulator of FtsZ ring formation in Bacillus subtilis.* Proc Natl Acad Sci U S A, 1999. **96**(17): p. 9642-7.
37. Haeusser, D.P., et al., *EzrA prevents aberrant cell division by modulating assembly of the cytoskeletal protein FtsZ.* Mol Microbiol, 2004. **52**(3): p. 801-14.
38. Steele, V.R., et al., *Multiple essential roles for EzrA in cell division of Staphylococcus aureus.* Mol Microbiol, 2011. **80**(2): p. 542-55.
39. Adams, D.W. and J. Errington, *Bacterial cell division: assembly, maintenance and disassembly of the Z ring.* Nat Rev Microbiol, 2009. **7**(9): p. 642-53.
40. Bisson-Filho, A.W., et al., *Treadmilling by FtsZ filaments drives peptidoglycan synthesis and bacterial cell division.* Science, 2017. **355**(6326): p. 739-743.
41. Gao, Y., et al., *Free SepF interferes with recruitment of late cell division proteins.* Sci Rep, 2017. **7**(1): p. 16928.
42. Eswara, P.J., et al., *An essential Staphylococcus aureus cell division protein directly regulates FtsZ dynamics.* Elife, 2018. **7**.
43. Monteiro, J.M., et al., *Peptidoglycan synthesis drives an FtsZ-treadmilling-independent step of cytokinesis.* Nature, 2018. **554**(7693): p. 528-532.
44. Pinho, M.G. and J. Errington, *Recruitment of penicillin-binding protein PBP2 to the division site of Staphylococcus aureus is dependent on its transpeptidation substrates.* Mol Microbiol, 2005. **55**(3): p. 799-807.

45. Do, T., et al., *Staphylococcus aureus cell growth and division are regulated by an amidase that trims peptides from uncrosslinked peptidoglycan.* Nat Microbiol, 2020. **5**(2): p. 291-303.
46. Atilano, M.L., et al., *Teichoic acids are temporal and spatial regulators of peptidoglycan cross-linking in Staphylococcus aureus.* Proc Natl Acad Sci U S A, 2010. **107**(44): p. 18991-6.
47. Leski, T.A. and A. Tomasz, *Role of penicillin-binding protein 2 (PBP2) in the antibiotic susceptibility and cell wall cross-linking of Staphylococcus aureus: evidence for the cooperative functioning of PBP2, PBP4, and PBP2A.* J Bacteriol, 2005. **187**(5): p. 1815-24.
48. Jensen, C., et al., *The ClpX chaperone controls autolytic splitting of Staphylococcus aureus daughter cells, but is bypassed by beta-lactam antibiotics or inhibitors of WTA biosynthesis.* PLoS Pathog, 2019. **15**(9): p. e1008044.
49. Thalso-Madsen, I., et al., *The Sle1 Cell Wall Amidase Is Essential for beta-Lactam Resistance in Community-Acquired Methicillin-Resistant Staphylococcus aureus USA300.* Antimicrob Agents Chemother, 2019. **64**(1).
50. Zoll, S., et al., *Structural basis of cell wall cleavage by a staphylococcal autolysin.* PLoS Pathog, 2010. **6**(3): p. e1000807.
51. Oshida, T., et al., *A Staphylococcus aureus autolysin that has an N-acetylmuramoyl-L-alanine amidase domain and an endo-beta-N-acetylglucosaminidase domain: cloning, sequence analysis, and characterization.* Proc Natl Acad Sci U S A, 1995. **92**(1): p. 285-9.
52. Schlag, M., et al., *Role of staphylococcal wall teichoic acid in targeting the major autolysin Atl.* Mol Microbiol, 2010. **75**(4): p. 864-73.
53. Zoll, S., et al., *Ligand-binding properties and conformational dynamics of autolysin repeat domains in staphylococcal cell wall recognition.* J Bacteriol, 2012. **194**(15): p. 3789-802.
54. Frankel, M.B. and O. Schneewind, *Determinants of murein hydrolase targeting to cross-wall of Staphylococcus aureus peptidoglycan.* J Biol Chem, 2012. **287**(13): p. 10460-71.
55. Kajimura, J., et al., *Identification and molecular characterization of an N-acetylmuramyl-L-alanine amidase Sle1 involved in cell separation of Staphylococcus aureus.* Mol Microbiol, 2005. **58**(4): p. 1087-101.
56. Touhami, A., M.H. Jericho, and T.J. Beveridge, *Atomic force microscopy of cell growth and division in Staphylococcus aureus.* J Bacteriol, 2004. **186**(11): p. 3286-95.
57. Monteiro, J.M., et al., *Cell shape dynamics during the staphylococcal cell cycle.* Nat Commun, 2015. **6**: p. 8055.
58. Frankel, M.B., et al., *LytN, a murein hydrolase in the cross-wall compartment of Staphylococcus aureus, is involved in proper bacterial growth and envelope assembly.* J Biol Chem, 2011. **286**(37): p. 32593-605.
59. Giesbrecht, P., et al., *Staphylococcal cell wall: morphogenesis and fatal variations in the presence of penicillin.* Microbiol Mol Biol Rev, 1998. **62**(4): p. 1371-414.
60. Percy, M.G. and A. Grundling, *Lipoteichoic acid synthesis and function in gram-positive bacteria.* Annu Rev Microbiol, 2014. **68**: p. 81-100.
61. Schirner, K., et al., *Distinct and essential morphogenic functions for wall- and lipo-teichoic acids in Bacillus subtilis.* EMBO J, 2009. **28**(7): p. 830-42.
62. Swoboda, J.G., et al., *Wall teichoic acid function, biosynthesis, and inhibition.* Chembiochem, 2010. **11**(1): p. 35-45.
63. Chan, Y.G., et al., *Staphylococcus aureus mutants lacking the LytR-CpsA-Psr family of enzymes release cell wall teichoic acids into the extracellular medium.* J Bacteriol, 2013. **195**(20): p. 4650-9.
64. Brown, S., J.P. Santa Maria, Jr., and S. Walker, *Wall teichoic acids of gram-positive bacteria.* Annu Rev Microbiol, 2013. **67**: p. 313-36.
65. Reichmann, N.T., et al., *Differential localization of LTA synthesis proteins and their interaction with the cell division machinery in Staphylococcus aureus.* Mol Microbiol, 2014. **92**(2): p. 273-86.

66. Walter, A., et al., *Phosphoglycerol-type wall and lipoteichoic acids are enantiomeric polymers differentiated by the stereospecific glycerophosphodiesterase GlpQ.* J Biol Chem, 2020. **295**(12): p. 4024-4034.
67. Reichmann, N.T. and A. Grundling, *Location, synthesis and function of glycolipids and polyglycerolphosphate lipoteichoic acid in Gram-positive bacteria of the phylum Firmicutes.* FEMS Microbiol Lett, 2011. **319**(2): p. 97-105.
68. Grundling, A. and O. Schneewind, *Genes required for glycolipid synthesis and lipoteichoic acid anchoring in Staphylococcus aureus.* J Bacteriol, 2007. **189**(6): p. 2521-30.
69. Zhang, B., et al., *Structure of a proton-dependent lipid transporter involved in lipoteichoic acids biosynthesis.* Nat Struct Mol Biol, 2020. **27**(6): p. 561-569.
70. Grundling, A. and O. Schneewind, *Synthesis of glycerol phosphate lipoteichoic acid in Staphylococcus aureus.* Proc Natl Acad Sci U S A, 2007. **104**(20): p. 8478-83.
71. Karatsa-Dodgson, M., M.E. Wormann, and A. Grundling, *In vitro analysis of the Staphylococcus aureus lipoteichoic acid synthase enzyme using fluorescently labeled lipids.* J Bacteriol, 2010. **192**(20): p. 5341-9.
72. Hesser, A.R., et al., *The length of lipoteichoic acid polymers controls Staphylococcus aureus cell size and envelope integrity.* J Bacteriol, 2020.
73. Wormann, M.E., et al., *Proteolytic cleavage inactivates the Staphylococcus aureus lipoteichoic acid synthase.* J Bacteriol, 2011. **193**(19): p. 5279-91.
74. Fischer, W., *Lipoteichoic acid and lipids in the membrane of Staphylococcus aureus.* Med Microbiol Immunol, 1994. **183**(2): p. 61-76.
75. Reichmann, N.T., C.P. Cassona, and A. Grundling, *Revised mechanism of D-alanine incorporation into cell wall polymers in Gram-positive bacteria.* Microbiology (Reading), 2013. **159**(Pt 9): p. 1868-1877.
76. Wood, B.M., et al., *A partial reconstitution implicates DltD in catalyzing lipoteichoic acid d-alanylation.* J Biol Chem, 2018. **293**(46): p. 17985-17996.
77. Haas, R., H.U. Koch, and W. Fischer, *Alanyl turnover from lipoteichoic acid to teichoic acid in Staphylococcus aureus.* FEMS Microbiology Letters, 1984. **21**(1): p. 27-31.
78. Schneewind, O. and D. Missiakas, *Lipoteichoic acids, phosphate-containing polymers in the envelope of gram-positive bacteria.* J Bacteriol, 2014. **196**(6): p. 1133-42.
79. Kho, K. and T.C. Meredith, *Salt-Induced Stress Stimulates a Lipoteichoic Acid-Specific Three-Component Glycosylation System in Staphylococcus aureus.* J Bacteriol, 2018. **200**(12).
80. Rismondo, J., M.G. Percy, and A. Grundling, *Discovery of genes required for lipoteichoic acid glycosylation predicts two distinct mechanisms for wall teichoic acid glycosylation.* J Biol Chem, 2018. **293**(9): p. 3293-3306.
81. Corrigan, R.M., et al., *c-di-AMP is a new second messenger in Staphylococcus aureus with a role in controlling cell size and envelope stress.* PLoS Pathog, 2011. **7**(9): p. e1002217.
82. Baek, K.T., et al., *The Cell Wall Polymer Lipoteichoic Acid Becomes Nonessential in Staphylococcus aureus Cells Lacking the ClpX Chaperone.* mBio, 2016. **7**(4).
83. Karinou, E., et al., *Inactivation of the Monofunctional Peptidoglycan Glycosyltransferase SgtB Allows Staphylococcus aureus To Survive in the Absence of Lipoteichoic Acid.* J Bacteriol, 2019. **201**(1).
84. Kiriukhin, M.Y., et al., *Biosynthesis of the glycolipid anchor in lipoteichoic acid of Staphylococcus aureus RN4220: role of YpfP, the diglucosyldiacylglycerol synthase.* J Bacteriol, 2001. **183**(11): p. 3506-14.
85. Lazarevic, V., et al., *Bacillus subtilis alpha-phosphoglucomutase is required for normal cell morphology and biofilm formation.* Appl Environ Microbiol, 2005. **71**(1): p. 39-45.
86. Weart, R.B., et al., *A metabolic sensor governing cell size in bacteria.* Cell, 2007. **130**(2): p. 335-47.
87. Cox, G. and G.D. Wright, *Intrinsic antibiotic resistance: mechanisms, origins, challenges and solutions.* Int J Med Microbiol, 2013. **303**(6-7): p. 287-92.

88. Foster, T.J., *Can beta-Lactam Antibiotics Be Resurrected to Combat MRSA?* Trends Microbiol, 2019. **27**(1): p. 26-38.
89. Roemer, T., T. Schneider, and M.G. Pinho, *Auxiliary factors: a chink in the armor of MRSA resistance to beta-lactam antibiotics.* Curr Opin Microbiol, 2013. **16**(5): p. 538-48.
90. Berger-Bachi, B., et al., *FemA, a host-mediated factor essential for methicillin resistance in Staphylococcus aureus: molecular cloning and characterization.* Mol Gen Genet, 1989. **219**(1-2): p. 263-9.
91. Lee, S.H., et al., *Antagonism of chemical genetic interaction networks resensitize MRSA to beta-lactam antibiotics.* Chem Biol, 2011. **18**(11): p. 1379-89.
92. Gustafson, J., et al., *The femC locus of Staphylococcus aureus required for methicillin resistance includes the glutamine synthetase operon.* J Bacteriol, 1994. **176**(5): p. 1460-7.
93. Memmi, G., et al., *Staphylococcus aureus PBP4 is essential for beta-lactam resistance in community-acquired methicillin-resistant strains.* Antimicrob Agents Chemother, 2008. **52**(11): p. 3955-66.
94. Pinho, M.G., H. de Lencastre, and A. Tomasz, *An acquired and a native penicillin-binding protein cooperate in building the cell wall of drug-resistant staphylococci.* Proc Natl Acad Sci U S A, 2001. **98**(19): p. 10886-91.
95. Tan, C.M., et al., *Restoring methicillin-resistant Staphylococcus aureus susceptibility to beta-lactam antibiotics.* Sci Transl Med, 2012. **4**(126): p. 126ra35.
96. Jousselin, A., et al., *The Staphylococcus aureus Chaperone PrsA Is a New Auxiliary Factor of Oxacillin Resistance Affecting Penicillin-Binding Protein 2A.* Antimicrob Agents Chemother, 2015. **60**(3): p. 1656-66.
97. Renzoni, A., et al., *Molecular Bases Determining Daptomycin Resistance-Mediated Resensitization to beta-Lactams (Seesaw Effect) in Methicillin-Resistant Staphylococcus aureus.* Antimicrob Agents Chemother, 2017. **61**(1).
98. Therien, A.G., et al., *Broadening the spectrum of beta-lactam antibiotics through inhibition of signal peptidase type I.* Antimicrob Agents Chemother, 2012. **56**(9): p. 4662-70.
99. Schneewind, O. and D. Missiakas, *Sec-secretion and sortase-mediated anchoring of proteins in Gram-positive bacteria.* Biochim Biophys Acta, 2014. **1843**(8): p. 1687-97.
100. Meredith, T.C., et al., *Harnessing the power of transposon mutagenesis for antibacterial target identification and evaluation.* Mob Genet Elements, 2012. **2**(4): p. 171-178.
101. Nakao, A., S. Imai, and T. Takano, *Transposon-mediated insertional mutagenesis of the D-alanyl-lipoteichoic acid (dlt) operon raises methicillin resistance in Staphylococcus aureus.* Res Microbiol, 2000. **151**(10): p. 823-9.
102. Pasquina, L., et al., *A synthetic lethal approach for compound and target identification in Staphylococcus aureus.* Nat Chem Biol, 2016. **12**(1): p. 40-5.
103. Komatsuzawa, H., et al., *Cloning and characterization of the fmt gene which affects the methicillin resistance level and autolysis in the presence of triton X-100 in methicillin-resistant Staphylococcus aureus.* Antimicrob Agents Chemother, 1997. **41**(11): p. 2355-61.
104. Rahman, M.M., et al., *The Staphylococcus aureus Methicillin Resistance Factor FmtA Is a d-Amino Esterase That Acts on Teichoic Acids.* mBio, 2016. **7**(1): p. e02070-15.
105. Brown, S., et al., *Methicillin resistance in Staphylococcus aureus requires glycosylated wall teichoic acids.* Proc Natl Acad Sci U S A, 2012. **109**(46): p. 18909-14.
106. Rajagopal, M., et al., *Multidrug Intrinsic Resistance Factors in Staphylococcus aureus Identified by Profiling Fitness within High-Diversity Transposon Libraries.* mBio, 2016. **7**(4).
107. Gallagher, L.A., et al., *Impaired Alanine Transport or Exposure to d-Cycloserine Increases the Susceptibility of MRSA to beta-lactam Antibiotics.* J Infect Dis, 2020. **221**(6): p. 1000-1016.
108. Samson, J.E., et al., *Revenge of the phages: defeating bacterial defences.* Nat Rev Microbiol, 2013. **11**(10): p. 675-87.
109. Depardieu, F., et al., *A Eukaryotic-like Serine/Threonine Kinase Protects Staphylococci against Phages.* Cell Host Microbe, 2016. **20**(4): p. 471-481.

110. Labrie, S.J., J.E. Samson, and S. Moineau, *Bacteriophage resistance mechanisms.* Nat Rev Microbiol, 2010. **8**(5): p. 317-27.
111. Hampton, H.G., B.N.J. Watson, and P.C. Fineran, *The arms race between bacteria and their phage foes.* Nature, 2020. **577**(7790): p. 327-336.
112. Makarova, K.S., et al., *Evolutionary classification of CRISPR-Cas systems: a burst of class 2 and derived variants.* Nat Rev Microbiol, 2020. **18**(2): p. 67-83.
113. Jansen, R., et al., *Identification of genes that are associated with DNA repeats in prokaryotes.* Mol Microbiol, 2002. **43**(6): p. 1565-75.
114. Ishino, Y., et al., *Nucleotide sequence of the iap gene, responsible for alkaline phosphatase isozyme conversion in Escherichia coli, and identification of the gene product.* J Bacteriol, 1987. **169**(12): p. 5429-33.
115. Bolotin, A., et al., *Clustered regularly interspaced short palindrome repeats (CRISPRs) have spacers of extrachromosomal origin.* Microbiology (Reading), 2005. **151**(Pt 8): p. 2551-2561.
116. Mojica, F.J., et al., *Intervening sequences of regularly spaced prokaryotic repeats derive from foreign genetic elements.* J Mol Evol, 2005. **60**(2): p. 174-82.
117. Barrangou, R., et al., *CRISPR provides acquired resistance against viruses in prokaryotes.* Science, 2007. **315**(5819): p. 1709-12.
118. Hille, F., et al., *The Biology of CRISPR-Cas: Backward and Forward.* Cell, 2018. **172**(6): p. 1239-1259.
119. Pyenson, N.C. and L.A. Marraffini, *Type III CRISPR-Cas systems: when DNA cleavage just isn't enough.* Curr Opin Microbiol, 2017. **37**: p. 150-154.
120. Cao, L., et al., *Identification and functional study of type III-A CRISPR-Cas systems in clinical isolates of Staphylococcus aureus.* Int J Med Microbiol, 2016. **306**(8): p. 686-696.
121. Li, Q., et al., *Characterization of CRISPR-Cas system in clinical Staphylococcus epidermidis strains revealed its potential association with bacterial infection sites.* Microbiol Res, 2016. **193**: p. 103-110.
122. Carte, J., et al., *Cas6 is an endoribonuclease that generates guide RNAs for invader defense in prokaryotes.* Genes Dev, 2008. **22**(24): p. 3489-96.
123. Hatoum-Aslan, A., I. Maniv, and L.A. Marraffini, *Mature clustered, regularly interspaced, short palindromic repeats RNA (crRNA) length is measured by a ruler mechanism anchored at the precursor processing site.* Proc Natl Acad Sci U S A, 2011. **108**(52): p. 21218-22.
124. Niewoehner, O., et al., *Type III CRISPR-Cas systems produce cyclic oligoadenylate second messengers.* Nature, 2017. **548**(7669): p. 543-548.
125. Samai, P., et al., *Co-transcriptional DNA and RNA Cleavage during Type III CRISPR-Cas Immunity.* Cell, 2015. **161**(5): p. 1164-1174.
126. Makarova, K.S., et al., *Defense islands in bacterial and archaeal genomes and prediction of novel defense systems.* J Bacteriol, 2011. **193**(21): p. 6039-56.
127. Nunez, J.K., et al., *Cas1-Cas2 complex formation mediates spacer acquisition during CRISPR-Cas adaptive immunity.* Nat Struct Mol Biol, 2014. **21**(6): p. 528-34.
128. Wang, J., et al., *Structural and Mechanistic Basis of PAM-Dependent Spacer Acquisition in CRISPR-Cas Systems.* Cell, 2015. **163**(4): p. 840-53.
129. Marraffini, L.A. and E.J. Sontheimer, *Self versus non-self discrimination during CRISPR RNA-directed immunity.* Nature, 2010. **463**(7280): p. 568-71.
130. Jia, N., et al., *Type III-A CRISPR-Cas Csm Complexes: Assembly, Periodic RNA Cleavage, DNase Activity Regulation, and Autoimmunity.* Mol Cell, 2019. **73**(2): p. 264-277 e5.
131. McGinn, J. and L.A. Marraffini, *CRISPR-Cas Systems Optimize Their Immune Response by Specifying the Site of Spacer Integration.* Mol Cell, 2016. **64**(3): p. 616-623.
132. Koonin, E.V., K.S. Makarova, and F. Zhang, *Diversity, classification and evolution of CRISPR-Cas systems.* Curr Opin Microbiol, 2017. **37**: p. 67-78.
133. Wei, Y., R.M. Terns, and M.P. Terns, *Cas9 function and host genome sampling in Type II-A CRISPR-Cas adaptation.* Genes Dev, 2015. **29**(4): p. 356-61.

134. Pyenson, N.C., et al., *Broad Targeting Specificity during Bacterial Type III CRISPR-Cas Immunity Constrains Viral Escape.* Cell Host Microbe, 2017. **22**(3): p. 343-353 e3.
135. Hatoum-Aslan, A., et al., *Genetic characterization of antiplasmid immunity through a type III-A CRISPR-Cas system.* J Bacteriol, 2014. **196**(2): p. 310-7.
136. Golding, G.R., et al., *Livestock-associated methicillin-resistant Staphylococcus aureus sequence type 398 in humans, Canada.* Emerg Infect Dis, 2010. **16**(4): p. 587-94.
137. Sieber, R.N., et al., *Complete Genome Sequences of Methicillin-Resistant Staphylococcus aureus Strains 110900 and 128254, Two Representatives of the CRISPR-Cas-Carrying Sequence Type 630/spa Type t4549 Lineage.* Microbiol Resour Announc, 2020. **9**(41).
138. Larsen, J., et al., *Staphylococcus aureus CC395 harbours a novel composite staphylococcal cassette chromosome mec element.* J Antimicrob Chemother, 2017. **72**(4): p. 1002-1005.
139. Bebel, A., et al., *A novel DNA primase-helicase pair encoded by SCCmec elements.* Elife, 2020. **9**.
140. Mir-Sanchis, I., et al., *Staphylococcal SCCmec elements encode an active MCM-like helicase and thus may be replicative.* Nat Struct Mol Biol, 2016. **23**(10): p. 891-898.
141. Wisplinghoff, H., et al., *Related clones containing SCCmec type IV predominate among clinically significant Staphylococcus epidermidis isolates.* Antimicrob Agents Chemother, 2003. **47**(11): p. 3574-9.

Manuscript 1:

Correlating susceptibility to genomes: Search for “non-obvious” resistance genes by pan-GWAS analysis of 100 Danish MRSA isolates

Author list:

Kasper Mikkelsen[1], Sharmin Baig[2], Paal Skytt Andersen[1,2], Hanne Ingmer[1]

* These authors contributed equally to this work

1. Department of Veterinary and Animal Sciences, University of Copenhagen, Denmark
2. Department of Bacteria, Parasites and Fungi, Statens Serum Institut, Copenhagen, Denmark

Author contributions

SJB assembled and annotated the genomes and prepared a genome matrix file using roary. KM did the scoary analysis, lab experiments, and wrote the manuscript. PSA and HI provided invaluable guidance.

Abstract

Even though carrying the identical resistance genes, MRSA clinical isolates can vary quite significantly in susceptibility. In this study, we analyzed the genome profiles of 100 MRSA strains and matched them with susceptibility data against eight different antimicrobial agents using the pan-GWAS software, scoary. We confirmed the high influence of already known resistance genes in relation to kanamycin and erythromycin resistance. We were as well able to confirm mutations that lead to alterations in the gyrase and topoisomerase IV proteins as necessary for norfloxacin resistance. The analysis of genomic profiles in relation to β-lactam antimicrobials lead to hits in the J1 region of the staphylococcal chromosome cassette *mec* type IVh, prophage-associated genes, and the *sraP* gene. Deletion of the J1 region did not alter β-lactam susceptibility, whereas lysogens carrying the MRSA phages showed slight changes in β-lactam susceptibility. Testing of vancomycin, daptomycin and linezolid did not reveal any obvious hits. This study confirm previously known resistance mechanisms, while prediction of non-obvious resistance genes from genomic data seem more difficult.

Introduction

Staphylococcus aureus has been susceptible to any antibiotic ever developed [1]. However, *S. aureus* is constantly adapting and via uptake of mobile genetic elements and acquisitions of chromosomal mutations, it has evolved into a feared, multidrug resistant pathogen [2, 3]. Antibiotic resistance arise by several mechanisms that include reduced drug affinity, enzymatic drug inactivation, drug extrusion, and decreased drug accessibility [4]. These resistance mechanisms can be transferred between strains by mobile genetic elements such as plasmids, transposons, bacteriophages, *S. aureus* pathogenicity islands (SaPIs) and staphylococcal chromosome cassettes (SCCs) [5].

There are multiple classes of drugs that target different parts or pathways of the *S. aureus* cell. The primary target used to kill *S. aureus* is the cell envelope. This is the target of both β-lactam antimicrobials and vancomycin, the preferred drugs for treatment of methicillin-sensitive (MSSA) and methicillin-resistant *S. aureus* (MRSA) infections, respectively [6]. The defining feature of MRSA is the presence of the staphylococcal cassette chromosome *mec* (SCC*mec*), which carries the *mecA* gene encoding PBP2a, a low β-lactam affinity penicillin-binding protein [7]. A number of alternatives to vancomycin exist for the treatment of invasive MRSA infections. Linezolid is bacteriostatic but has proven effective against pneumonia and osteomyelitis, whereas daptomycin has been used for treating bloodstream infections and right-sided endocarditis [6]. Linezolid inhibits the initiation of bacterial protein synthesis [8], and daptomycin interacts with the membrane component phosphatidylglycerol and the cell envelope precursor, lipid II, resulting in membrane leakage [9]. A new agent is the fifth generation cephalosporin ceftaroline that is able to inhibit the methicillin-resistance determinant, PBP2a [10].

Multilocus sequence typing (MLST), based on sequences of seven housekeeping genes of *S. aureus* that enables grouping of isolates into sequence types (STs) and clonal complexes (CCs), has made it possible to study the evolution of *S. aureus* [1]. However, the introduction of whole genome sequencing (WGS) as a new typing method of bacterial infections, provides an immense amount of additional useful information that allow researchers to carefully monitor an ongoing outbreak, and provide initial predictions of resistance and virulence patterns, applicable to assist in treatment measures [11].

The search for the presence of known resistance genes in *S. aureus* isolates can e.g. be done using the ResFinder and PointFinder platforms [12]. However, isolates with identical resistance gene profiles can vary quite drastically in minimum inhibitory concentrations (MICs), why supportive resistance mechanisms must be hiding within their genomes. Genome-wide association studies (GWAS) have gained attention to associate single nucleotide polymorphisms (SNPs) to a specific phenotype [13]. GWAS approaches can as well be used to associate genes to a specific phenotype, which is applicable when studying pan-genomes, which is defined as the complete genetic content in a set of genomes of the same species [14]. Scoary is a gene-scoring program that perform pan-genome GWAS using a genome matrix file, created via the pan-genome construction software roary [15], and a trait file to associate a given phenotype (e.g. susceptibility data) with genes of the pan-genome [16].

In this study, we used scoary to perform pan-GWAS analysis on WGS data from 100 MRSA isolates across multiple CCs, to search for possible acquired “non-obvious” resistance genes that support known resistance mechanisms and assist to protect the cell from antimicrobials.

Results

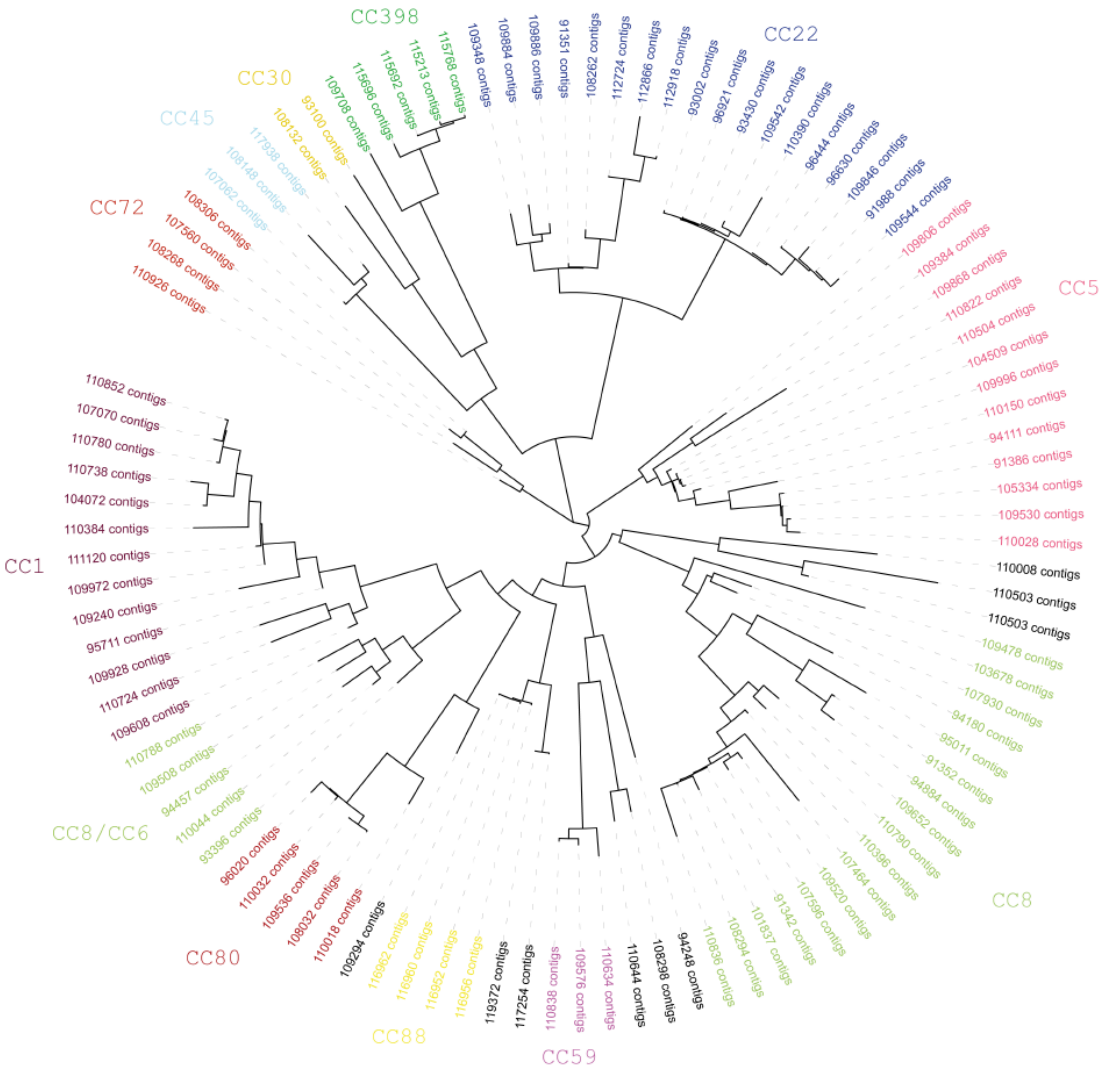

Figure 1. Phylogenetic tree based of 100 MRSA isolates included in the analysis. *Isolates are colored based on clonal complex (CC), and include the most common CCs (5, 8, 22, 30 and 45) of MRSA isolates.*

To search for genes that support resistance in MRSA isolates, we selected 100 whole genome sequenced strains with origins ranging from animal or human clinical infections to nasal colonizers of healthy individuals. We selected strains to represent a wide panel of CC types and include both resistant and susceptible isolates to various drug types from an initial standard susceptibility screen (Figure 1). We performed susceptibility testing on individual strains against eight antimicrobial agents of different classes and with different targets (Table 1).

Table 1. *List of antimicrobial agents used in this study and their respective targets. Isolates above the EUCAST clinical MIC breakpoints (BP) 2021 [17] are noted as resistant (R) above the given value.*

Agent	Class	General target	Specific target	EUCAST MIC BP R > [ug/ml]
Penicillin G	β-lactam	Cell wall	PBP1, PBP2 and PBP3 [18]	0.125
Ceftaroline	5th Cephalosporin	Cell wall	PBPs including PBP2a [10]	1
Vancomycin	Glycopeptide	Cell wall	D-Ala-D-Ala of peptidoglycan stem peptide[19]	2
Daptomycin	Lipopeptide	Cell membrane	Phosphatidylglycerol and Lipid II [9]	1
Kanamycin	Aminoglycoside	Protein synthesis	30S ribosomal subunit, Recognition site distortion [20]	8
Erythromycin	Macrolide	Protein synthesis	50S ribosomal subunit, Peptide elongation [21]	2
Linezolid	Oxazolidinone	Protein synthesis	50 S ribosomal subunit, Peptide initiation [8]	4
Norfloxacin	Fluoroquinolone	DNA Replication	DNA gyrase, topoisomerase IV [22]	1

The MIC profiles varied between the different types of antimicrobials with isolates being either highly resistant or susceptible against kanamycin, erythromycin and norfloxacin, which could indicate that a single gene or gene cluster on an easily transferable mobile genetic element (MGE) could be responsible (Figure 2). No isolates had MICs above the European Committee on Antimicrobial Susceptibility Testing (EUCAST) clinical breakpoint (BP) for vancomycin and daptomycin, while only a few isolates were resistant against linezolid and ceftaroline. Three MRSA isolates were susceptible to penicillin G, none of which carried the *blaZ* β-lactamase gene. Despite classified as resistant, the remaining 97 MRSAs showed a great variety in levels of resistance against penicillin G, which point to additional factors besides *mecA* and *blaZ* as important to drive high β-lactam resistance.

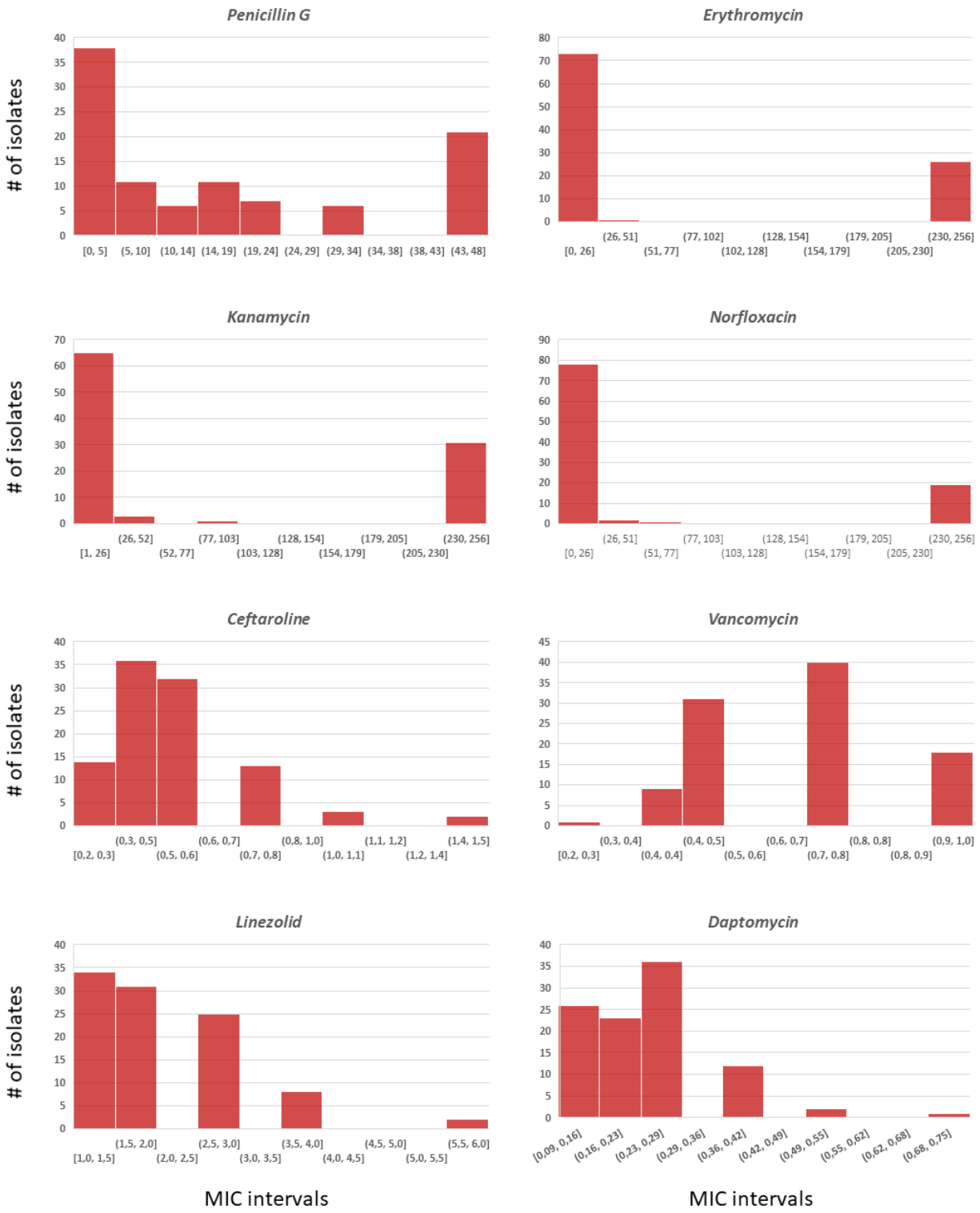

Figure 2. *Histograms of MIC values of the 100 MRSA isolates against 8 different antibiotics.*

Kanamycin, erythromycin and norfloxacin are dependent on known resistance genes or chromosomal mutations. To see if we could correlate specific genes with a high or low resistance profile, we used scoary; a pan-GWAS software package able to relate a genomic

matrix with phenotype data on gene presence/absence level [16]. For kanamycin we found hits to four previously described aminoglycoside resistance genes *aphA*, *wecD*, *aadk* and *aacA-aphD* (Table 2), able to explain the resistance profiles seen in the MRSA isolates. This serves as a nice verification of the scoary method. Likewise, the scoary output for erythromycin showed top hits to ermC' and hypothetical protein group_1726 (Table 2). Group_1726 is found on the same plasmid as ermC' why this shows up as a top hit. Looking down the list another erm resistance gene showed up and was present in high erythromycin resistance isolates not carrying ermC'. ResFinder found resistance genes that could explain the resistance patterns for the remainder of the resistant isolates. No significant hits were found for norfloxacin, which correlates with the described resistance mechanisms as being related to mutations of the genes encoding DNA gyrase and topoisomerase IV [22]. We tested this and confirmed that this was indeed the case (data not shown).

Table 2. Scoary hits for kanamycin and erythromycin. *Pos/neg and present/absent represent number of MRSA isolates with MIC values above (positive) or below (negative) the cutoff value with the gene present or absent.*

Gene	Annotation	pos present	neg present	pos absent	neg absent
	Kanamycin (cutoff: >8 µg/ml)				
aadK	Aminoglycoside 6-adenylyltransferase	15	0	21	64
aacA-aphD	Bifunctional AAC/APH	11	0	25	64
aphA	Aminoglycoside 3'-phosphotransferase	27	1	9	63
wecD	dTDP-fucosamine acetyltransferase	27	1	9	63
	Erythromycin (cutoff: >8 µg/ml)				
ermC'	rRNA adenine N-6-methyltransferase	19	7	15	59
group_1726	hypothetical protein	19	8	15	58
erm	rRNA adenine N-6-methyltransferase	5	0	29	66

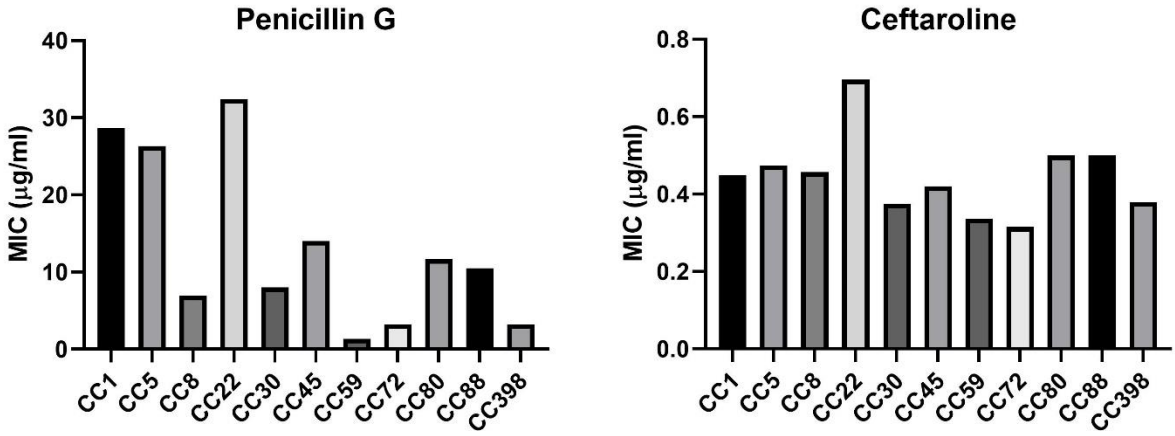

Figure 3. Mean β-lactam MIC levels of different clonal complexes (CCs) among the MRSA *isolates. Some penicillin G ETEST strips had a maximum of 32 µg/ml, why all isolates with a MIC >32 µg/ml was set to 48 µg/ml (the next detectable value on other ETEST strips).*

Clonal complex 22 show a high level of β-lactam tolerance. Isolates of CC22 had the highest mean MIC of the different MRSA clonal complexes against Penicillin G and ceftaroline (Figure 3). When running scoary, the top hits encoded hypothetical proteins and SraP, and overlapped for both Penicillin G and ceftaroline. Five of these hypothetical protein open reading frames were located adjacently in the joining region (J region) 1 of the SCC*mec* type IVh. We deleted all five genes from the chromosome of two of the CC22 MRSA isolates and did disk diffusion assays of six different β-lactam antimicrobials. Yet, we were unable to detect any differences in clearing zones against any of the six antimicrobials between the mutants and the wild type strains (data not shown).

Additional hits to hypothetical protein open reading frames were located within prophage sequences. We made phage lysates of multiple CC22 isolates and lysogenized them into the RN4220 MSSA lab strain, which is cured of any inherent prophages. Three CC22 lysates succeeded to infect and integrate into the RN4220 chromosome, and these lysogens were tested against three different β-lactam antibiotics using E-tests. We noted a 4-fold increase in MIC of one lysogen strain against cefotaxime and 2-fold increase against oxacillin. However, it is unclear whether this is due to phage integrations or possible alterations of the cell surface during attachment of the phage particle. We did not examine correlation of the *sraP* gene with β-lactam resistance. Analysis of vancomycin, linezolid and daptomycin did not yield

obvious hits of interest, which might be ascribed the lack of high MIC isolates against these drugs.

Table 3. Scoary hits for ceftaroline with cutoff set to ≥0.75 µg/ml. *Descriptions as in table 2.*

Gene	Annotation	pos present	neg present	pos absent	neg absent
		Ceftaroline (cutoff: ≥0.75 µg/ml)			
group_1197	SCCmecIVh hypothetical protein	9	1	7	83
group_1917	SCCmecIVh hypothetical protein	9	1	7	83
group_2852	Phage hypothetical protein	9	1	7	83
group_2853	SCCmecIVh hypothetical protein	9	1	7	83
group_2854	Phage hypothetical protein	9	1	7	83
group_2856	SCCmecIVh hypothetical protein	9	1	7	83
group_2861	SCCmecIVh hypothetical protein	9	1	7	83
group_1918	Serine-rich surface protein *sraP*	8	0	8	84

Discussion

The European committee on antimicrobial susceptibility testing (EUCAST) have put forward guidelines and breakpoint values for antimicrobials to decide whether isolates are resistant or susceptible. Isolates crossing these breakpoints are often carrying resistance genes. However, for some antimicrobials there are great varieties in the level of resistance between isolates, in spite carrying identical sets of resistance genes or mutations. The key to this variance might lie within the accessory genome of these isolates, which accounts for around 25 % of the *S. aureus* genome [23], where horizontally acquired non-resistance genes might assist a resistant isolate to withstand even higher concentrations of a certain drug.

Susceptibility testing of 100 MRSA isolates against kanamycin, erythromycin and norfloxacin showed that some isolates carry a very high resistance level, which would necessitate the use of other drugs in case of an infection with any of these isolates. We saw a high variability of penicillin G MICs between the isolates (Figure 2). This is probably a consequence of the high selection pressure due to the popularity of β-lactam antimicrobials for the treatment of both gram-positive and gram-negative infections [24]. Two isolates was above the EUCAST

breakpoint value against the other β-lactam included in this study, ceftaroline. This could be of concern as ceftaroline is used as a salvage therapy in case of vancomycin or daptomycin treatment failure [6]. None of the isolates were though resistant to neither vancomycin nor daptomycin.

As was anticipated judging by the binary nature of the MIC histograms (Figure 2), kanamycin and erythromycin resistance is highly dependent on presence of a single resistance gene, typically located on plasmids or transposons, able to inactivate the drug [20, 21], whereas norfloxacin resistance is due to single point mutations in the target of the drug [22].

The bacterial fight against β-lactam antimicrobials seem to be influenced by several factors. We here investigated the influence of genes present in the J1 region of the SCC*mec* type IVh and the contribution of lysogenized phages to increase β-lactam resistance levels, though, with limited success. The J1 region as a hit in this analysis might be a hit to the entire SCC*mec* type IVh, which could provide an additional protection against β-lactam antimicrobials than other SCC types.

That phage integration into the bacterial chromosome can be beneficial is well-known [25], and the thought of phages contributing to bacterial proliferation during β-lactam stress in intriguing. However, the slight increases we saw from one of the lysogens could either be contributions from the phage genome, or mutations leading to changes in the bacterial cell surface pushed by the phage adherence process. As all the hits presented in Table 3 are present in the same high-level β-lactam resistant isolates, it is plausible that the SCC*mec* type IVh provides the resistance phenotype, whereas prophages and SraP increase virulence to equip the CC22s with good odds of establishing an infection.

Acknowledgements

HI was supported by grants from Danmarks Fri Forskningsfond (7017-00079B).

Materials and methods

Bacterial strains and antimicrobial agents. The 100 MRSA isolates were acquired from, and sequenced at, Statens Serum Institut (SSI) by paired-end sequencing using the NextSeq 550 system (Illumina). ETEST strips were acquired from BIOMÉRIEUX, whereas antimicrobial discs and chloramphenicol, anhydrotetracycline, and mitomycin C were from Merck KGaA.

Genome matrix preparation. Assembled genomes were annotated using Prokka [26] and run through Roary [15] that extracts protein sequences from open reading frames and provides a matrix output of gene presence/absence from all MRSA isolates.

Susceptibility testing. For the initial susceptibility testing of eight different antibiotics against the 100 MRSA isolates, we applied ETESTs to a lawn of McFarland 0.5 adjusted bacterial suspensions in saline water and inspected the MIC value after 24 hours of growth at 37 °C. Subsequent susceptibility testing was done on bacterial lawns with antibiotic discs or ETESTs when noted.

Scoary analysis. Trait files were constructed in excel, where isolates were assigned '1' for resistant and '0' for susceptible according to the results of susceptibility testings. Scoary was run by supplying the genome matix file and trait file. This was done for multiple breakpoint values across the eight tested antimicrobials to assess the best output.

Chromosomal deletion of the SCC*mec* IVh J1 region. 1000 bp upstream and downstream sequences were amplified, subsequently fused by overlap extension PCR, and sub-cloned into the temperature-sensitive shuttle vector pBASE6 using SacI/BglII restriction sites. The resulting plasmid was purified from *E. coli* IM08B [27] and transformed into CC22 strains 96444 and 110390 at 30°C followed by chromosomal integration by plating on tryptic soy agar (TSA, Merck KGaA) (10 µg/ml chloramphenicol) at 44°C overnight. Plasmids were crossed-out by passage at 30°C followed by plating on TSA (500 ng/ml anhydrotetracycline), and successful allelic exchange was done by sequencing across the deleted area.

Lysogenization of MRSA prophages into RN4220. Prophage excision of CC22 MRSA cultures was induced by mitomycin C (1 µg/ml) and grown at 30°C until cultures were evident. Lysates were spotted on RN4220 recipient lawns and grown at 30°C overnight. Bacterial lysogens

appearing within the spotted area and phage integration was confirmed by multiplex PCR for the presence of phage integrase genes.

References

1. Chambers, H.F. and F.R. Deleo, *Waves of resistance: Staphylococcus aureus in the antibiotic era.* Nat Rev Microbiol, 2009. **7**(9): p. 629-41.
2. Aryee, A. and J.D. Edgeworth, *Carriage, Clinical Microbiology and Transmission of Staphylococcus aureus.* Curr Top Microbiol Immunol, 2017. **409**: p. 1-19.
3. Lowy, F.D., *Antimicrobial resistance: the example of Staphylococcus aureus.* J Clin Invest, 2003. **111**(9): p. 1265-73.
4. Vestergaard, M., D. Frees, and H. Ingmer, *Antibiotic Resistance and the MRSA Problem.* Microbiol Spectr, 2019. **7**(2).
5. Haaber, J., J.R. Penades, and H. Ingmer, *Transfer of Antibiotic Resistance in Staphylococcus aureus.* Trends Microbiol, 2017. **25**(11): p. 893-905.
6. David, M.Z. and R.S. Daum, *Treatment of Staphylococcus aureus Infections.* Curr Top Microbiol Immunol, 2017. **409**: p. 325-383.
7. International Working Group on the Classification of Staphylococcal Cassette Chromosome, E., *Classification of staphylococcal cassette chromosome mec (SCCmec): guidelines for reporting novel SCCmec elements.* Antimicrob Agents Chemother, 2009. **53**(12): p. 4961-7.
8. Swaney, S.M., et al., *The oxazolidinone linezolid inhibits initiation of protein synthesis in bacteria.* Antimicrob Agents Chemother, 1998. **42**(12): p. 3251-5.
9. Grein, F., et al., *Ca(2+)-Daptomycin targets cell wall biosynthesis by forming a tripartite complex with undecaprenyl-coupled intermediates and membrane lipids.* Nat Commun, 2020. **11**(1): p. 1455.
10. Saravolatz, L.D., G.E. Stein, and L.B. Johnson, *Ceftaroline: a novel cephalosporin with activity against methicillin-resistant Staphylococcus aureus.* Clin Infect Dis, 2011. **52**(9): p. 1156-63.
11. Price, J., et al., *The usefulness of whole genome sequencing in the management of Staphylococcus aureus infections.* Clin Microbiol Infect, 2013. **19**(9): p. 784-9.
12. Bortolaia, V., et al., *ResFinder 4.0 for predictions of phenotypes from genotypes.* J Antimicrob Chemother, 2020. **75**(12): p. 3491-3500.
13. Laabei, M., et al., *Predicting the virulence of MRSA from its genome sequence.* Genome Res, 2014. **24**(5): p. 839-49.
14. Sherman, R.M. and S.L. Salzberg, *Pan-genomics in the human genome era.* Nat Rev Genet, 2020. **21**(4): p. 243-254.
15. Page, A.J., et al., *Roary: rapid large-scale prokaryote pan genome analysis.* Bioinformatics, 2015. **31**(22): p. 3691-3.
16. Brynildsrud, O., et al., *Rapid scoring of genes in microbial pan-genome-wide association studies with Scoary.* Genome Biol, 2016. **17**(1): p. 238.
17. EUCAST, *The European Committee on Antimicrobial Susceptibility Testing. Breakpoint tables for interpretation of MICs and zone diameters.* 2021.
18. Fontana, R., et al., *The final goal: penicillin-binding proteins and the target of cephalosporins.* Clin Microbiol Infect, 2000. **6 Suppl 3**: p. 34-40.
19. Reynolds, P.E., *Structure, biochemistry and mechanism of action of glycopeptide antibiotics.* Eur J Clin Microbiol Infect Dis, 1989. **8**(11): p. 943-50.
20. Magnet, S. and J.S. Blanchard, *Molecular insights into aminoglycoside action and resistance.* Chem Rev, 2005. **105**(2): p. 477-98.

21. Gaynor, M. and A.S. Mankin, *Macrolide antibiotics: binding site, mechanism of action, resistance.* Curr Top Med Chem, 2003. **3**(9): p. 949-61.
22. Blondeau, J.M., *Fluoroquinolones: mechanism of action, classification, and development of resistance.* Surv Ophthalmol, 2004. **49 Suppl 2**: p. S73-8.
23. Lindsay, J.A. and M.T. Holden, *Staphylococcus aureus: superbug, super genome?* Trends Microbiol, 2004. **12**(8): p. 378-85.
24. Llarrull, L.I., et al., *The future of the beta-lactams.* Curr Opin Microbiol, 2010. **13**(5): p. 551-7.
25. Bondy-Denomy, J. and A.R. Davidson, *When a virus is not a parasite: the beneficial effects of prophages on bacterial fitness.* J Microbiol, 2014. **52**(3): p. 235-42.
26. Seemann, T., *Prokka: rapid prokaryotic genome annotation.* Bioinformatics, 2014. **30**(14): p. 2068-9.
27. Monk, I.R., et al., *Complete Bypass of Restriction Systems for Major Staphylococcus aureus Lineages.* mBio, 2015. **6**(3): p. e00308-15.

Manuscript 2:

The Novel Membrane-Associated Auxiliary Factors AuxA and AuxB Modulate β-lactam Resistance in MRSA by stabilizing Lipoteichoic Acids

Kasper Mikkelsen[1]*, Wanchat Sirisarn[2]*, Ohood Alharbi[2], Mohanned Alharbi[2], Huayong Liu[2], Katrine Nøhr-Meldgaard[1], Katharina Mayer[3], Martin Vestergaard[1], Laura M. Gallagher[4], Jeremy P. Derrick[2], Andrew J McBain[5], Jacob Biboy[6], Waldemar Vollmer[6], James P. O'Gara[4], Tom Grunert[3], Hanne Ingmer[1]• and Guoqing Xia[2]•

1. Department of Veterinary and Animal Sciences, University of Copenhagen, Denmark

2. Lydia Becker Institute of Immunology and Inflammation, Division of Infection, Immunity and Respiratory Medicine, School of Biological Sciences, Faculty of Biology, Medicine and Health, University of Manchester, Manchester Academic Health Science Centre, Manchester, M13 9PT, United Kingdom

3. Functional Microbiology, Institute of Microbiology, Department of Pathobiology, University of Veterinary Medicine, Vienna, Austria

4. Department of Microbiology, School of Natural Sciences, National University of Ireland Galway, Galway, Ireland

5. Division of Pharmacy and Optometry, Faculty of Biology, Medicine and Health, The University of Manchester, Manchester, M13 9PT, United Kingdom

6. Centre for Bacterial Cell Biology, NU Biosciences Institute, Newcastle University, Newcastle upon Tyne, NE2 4AX, United Kingdom

(*) Equal contribution (•) correspondence to: guoqing.xia@manchester.ac.uk or hi@sund.ku.dk

Author contributions

WS, OA, MA, PD & HL did susceptibility testing of β-lactam antibiotics, transferred transposon insertions into other strain backgrounds and created deletion mutation. KM & KNM did susceptibility testing of non-β-lactam antibiotics. KM and MV did suppressor mutations and analysis. KM did all western blot analysis and triton X-100 assay. OA did *Galleria mellonella* assay. Peptidoglycan analysis was done by KM, JB, WV and DV (acknowledgements) and TG and KM did WTA analysis. KM, WS, MV, GX and HI wrote the manuscript with discussion and comments from all authors.

This manuscript was submitted to the International Journal of Antimicrobial Agents on Oct 30, 2020 and a revised version was accepted for publication on Jan 14, 2021.

Abstract

A major determinant of β-lactam resistance in methicillin-resistant *Staphylococcus aureus* (MRSA) is the drug insensitive transpeptidase, PBP2a, encoded by *mecA*. However, full expression of the resistance phenotype requires auxiliary factors. We identified two such factors, auxiliary factor A (*auxA*, *SAUSA300_0980*) and B (*auxB*, *SAUSA300_1003*) in a screen against mutants with increased susceptibility to β-lactams in the MRSA strain JE2. *auxA* and *auxB* encode transmembrane proteins, with AuxA predicted to be a transporter. Inactivation of *auxA* or *auxB* enhanced β-lactam susceptibility in community-, hospital- and livestock associated MRSA strains without affecting PBP2a expression, peptidoglycan cross-linking or wall teichoic acid synthesis. Both mutants displayed increased susceptibility to inhibitors of lipoteichoic acid synthesis (LTA) and alanylation pathways, and released LTA even in the absence of β-lactams. The β-lactam susceptibility of the *aux* mutants was suppressed by mutations inactivating *gdpP*, which was previously found to allow growth of mutants lacking the lipoteichoic synthase enzyme, LtaS. Using the *Galleria mellonella* infection model, we observed enhanced survival of larvae inoculated with either *auxA* or *auxB* mutants compared to the wild type strain following treatment with amoxicillin. Collectively, our results indicate that AuxA and AuxB are central for LTA stability and potential inhibitors can be an efficient tool to re-sensitize MRSA strains to β-lactams and combat MRSA infections.

Introduction

Staphylococcus aureus is a leading cause of bacterial infections, ranging from mild skin to life-threatening infections. One major class of antibiotics used to treat *S. aureus* infections are the β-lactams, which target penicillin-binding proteins and inhibit the transpeptidation step in peptidoglycan biosynthesis. Since the introduction of penicillin in the early 1940s, *S. aureus* has acquired mechanisms to overcome the bactericidal activity of β-lactam antibiotics. The acquisition of the *bla*Z gene by *S. aureus*, which encodes a penicillinase able to inactivate β-lactams, left these drugs ineffective [1]. New generations of penicillinase-resistant β-lactams (e.g. oxacillin and methicillin) restored the bactericidal effect, but the benefits were neutralized when *S. aureus* acquired the *mecA* gene that encodes PBP2a, a penicillin binding protein with low affinity to β-lactams [2]. Even though the gain of the *mecA* gene has made methicillin-resistant *S. aureus* (MRSA) resistant to almost all β-lactams, they remain an important class of antibiotics, as they have superior efficiency against methicillin-sensitive *S. aureus* (MSSA) infections compared to MRSA standard-of-care drugs (e.g. vancomycin) and are safe to use [3].

One approach suggested to treat MRSA infections has been to target the so-called auxiliary factors that assist PBP2a in conferring β-lactam resistance. Several known auxiliary factors are involved cell wall biogenesis and regulation, for examples, the Fem peptidyltransferases that add a penta-glycine stem to lipid II [4], PBP4 that synthetize peptidoglycan [5], GlcNAc-1-P-transferase TarO that initiates the biogenesis of wall teichoic acid (WTA) [6], the WTA GlcNAc glycosyltransferases TarS and TarP [7], the polymerizing division protein FtsZ [8], and the two-component system VraSR [9]. Mutations or inhibitors of auxiliary factors are synergistic in combination with β-lactams both *in vitro* and *in vivo*, and markedly increase β-lactam susceptibility [10].

Here we screened the Nebraska Transposon Mutant Library for mutants that exhibited increased susceptibility to three classes of β-lactams namely cephalosporins, carbapenems or penicillins. Along with previously identified auxiliary factors, the screens revealed two mutants with transposon (Tn) inserts in either gene *SAUSA300_0980* or *SAUSA300_1003* that both failed to grow in the presence of sub-lethal concentrations of β–lactam antibiotics. Previous studies have found *SAUSA300_0980* and *SAUSA300_1003* mutants to be sensitive to

inhibitors of lipoteichoic acid (LTA) synthesis apparatus [11, 12]. LTA is a phosphoglycerol polymer that is polymerized outside of the cell by the membrane-linked lipoteichoic synthase enzyme LtaS and is attached to the cell membrane via a glycolipid anchor, diglucosyl-diacylglycerol. This anchor is formed by YpfP and flipped across the membrane by LtaA [13]. In addition, LTA is decorated with D-alanine moieties that introduce positive charge to the negatively charged polymer backbone [14]. LTA and the machinery behind its synthesis and modification have amongst others been ascribed roles in cell division [15, 16], cationic antimicrobial peptide resistance [17], β–lactam resistance [16], and autolytic activity regulation [18]. Here, we have named *SAUSA300_0980* and *SAUSA300_1003* as auxiliary factors A (*auxA*) and B (*auxB*), respectively. We report the characterization of these mutants and provide evidence that AuxA and AuxB are suitable *in vivo* targets for the development of β-lactam adjuvants to treat MRSA infections.

Results and discussion

Transposon inactivation of *auxA* and *auxB* decreases β-lactam resistance in MRSA. To identify modulators of β-lactam susceptibility in MRSA, we screened the Nebraska Transposon Mutant Library, which is derived from the community-acquired MRSA strain JE2, for lack of growth on agar plates supplemented with three classes of β-lactams, namely cephalosporins (ceftazidime), carbapenems (meropenem) or penicillins (oxacillin), at concentrations corresponding to half the minimal inhibitory concentration (MIC). We found growth to be compromised by inactivation of genes already described to affect β-lactam susceptibility in *S. aureus*, including *mecA*, *pbpD* encoding PBP4 [5, 19], two-component system member *VraS* [9], and the global regulator *sarA* [20]. Additionally, we identified two genes, *SAUSA300_0980* and *SAUSA300_1003*, which previously had been found in a screen for mutants with increased susceptibility towards clinically relevant antibiotics including β-lactams [21]. We set out to further characterize these mutations and designated the affected genes auxiliary factor A (*auxA*; *SAUSA300_0980*) and B (*auxB*; *SAUSA300_1003*).

When assessing the minimal inhibitory concentration (MIC) of the mutants to representatives of different β-lactam classes we found that the JE2_*auxA::Tn* mutant (henceforth JE2_*auxA*) had an 8- to 256-fold reduction in MIC towards penicillins (oxacillin, amoxicillin and carbenicillin), cephalosporins (cefalotin, cefoxitin, cefuroxime and ceftazidime) and carbapenems (meropenem). Inactivation of *auxB* in JE2_*auxB::Tn* (henceforth JE2_*auxB*) led to a 2- to 16-fold reduction towards β-lactams (Table 1). In contrast, susceptibility to antimicrobials targeting cell membrane and protein or DNA synthesis was unaffected (Table 2). Complementation of the transposon mutants with a vector expressing either the wild type *auxA* or *auxB* partially restored β-lactam MICs (Table 1). The effect of *auxA* and *auxB* on β-lactam susceptibility was further confirmed in deletion mutants (Δ*auxA* and Δ*auxB*) (Table 1).

Upon transduction of the *auxA* and *auxB* mutations into livestock-associated (ST398), hospital-acquired (COL) and community-acquired (MW2) MRSA strains we confirmed that the mutations also led to an increased β-lactam susceptibility in these strain backgrounds. Furthermore, inactivation of *auxA* and *auxB* in strain Newman, a methicillin sensitive *S aureus* strain (MSSA) strain, also resulted in an increased β-lactam sensitivity, albeit to a lesser extent than observed in the MRSA strains (Table 3). This agrees with a previous study, where

inactivation of the same genes reduced oxacillin resistance in the MSSA strain HG003 [21]. Thus, our results suggest that AuxA and AuxB influence β-lactam resistance independently of *mecA* and that their activities are ubiquitous amongst *S. aureus* strains.

Topological and structural prediction of the AuxA and AuxB proteins. BlastN analysis showed that both *auxA* and *auxB* are conserved among *S. aureus* strains, whereas BlastP analysis with AuxA or AuxB as probes failed to identify any homologues of known function. Membrane topology analysis by TMHMM [22] predicted that AuxA contains 10 transmembrane segments with a 94 amino acid intracellular domain between helices 6 and 7, and AuxB contains 3 transmembrane segments and an extracellular 192 amino acid C-terminal domain.

In order to obtain further insight into the AuxA structure, and hence its potential function, we used the I-TASSER structure prediction server, which relies on a multiple template threading approach [23]. I-TASSER identified the closest structure in the PDB database as SecDF from *Thermus thermophilus* (TM-Score: 0.90). SecDF is an accessory factor of the conserved Sec protein translocation machinery and it has been shown in *Escherichia coli* and *Bacillus subtilis* to be involved in the export of proteins [24, 25]. Inactivation of *secDF* in *S. aureus* leads to increased susceptibility towards β-lactams and vancomycin, which was unrelated to the expression of PBP1-4 and PBP2a, but associated with increased autolysis, possibly via increased levels of the autolysin LytM [26, 27]. Using the AuxB protein sequence as a query, we did not find any significant similarities to well-described proteins.

PBP expression, peptidoglycan composition, and wall teichoic acid modifications are not altered in *auxA* and *auxB* mutants. Initially we examined whether the increase in β-lactam susceptibility observed in the *auxA* and *auxB* mutants was influenced by decreased PBP2a expression. We found no differences in the amount of PBP2a in the membrane between WT and mutants, both with and without oxacillin added to the growth medium (Figure1A). Induction of PBP2a expression by oxacillin appears to be strain specific as others have reported a drastic increase under these conditions in the MRSA strain N315 [28]. This confirms the notion that AuxA and AuxB act independently of PBP2a. Furthermore, we saw no differences in PBP1, PBP2 and PBP4 levels when cell membranes were stained with Bocillin, a fluorescent β-lactam (Figure1B), indicating that PBP expression in general is not affected by the *auxA* and *auxB* mutations in exponential phase cultures.

As β-lactams target PBPs involved in cell wall cross-linking and modulation, we addressed if cell wall structure was affected by the inactivation of *auxA* and *auxB*. We found no differences in peptidoglycan (PG) profiles obtained after releasing the muropeptides with cellosyl and separating them on an HPCL column (Figure S1). Likewise, the wall teichoic acid (WTA) glycosylation examined by Fourier-transform infrared (FTIR) spectroscopic molecular fingerprinting [29] was similar to WT in both mutant strains (Figure S2).

Triton X-100-induced autolysis is decreased in *auxA* and *auxB* mutants. During growth the bacterial cell wall undergoes continuous re-modelling that requires a tight coordination between PG synthesizing and degrading enzymes [30, 31]. When treated with Triton X-100, both *auxA* and *auxB* mutants demonstrated less lysis in comparison to the parental JE2 strain (Figure 2A). When grown in the presence of 0.1 µg/ml oxacillin prior to Triton X-100 lysis induction, the mutants showed decreased lysis with profiles resembling mutants lacking either one of two major autolysins, Atl or Sle1, whereas WT cells retained their lysis profile (Figure 2B). Similar lysis profiles have been observed for a *dltA* mutant strain deficient in D-alanylation of teichoic acids [18].

Suppressor mutations in *gdpP* restore β-lactam resistance in *auxA* and *auxB* mutants. To further assess the role of *auxA* and *auxB* in β-lactam susceptibility we challenged mutant strains with cefotaxime 4× MIC and suppressor mutants were selected and genome sequenced. All mutants had mutations in *gdpP*, which encodes a phosphodiesterase capable of degrading c-di-AMP (c-di-AMP). 4/5 mutations truncated the gene to less than a third leaving the protein dysfunctional, while the last mutation is located in the DHH domain, which is essential for phosphodiesterase activity (Table 4) [32].

The connection between mutations in the *gdpP* gene and β-lactam resistance has been shown in laboratory strains [33] and clinical isolates [34]. Phenotypes related to *gdpP* inactivation include increased PG cross-linking (probably due to increased *pbpD* transcription) and a decrease in cell size [32]. GdpP inactivation mutations arise in diverse *mec*-negative MRSA clinical isolates [34] and can compensate for impaired growth in mutants lacking the LTA synthase, LtaS [32].

LTA stability is compromised by *auxA* and *auxB* mutations. Previous studies have found *SAUSA300_0980* (*auxA*) to be essential in the presence of the LtaS inhibitor Congo red [11]

and that both *auxA* and *auxB* are essential in the presence of amsacrine, which inhibits the *dlt* pathway responsible for D-alanylation of LTA [12]. Here we confirmed that the *auxA* and *auxB* mutations significantly reduced the Congo red and amsacrine MICs (Table 2). Further we found that both *auxA* and *auxB* mutants are susceptible to D-cycloserine (Table 2) which inhibits the Alr racemase and Ddl ligase responsible for the conversion of L-alanine to D-alanine and D-ala-D-ala ligation, respectively [35] .

To address how LTA may be compromised we examined LTA size and quantities by Western blot with an antibody recognizing the LTA phosphoglycerol backbone. When analyzing LTA of pellet fractions we saw no differences in either size or quantity between the *aux* mutants and WT (Figure 3A). However, when analyzing the supernatant fractions we saw LTA being released to the medium by both *aux* mutants in presence or absence of sub-MIC oxacillin (0.05 µg/ml) (Figure 3B). This was specific to the *aux* mutants as both the WT strain and a mutant of another auxiliary factor, PBP4 (*pbpD*), did not show a release of LTA into the medium. The size of the bands did not indicate an increased LTA chain length as seen in an *ltaA* mutant that produces high quantities of extended LTA polymers [16, 36]. This indicates that *auxA* and *auxB* are involved in LTA stability rather than LTA synthesis. The released LTA polymers could explain the attenuated lysis profiles (Figure 2), as the negatively charged phosphoglycerol backbone was shown to bind autolysins and reduce autolytic activity [18].

***auxA* and *auxB* are required for amoxicillin resistance in *Galleria mellonella*.** The *Galleria mellonella in vivo* model was used to evaluate β-lactam treatment potential combined with *aux* gene inactivation [37]. After injection of JE2 WT or mutant cultures, survival of infected larvae was monitored over time (Figure 4). While all WT infected larvae died within three days post infection (d.p.i.), 30% of JE2_*auxA*-infected larvae and 10% JE2_*auxB*-infected larvae survived, indicating that the *auxA* and *auxB* mutations lowered virulence levels. This agrees with a recent report of attenuated virulence of JE2_*auxA* in a silkworm and mouse model [38]. Treatment of WT-infected larvae with amoxicillin did not significantly improve survival rates. In contrast, amoxicillin treatment significantly increased the survival rates of larvae infected with the *auxA* and *auxB* mutants from 10% to 60% and 50%, respectively at 7 d.p.i. (Figure 4). These data demonstrate that inactivation of *auxA* and *auxB* improves efficacy of amoxicillin in the treatment of MRSA infections in *Galleria mellonella*.

The role of AuxA and AuxB in LTA stability. The data presented here suggests a role of AuxA and AuxB in stabilizing LTA. The I-TASSER server predicts with high confidence a structural similarity between AuxA and the accessory factor of the Sec translocation pathway, SecDF. Hence, AuxA and AuxB might act together in assisting the Sec pathway or perhaps they could single-handedly transport yet unknown factors across the membrane that could stabilize the LTA polymers (Figure 5A). Alternatively, as the *aux* mutants show increased sensitivity towards β-lactams, amsacrine and Congo red, and suppressor mutations in *gdpP* correlate with mutant phenotypes of the LTA synthesis pathway, AuxA and AuxB could stabilize the LTA polymer directly or via interactions with YpfP, LtaA and/or LtaS (Figure 5B). Our data provide the foundation for further studies aiming to decipher the exact role of these two novel important auxiliary factors in LTA stability and β-lactam resistance.

Acknowledgements

We thank Dr. Daniela Vollmer (Newcastle University) for help with PG isolation. This work was financed by grants from the Ministry of Science and Technology, Thailand to WS; the Ministry of Education, Saudi Arabia to OA and MA; the Austrian Science Fund FWF-P29304-B22 to TG; the Health Research Board Ireland (HRA-POR-2015-1158) to JOG; the UKRI Strategic Priorities Fund (grant no. EP/T002778/1) to WV, Danmarks Fri Forskningsfond (7017-00079B) to KM and HI.

Materials and methods

Bacterial strains and culture conditions. Bacterial strains (Table S1) were cultured in tryptic soy broth (TSB), tryptic soy agar (TSA), and Mueller–Hinton Broth (Thermo Fisher Scientific). Antibiotics (Merck KGaA) used in this study include β-lactams (oxacillin, amoxicillin, carbenicillin, cefalothin, cephradine, cefoxitin, cefuroxime, ceftazidime and meropenem), chloramphenicol, vancomycin, bacitracin, D-cycloserine, tunicamycin, congo red, amsacrine, daptomycin, nisin, gentamicin, ciprofloxacin and erythromycin.

Screening of transposon mutant library. The Nebraska Transposon Mutant Library is stored in glycerol in 96-wells microtiter plates at -80 ^{o}C. Material from the frozen stock was

transferred directly with a Deutz 96 cryo-replicator from the 96 wells microtiter plates onto TSA plates supplemented with 5 µg/ml erythromycin and half the minimal inhibitory concentration (MIC) of ceftazidime, oxacillin or meropenem. The plates were incubated at 37°C for 24 hours and visually inspected for lack of growth of individual mutants.

Construction and complementation of *aux* mutants. To construct *auxA* and *auxB* mutants, the *auxA* and *auxB* transposon mutations were transduced by phage ϕ11 from donor strains JE2_*auxA* and JE2_*auxB* into other *S. aureus* strains, including MW2, COL, ST398 and Newman. Briefly, ϕ11 was propagated with donor strains and ϕ11 lysate with a titre of 10^{11} pfu/ml was incubated with the recipient *S. aureus* strains for 10 minutes before plating on TSA with 2.5 µg/ml of erythromycin. Transductants were then genotyped by PCR with primer pair auxA-for/auxA-rev for the *auxA* mutation or auxB-for/auxB–rev for the *auxB* mutation (Table S2).

To construct marker-less clean deletion mutants, the DNA fragments flanking *auxA* or *auxB* were amplified using primers A5/A3 or B5/B3 (Table S2) and ligated before sub-cloned into the pIMay vector [39]. The resulting knockout vectors were transformed into MRSA JE2 strain and the *auxA* and *auxB* deletion mutants was constructed by allelic exchange following a previously published procedure [39].

To construct *auxA* and *auxB* expression vectors, the open reading frame of both genes were amplified by PCR reactions with Phusion High-Fidelity DNA Polymerase (New England Biolabs) and primer pair, A5/A3 for *auxA* and B5/B3 for *auxB*. The amplicons were sub-cloned into expression vector pRB474 at *BamHI/EcoRI* sites using the infusion cloning kit (Takara Bio Inc.). The recombinant expression vectors were propagated in transition host *E. coli* DC10B cells before being electroporated into *auxA* and *auxB* transposon and deletion mutants. The complemented mutants were selected on TSA containing 10 µg/ml of chloramphenicol.

Antimicrobial susceptibility tests. The broth microdilution method was used to assess the minimum inhibitory concentration (MIC) for β-lactams, nisin, D-cycloserine, congo red, amsacrine and tunicamycin. Briefly, the tested antibiotics were dissolved in Mueller-Hinton Broth (Thermo Fisher Scientific) and serial two-fold dilution of each antibiotic placed into the wells of a 96 well round bottom microtiter plate (Corning). A bacterial culture was adjusted with saline to 0.1 OD_{600} and 5 µl of the bacterial suspension transferred into each well of the

microtiter plate. The plate was incubated at 37°C overnight and the MICs were recorded as the lowest concentration with no growth. MICs for vancomycin, bacitracin, daptomycin, gentamicin and ciprofloxacin were determined using E-tests (bioMérieux) on TSA plates without erythromycin supplementation according to the instruction of the manufacturer.

Raising β-lactam suppressor mutations. To select mutations that would revert the β-lactam sensitive phenotype of JE2_*auxA* and JE2_*auxB*, we grew the strains overnight and plated 50 µl undiluted culture on TSA with 4 µg/ml cefotaxime and incubated at 37 °C for 24 hrs. Three colonies from each plate were re-streaked onto TSB agar with 4 µg/ml cefotaxime and chromosomal DNA from individual colonies were isolated using the DNeasy Blood & Tissue Kit (Qiagen). DNA samples were sent to Statens Serum Institut for paired-end sequencing using the NextSeq 550 system (Illumina). One run failed, leaving 5 sequenced suppressor mutants. Analysis of output reads was performed in CLC Genomics Workbench.

Fourier transform infrared (FTIR) spectroscopic analysis. FTIR spectroscopic measurement and spectral processing were performed as reported previously [29]. In brief, the bacteria were grown on TSA at 30°C for 24 h and the measurement was conducted on a Tensor 27/ HTS-XT microplate adapter FTIR spectrometer (Bruker Optics GmbH). Principal component analysis (PCA) computation at the spectral region for carbohydrates (1200 – 800 cm^{-1}) was based on the NIPALS algorithm and the first and second components were projected for PCA using the software Unscrambler X (CAMO Software).

Western blot analysis of PBP2a. Cultures of JE2 WT, JE2_*auxA* and JE2_*auxB* were diluted to 0.05 OD_{600} and grown to 0.8 OD_{600}. A volume of 20 ml culture was centrifuged at 12000 × g for 5 min and the pellet was re-suspended in 800 µl 50 mM Tris-HCl. Cells were lysed by bead beating (6.0 m/sec, 45 sec, 3 times) using a FastPrep-24 homogenizer (MP Biomedicals, CA, USA) and spun down. The supernatant was centrifuged at 100,000 ×g for one hour and the membrane fraction (pellet) was re-suspended in 50 µl 50 mM Tris-HCl. 13 µl of cell membrane fractions were mixed with reducing agent and sample buffer and loaded onto a NuPAGE Novex 4-12% Bis-Tris protein gel and run for 45 min at 200V and 350A in MOPS running buffer (Thermo Fisher Scientific). Protein was transferred to a PVDF membrane and the WesternBreeze Chemiluminescent Kit (Thermo Fisher Scientific) was applied following the manufacturer's protocol. Protein bands were developed using an anti-PBP2a antibody [1

µg/ml] (Ray Biotech) and human IgG [1 µg/ml] were added to all buffers to block unspecific Protein A binding.

Western Blot analysis of LTA. Overnight cultures of JE2 WT, JE2_*auxA*, JE2_*auxB*, JE2_*ltaA*, and JE2_*pbpD* were diluted to 0.05 OD_{600} and grown for 8 hours in TSB medium with or without 0.05 µg/ml oxacillin and samples were withdrawn for analysis of both pellet and supernatant fractions. For pellet fraction analysis, 100 µl of the bacterial culture was collected by centrifugation and re-suspended in 50 µl lysis buffer (normalized to OD_{600}) containing 50 mM Tris (pH 7.4), 150 mM NaCl, and 200 µg/ml lysostaphin, before being incubated at 37 °C for 10 min. The cells were diluted with one volume of 4x LDS sample buffer (Thermo Fisher Scientific), and boiled for 30 min. Insoluble material in the samples was collected by centrifugation at 16,000 ×g and the supernatant was diluted with one volume of water and treated with 0.5 µl of proteinase K [20 mg/ml] for 2 hours.

For LTA analysis in supernatant 500 µl of overnight culture was subjected to centrifugation at 16,000 ×g. 75 µl of supernatant was mixed with 25 µl 4x LDS sample buffer and boiled for 30 min. Insoluble material in the samples was collected by centrifugation at 16,000 ×g. Pellet and supernatant fractions were loaded onto a NuPAGE Novex 4-12% Bis-Tris protein gel and run for 90 min at 100V and 200A in MES running buffer. LTA was transferred to a PVDF membrane and bands were developed using the WesternBreeze Chemiluminescent Kit with the anti-LTA mAb 55 antibody from Hycult Biotech.

Bocillin-FL labelling of PBPs. 15 µg of membrane proteins were labelled with 15 µM bocillin-FL (Thermo Fisher Scientific) for 10 min at 30 °C. The reaction was stopped by addition of 4 x SDS-PAGE sample buffer (Merck), and labelled membrane proteins were separated on a NuPAGE Novex 4-12% Bis-Tris protein gel and visualized on a Gel-Doc XR+ imager (Bio-Rad).

Preparation and analysis of peptidoglycan. Overnight cultures of *S. aureus* strains JE2 WT, JE2_*auxA* and JE2_*auxB* were used to inoculate 1 l of TSB, which was grown to 0.5 OD_{600}, before being cooled on ice and collected by centrifugation. Peptidoglycan preparation and high performance liquid chromatography (HPLC) analysis of the digested peptidoglycan samples were performed as previously described [40]. The distribution of monomeric, dimeric, trimeric and higher oligomeric peptidoglycan was quantified by integration of peaks belonging to each group, relative to the total peak area.

Triton X-100-induced lysis assay. Overnight cultures were diluted to an 0.05 OD_{600} and grown until 0.8 OD_{600}. The cultures were chilled in an ice-ethanol bath, spun down (10,000 × g, 4 °C, 5 min) washed in ice-cold water and collected by centrifugation. The pellet was re-suspended in half of the initial volume of lysis-buffer (50 mM Glycine, 0.01% Triton X-100, pH 8). The samples were incubated at 37 °C and OD_{600} was measured every 15 min for 3 hours.

***Galleria mellonella* infection model**. *Galleria mellonella* larvae (Livefoods Direct Limited, Sheffield) were used as an infection host for investigating the virulence of pathogenic bacteria and evaluating efficacy of antibiotic therapy for bacterial infections [37]. The bacterial inoculum was prepared from overnight cultures and adjusted to 0.3 OD_{600} in sterile water. Aliquots of 5 µl (~$1.5x10^6$ CFU/larvae) were injected to each larvae using a Hamilton Microliter™ syringe via the last right pro-leg. Each group contains 10 larvae. After injection, larvae were incubated at 37 °C in petri dishes. To test the efficacy of amoxicillin against *S aureus* strains, a dose of 30 mg/kg was administered one hour post infection. Survival was inspected and recorded every 24 hours for seven days. Larvae are considered dead if they become black and crusty or discolored and unresponsive to touch. Two control groups were used, the first received no injection and the other received PBS only to evaluate death related to trauma.

Statistics. Data were analyzed using GraphPad Prism 7.04 (GraphPad Software Inc., CA) with statistical significance highlighted: no significance (ns), *($p<0.05$). The final survival rates of the *Galleria mellonella* infection model were compared using the Gehan-Breslow-Wilcoxon test.

References

1. Lowy, F.D., *Antimicrobial resistance: the example of Staphylococcus aureus.* J. Clin. Investig., 2003. **111**(9): p. 1265-1273.
2. Hartman, B.J. and A. Tomasz, *Low-Affinity Penicillin-Binding Protein Associated with β-Lactam Resistance in Staphylococcus aureus.* J. Bacteriol., 1984. **158**(2): p. 513-516.
3. Llarrull, L.I., et al., *The future of the β-lactams.* Curr. Opin. Microbiol., 2010. **13**(5): p. 551-557.
4. Rohrer, S., et al., *The essential Staphylococcus aureus gene fmhB is involved in the first step of peptidoglycan pentaglycine interpeptide formation.* Proc. Natl. Acad. Sci. U.S.A., 1999. **96**(16): p. 9351-9356.
5. Memmi, G., et al., *Staphylococcus aureus PBP4 is Essential for β-Lactam Resistance in Community-Acquired Methicillin-Resistant Strains.* Antimicrob. Agents Chemother., 2008. **52**(11): p. 3955-3966.
6. Campbell, J., et al., *Synthetic Lethal Compound Combinations Reveal a Fundamental Connection between Wall Teichoic Acid and Peptidoglycan Biosyntheses in Staphylococcus aureus.* ACS Chem. Biol., 2010. **6**(1): p. 106-116.
7. Brown, S., et al., *Methicillin resistance in Staphylococcus aureus requires glycosylated wall teichoic acids.* Proc. Natl. Acad. Sci. U.S.A., 2012. **109**(46): p. 18909-18914.
8. Lee, S.H., et al., *Antagonism of Chemical Genetic Interaction Networks Resensitize MRSA to β-Lactam Antibiotics.* Chem. Biol, 2011. **18**(11): p. 1379-1389.
9. Gardete, S., et al., *Role of VraSR in Antibiotic Resistance and Antibiotic-Induced Stress Response in Staphylococcus aureus.* Antimicrob. Agents Chemother., 2006. **50**(10): p. 3424-3434.
10. Foster, T.J., *Can β-Lactam Antibiotics Be Resurrected to Combat MRSA?* Trends Microbiol., 2019. **27**(1): p. 26-38.
11. DeFrancesco, A.S., et al., *Genome-wide screen for genes involved in eDNA release during biofilm formation by Staphylococcus aureus.* Proc. Natl. Acad. Sci. U.S.A., 2017. **114**(29): p. E5969-E5978.
12. Matano, L.M., et al., *Accelerating the discovery of antibacterial compounds using pathway-directed whole cell screening.* Bioorg. Med. Chem., 2016. **24**(24): p. 6307-6314.
13. Percy, M.G. and A. Gründling, *Lipoteichoic Acid Synthesis and Function in Gram-Positive Bacteria.* Annu. Rev. Microbiol., 2014. **68**: p. 81-100.
14. Rajagopal, M. and S. Walker, *Envelope Structures of Gram-Positive Bacteria.* Protein and Sugar Export and Assembly in Gram-positive Bacteria. Current Topics in Microbiology and Immunology, 2015. **404**: p. 1-44.
15. Gründling, A. and O. Schneewind, *Synthesis of glycerol phosphate lipoteichoic acid in Staphylococcus aureus.* Proc. Natl. Acad. Sci. U.S.A., 2007. **104**(20): p. 8478-8483.
16. Hesser AR, et al., *The Length of Lipoteichoic Acid Polymers Controls Staphylococcus aureus Cell Size and Envelope Integrity.* J. Bacteriol., 2020. **202**: p. e00149-20.
17. Peschel, A., et al., *Inactivation of the dlt Operon in Staphylococcus aureus Confers Sensitivity to Defensins, Protegrins, and Other Antimicrobial Peptides.* J. Biol. Chem., 1999. **274**(13): p. 8405-8410.
18. Peschel, A., et al., *The d-Alanine Residues of Staphylococcus aureus Teichoic Acids Alter the Susceptibility to Vancomycin and the Activity of Autolytic Enzymes.* Antimicrob. Agents Chemother., 2000. **44**(10): p. 2845-2847.
19. Hamilton, S.M., et al., *High-Level Resistance of Staphylococcus aureus to β-Lactam Antibiotics Mediated by Penicillin-Binding Protein 4 (PBP4).* Antimicrob. Agents Chemother., 2017. **61**(6): p. e02727-16.

20. Li, L., et al., *The Global Regulon sarA Regulates β-Lactam Antibiotic Resistance in Methicillin-Resistant Staphylococcus aureus In Vitro and in Endovascular Infections.* J. Infect. Dis., 2016. **214**(9): p. 1421-1429.
21. Rajagopal, M., et al., *Multidrug Intrinsic Resistance Factors in Staphylococcus aureus Identified by Profiling Fitness within High-Diversity Transposon Libraries.* mBio, 2016. **7**(4): p. e00950-16.
22. Krogh, A., et al., *Predicting transmembrane protein topology with a hidden Markov model: application to complete genomes.* J. Mol. Biol., 2001. **305**(3): p. 567-580.
23. Yang, J., et al., *The I-TASSER Suite: protein structure and function prediction.* Nat. Methods, 2015. **12**(1): p. 7-8.
24. Matsuyama, S.-i., Y. Fujita, and S. Mizushima, *SecD is involved in the release of translocated secretory proteins from the cytoplasmic membrane of Escherichia coli.* EMBO J., 1993. **12**(1): p. 265-270.
25. Bolhuis, A., et al., *SecDF of Bacillus subtilis, a Molecular Siamese Twin Required for the Efficient Secretion of Proteins.* J. Biol. Chem., 1998. **273**(33): p. 21217-21224.
26. Quiblier, C., et al., *Contribution of SecDF to Staphylococcus aureus resistance and expression of virulence factors.* BMC Microbiol., 2011. **11**.
27. Quiblier, C., et al., *Secretome Analysis Defines the Major Role of SecDF in Staphylococcus aureus Virulence.* PLoS ONE, 2013. **8**(5): p. e63513.
28. Aedo, S. and A. Tomasz, *Role of the Stringent Stress Response in the Antibiotic Resistance Phenotype of Methicillin-Resistant Staphylococcus aureus.* Antimicrob. Agents Chemother., 2016. **60**(4): p. 2311-2317.
29. Grunert, T., et al., *Analysis of Staphylococcus aureus wall teichoic acid glycoepitopes by Fourier Transform Infrared Spectroscopy provides novel insights into the staphylococcal glycocode.* Sci. Rep., 2018. **8**: p. 1889.
30. Antignac, A., K. Sieradzki, and A. Tomasz, *Perturbation of Cell Wall Synthesis Suppresses Autolysis in Staphylococcus aureus: Evidence for Coregulation of Cell Wall Synthetic and Hydrolytic Enzymes.* J. Bacteriol., 2007. **189**(21): p. 7573-7580.
31. Delaune, A., et al., *Peptidoglycan Crosslinking Relaxation Plays an Important Role in Staphylococcus aureus WalKR-Dependent Cell Viability.* PLoS ONE, 2011. **6**(2): p. e17054.
32. Corrigan, R.M., et al., *c-di-AMP Is a New Second Messenger in Staphylococcus aureus with a Role in Controlling Cell Size and Envelope Stress.* PLoS Pathog., 2011. **7**(9): p. e1002217.
33. Griffiths, J. and A. O'neill, *Loss of Function of the GdpP Protein Leads to Joint β-Lactam/Glycopeptide Tolerance in Staphylococcus aureus.* Antimicrob. Agents Chemother., 2012. **56**(1): p. 579-581.
34. Ba, X., et al., *Truncation of GdpP mediates β-lactam resistance in clinical isolates of Staphylococcus aureus.* J. Antimicrob. Chemother., 2019. **74**(5): p. 1182-1191.
35. Lambert, M.P. and F.C. Neuhaus, *Mechanism of D-Cycloserine Action: Alanine Racemase from Escherichia coli W.* J. Bacteriol., 1972. **110**(3): p. 978-987.
36. Gründling, A. and O. Schneewind, *Genes Required for Glycolipid Synthesis and Lipoteichoic Acid Anchoring in Staphylococcus aureus.* J. Bacteriol., 2007. **189**(6): p. 2521-2530.
37. Desbois, A.P. and P.J. Coote, *Wax moth larva (Galleria mellonella): an in vivo model for assessing the efficacy of antistaphylococcal agents.* J. Antimicrob. Chemother., 2011. **66**(8): p. 1785–1790.
38. Paudel, A., et al., *Large-Scale Screening and Identification of Novel Pathogenic Staphylococcus aureus Genes Using a Silkworm Infection Model* J. Infect. Dis., 2020. **221**(11): p. 1795-1804.
39. Monk, I.R., et al., *Transforming the Untransformable: Application of Direct Transformation To Manipulate Genetically Staphylococcus aureus and Staphylococcus epidermidis.* mBio, 2012. **3**(2): p. e00277-11.
40. De Jonge, B., et al., *Peptidoglycan composition of a highly methicillin-resistant Staphylococcus aureus strain. The role of penicillin binding protein 2A.* . J. Biol. Chem., 1992. **267**(16): p. 11248-11254.

Table 1. *MIC (µg/ml) of β-lactam antimicrobials against JE2, the isogenic auxA and auxB transposon mutants, auxA and auxB knock-out mutants (ΔauxA and ΔauxB) and complemented strains.*

Strains	Plasmid	Oxacillin	Amoxicillin	Carbenicillin	Cefalotin	Cefoxitin	Cefuroxime	Ceftazidime	Cefotaxime	Meropenem
JE2	-	32	32	64	32	64	>512	256	16	4
JE2	pRB474	64	64	64	32	64	>512	256	ND	4
JE2_*auxA*	-	1	4	4	1	8	2	32	0.75	0.125
JE2_*auxA*	pRB474	1	4	4	1	4	2	32	ND	0.125
JE2_*auxA*	pRB474-*auxA*	8	16	8	2	16	32	64	ND	2
JE2 Δ*auxA*	-	4	ND	ND	ND	ND	ND	8	ND	ND
JE2 Δ*auxA*	pRB474-*auxA*	8	ND	ND	ND	ND	ND	32	ND	ND
JE2_*auxB*	-	16	8	8	4	32	32	64	1	1
JE2_*auxB*	pRB474	8	8	8	4	32	32	64	ND	1
JE2_*auxB*	pRB474-*auxB*	32	32	64	16	64	512	128	ND	4
JE2 Δ*auxB*	-	2	ND	ND	ND	ND	ND	16	ND	ND
JE2 Δ*auxB*	pRB474-*auxB*	8	ND	ND	ND	ND	ND	32	ND	ND

Table 1. *MIC (µg/ml) of non-β-lactam antibiotics against auxA and auxB Tn mutants.*

Strains	Cell wall			Teichoic acids			Cell membrane		Protein synthesis	DNA synthesis
	Vanco-mycin	Baci-tracin	D-cyclo-serine	Tunicamycin	Congo Red	Amsa-crine	Dapto-mycin	Nisin	Genta-micin	Cipro-floxacin
JE2	1.5	256	32	>16	0.03%	>320	0.25	512	0.5	>32
JE2_*auxA*	0.38	128	8	>16	0.004%	5	0.19-0.38	256-512	0.38	>32
JE2_*auxB*	1	128	16	>16	<0.004 %	5	0.19-0.38	256-512	0.5	12-16

Table 3. *MICs (µg/ml) of oxacillin, cefoxitin and meropenem against CA-MRSA MW2, HA-MRSA COL, LA-MRSA ST398 and MSSA Newman.*

Strains	Oxacillin	Cefoxitin	Meropenem
MW2	32	32	2
MW2_*auxA*	8	16	0.25
MW2_*auxB*	8	16	0.5
COL	512	512	16
COL_*auxA*	32	64	2
COL_*auxB*	64	256	8
ST398	4	16	0.125
ST398_*auxA*	2	4	0.03
ST398_*auxB*	2	2	0.06
Newman	0.19	2	0.094
Newman_*auxA*	0.094	0.5	0.032
Newman_*auxB*	0.094	0.75	0.032

Table 4. *Suppressor mutations found in the gdpP gene of JE2_auxA and JE2_auxB mutants passaged with cefotaxime.*

Strains	Nucleotide change	Amino acid change
auxA_sup1	G1066A	Gly356Ser
auxA_sup2	C622T	Arg208*
auxB_sup1	C838T	Gln280*
auxB_sup2	T411A	Tyr137*
auxB_sup3	C376T	Gln126*

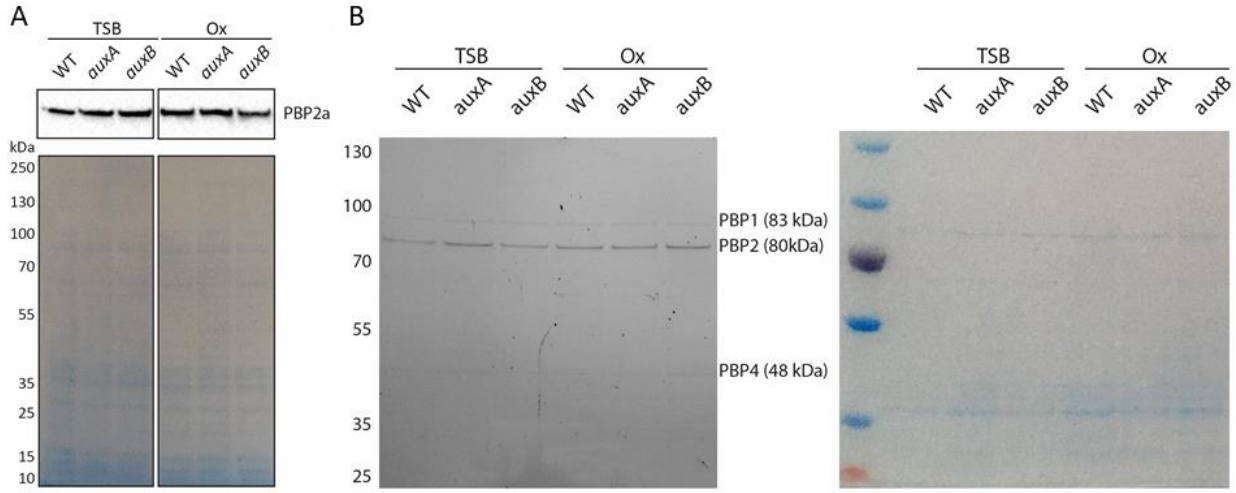

Figure 1. Analysis of PBP levels in auxA and auxB mutants. *Anti-PBP2a western blot analysis (n=3) (A), and Bocillin FL penicillin analysis (n=2) (B) of JE2_auxA, JE2_auxB and WT mid-exponential phase cultures +/- 0.1 µg/ml oxacillin. Comassie stained protein gels serve as loading controls (A lower, B right).*

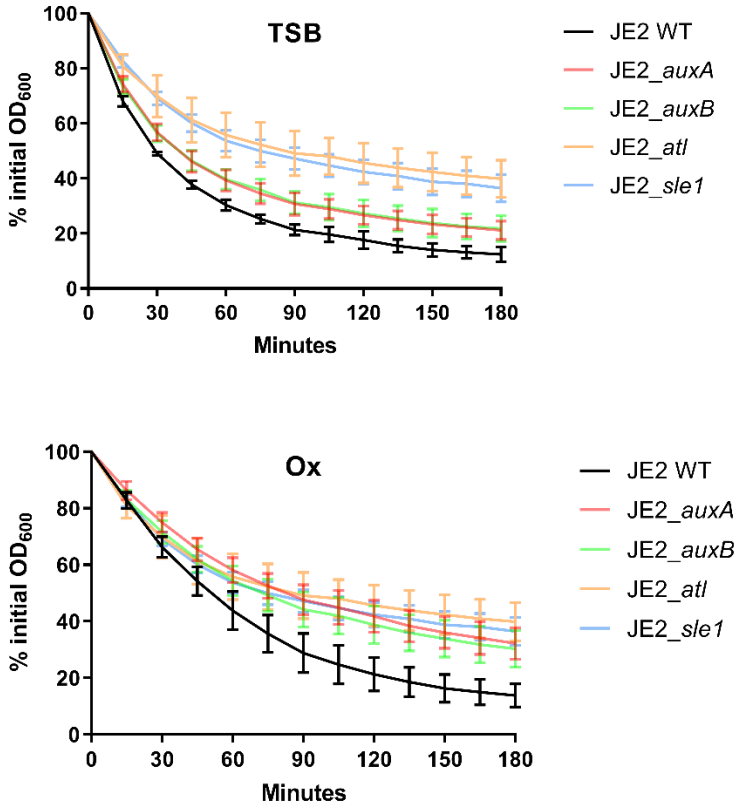

Figure 2. auxA and auxB mutants are less susceptible to Triton X-100 mediated lysis. *The decline in OD_{600} was measured for an exponential phase culture washed and re-suspended in lysis-buffer (50 mM Glycine, 0.01% Triton X-100, pH = 8). Cultures (n=3) were grown in TSB (A) or TSB with 0.1 µg/ml oxacillin (B) and standard deviations are shown.*

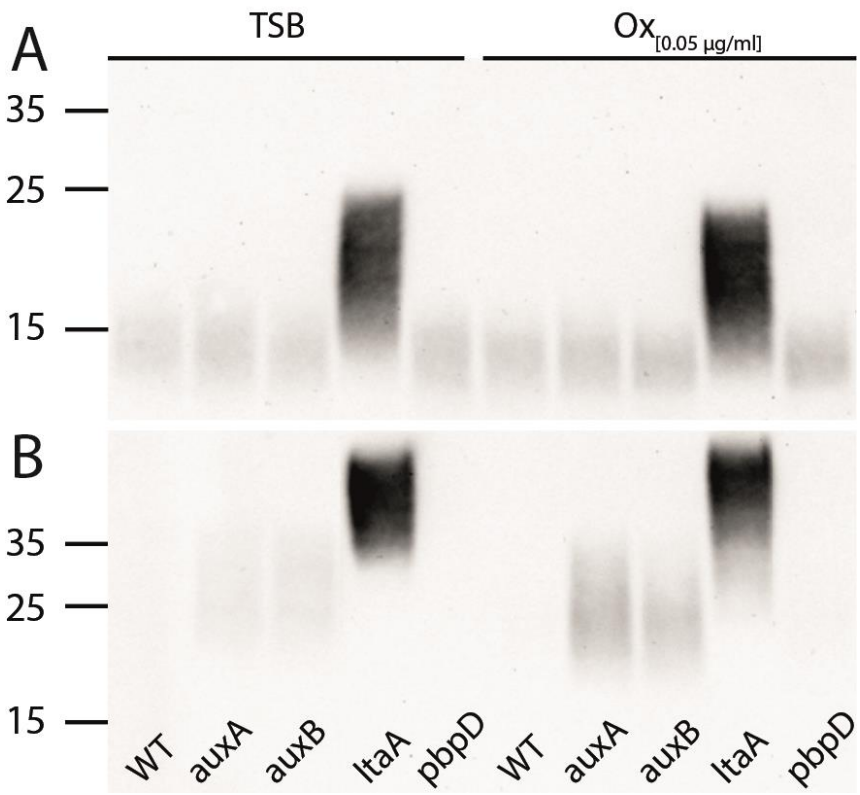

Figure 3. **auxA *and* auxB *mutants release LTA into the supernatant.*** *Anti-LTA western blot of cells grown for 8 hours. Pellet fractions (A) showed no difference in LTA content between aux mutants and WT. Release of LTA into the medium was detected from aux mutant cultures in TSB +/- 0.05 µg/ml oxacillin (B). Mutants of the LTA flippase ltaA and penicillin-binding protein pbpD was included as controls.*

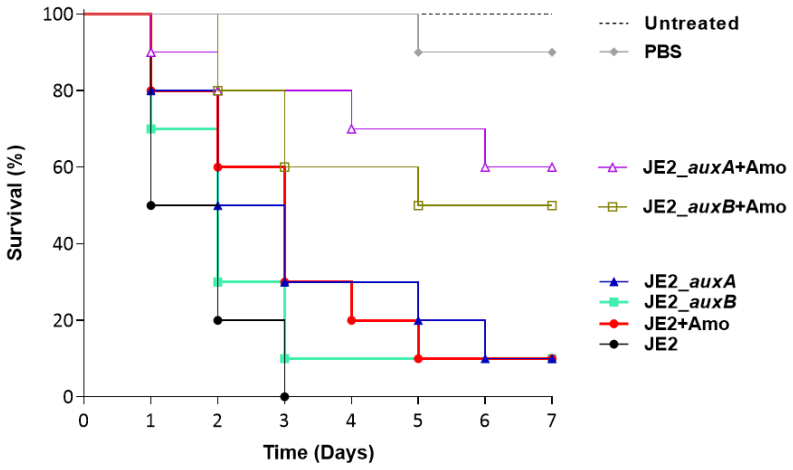

Figure 4. Amoxicillin treatment increases survival rates of JE2_auxA and JE2_auxB infected Galleria mellonella larvae. *Each larvae was injected with a bacterial inoculum of JE2 WT, JE2_auxA or JE2_auxB (~1.5x10^6 CFU) and 1 h.p.i. left untreated, injected with PBS, or treated with a single dose of amoxicillin (30 mg/kg). Amoxicillin treatment signifcantly improved the survival rate of JE2_auxA and JE2_auxB to 60% and 50% compared to 10% in JE2 infected larvae (p value <0.0001).*

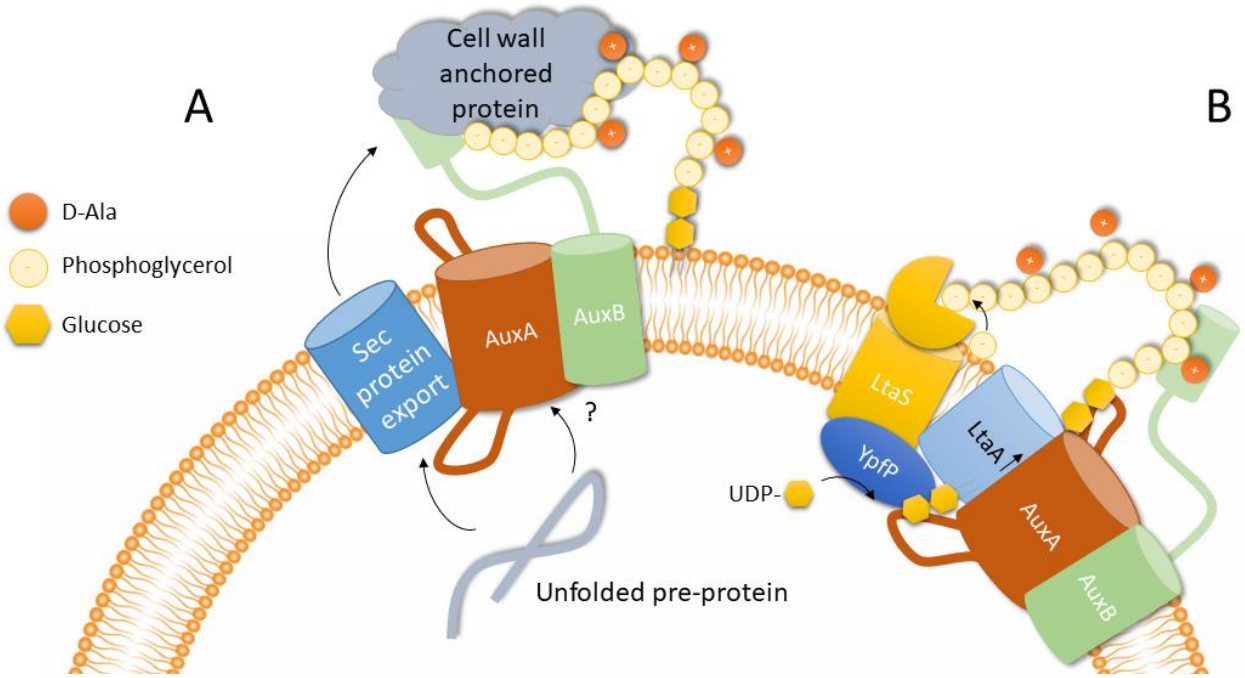

***Figure 5*. Possible models for AuxA and AuxB role in LTA stability.** *(A) AuxA and AuxB assists the Sec protein export pathway in translocating proteins to the extracellular space, where these proteins stabilize the LTA polymer, or AuxAB might transport small proteins or peptides across the membrane single-handedly. (B) AuxA and AuxB stabilizes LTA by physical interactions or assist members of the LTA pathway.*

***Supplementary Table S1**: Bacterial strains used in this study*

Name	Characteristics	Reference
E. coli IM08B	Lab strain used for cloning	[1]
JE2	USA300 CA-MRSA isolate and parent strain of the Nebraska Transposon Mutant Library	[2]
JE2_*auxA*	NE1044 NTML mutant (SAUSA300_0980)	[3]
JE2_*auxB*	NE1420 NTML mutant (SAUSA300_1003)	
JE2_*ltaA*	NE462 NTML mutant (SAUSA300_0917)	
JE2_*pbpD*	NE679 NTML mutant (SAUSA300_0629)	
JE2_*atl*	NE460 NTML mutant (SAUSA300_0955)	
JE2_*sle1*	NE1688 NTML mutant (SAUSA300_0438)	
JE2 Δ*auxA*	Clean deletion of *auxA* in JE2	This study
JE2 Δ*auxB*	Clean deletion of *auxB* in JE2	This study
auxA_sup1	JE2_*auxA* suppressor mutant #1	This study
auxA_sup2	JE2_*auxA* suppressor mutant #2	This study
auxB_sup1	JE2_*auxB* suppressor mutant #1	This study
auxB_sup2	JE2_*auxB* suppressor mutant #2	This study
auxB_sup3	JE2_*auxB* suppressor mutant #3	This study
MW2	CA-MRSA clinical isolate	[4]
MW2_*auxA*	MW2 carrying the NE1044 transposon insertion	This study
MW2_*auxB*	MW2 carrying the NE1420 transposon insertion	This study
COL	HA-MRSA clinical isolate	[5]
COL_*auxA*	COL carrying the NE1044 transposon insertion	This study
COL_*auxB*	COL carrying the NE1420 transposon insertion	This study
ST398	LA-MRSA clinical isolate	This study

ST398_*auxA*	ST398 carrying the NE1044 transposon insertion	This study
ST398_*auxB*	ST398 carrying the NE1420 transposon insertion	This study
Newman	MSSA clinical isolate	[6]
Newman_*auxA*	Newman carrying the NE1044 transposon insertion	This study
Newman_*auxB*	Newman carrying the NE1420 transposon insertion	This study
NRS384Δ*tagO*	Clean deletion of *tagO* in NRS384	[7]
NRS384Δ*tarM*	Clean deletion of *tarM* in NRS384	
NRS384Δ*tarS*	Clean deletion of *tarS* in NRS384	

***Supplementary Table S2**: Primers used in this study*

Primer	Sequence	Usage
auxA-for	5'-AAACTTACCCGCCATACCACGAT--3'	genotyping of *auxA*
auxA-rev	5'-TAGCCATTTGACCAAGTAACCACA-3'	
A5	5'-CGACTCTAGAGGATCCAAAGGAGGTTATAT AATGTCTTTTCTTAGGAAACACGC-3'	construction pRB474-*auxA*
A3	5'-CAGTGCAGCGGAATTCTTATGGTCGCTCTC GTAATTGT -3'	
koA-P1	5'-ATCGGAATTCAGGGATACTTATCAATCATAC C3'	amplification of *auxA* upstream fragments
KoA-P2	5'-TATGTTCACCTCAAAATCATTATATAT-3'	
KoA-P3	5'-TTAAAAGCATTATAAAAGTACTATCTATT-3'	amplification of *auxA* upstream fragments
KoA-P4	5'-TATCCTCTTCTTCAATTAAAGGAT-3'	
auxB-for	5'-ATCATTCCGATATTATTCTTTATTATTGCG-3'	genotyping of *auxB*
auxB-rev	5'-AACTTCAGGTTCTGCATAATAACCAT-3'	
B5	5'-CGACTCTAGAGGATCCAAAGGAGGTTATAT AATGACTGGAGAACAATTTACTCAAAT-3'	construction of pRB474-*auxB*
B3	5'-CAGTGCAGCGGAATTCTTATTCTTGCTCTTT TTTGTCCTTAACTT-3'	
KoB-P1	5'-TTTCGACTGAGCCTTTCGTTTTATTTGATG-3'	amplification of *auxB* upstream fragments
KoB-P2	5'-CAGCTTATCATCGAATTATAGGAATAGAGC-3'	
KoB-P3	5'-CGCAATATTATATGCTTGCTTTATCGG-3'	amplification of *auxB* upstream fragments
KoB-P4	5'-ACGCACTTTGCGCCGAATAAATAC-3'	

Supplementary Table S3. *Peptidoglycan crosslinking of JE2 WT, JE2_auxA, JE2_auxB. The relative percentage of Monomers, Dimers, Trimers and higher oligomers were estimated from the combined area of the peaks indicated, compared to total area.*

	Sum of relative peak area in strain (%)[1]					
Muropeptides	**WT 1**	**WT 2**	***auxA* 1**	***auxA* 2**	***auxB* 1**	***auxB* 2**
Monomers (peak 1-8)	9.1	9.5	7.2	9.7	8.4	9.5
Dimers (peak 9-13)	13.9	14.7	12.7	15.4	14.1	15.5
Trimers (peak 14-15)	13.4	14.6	12.4	15.0	13.2	14.6
> Trimers (peak 16 to end)	63.6	61.2	67.9	59.9	64.4	60.4

[1] numbers 1 and 2 after the strain name indicate two biological repeats.

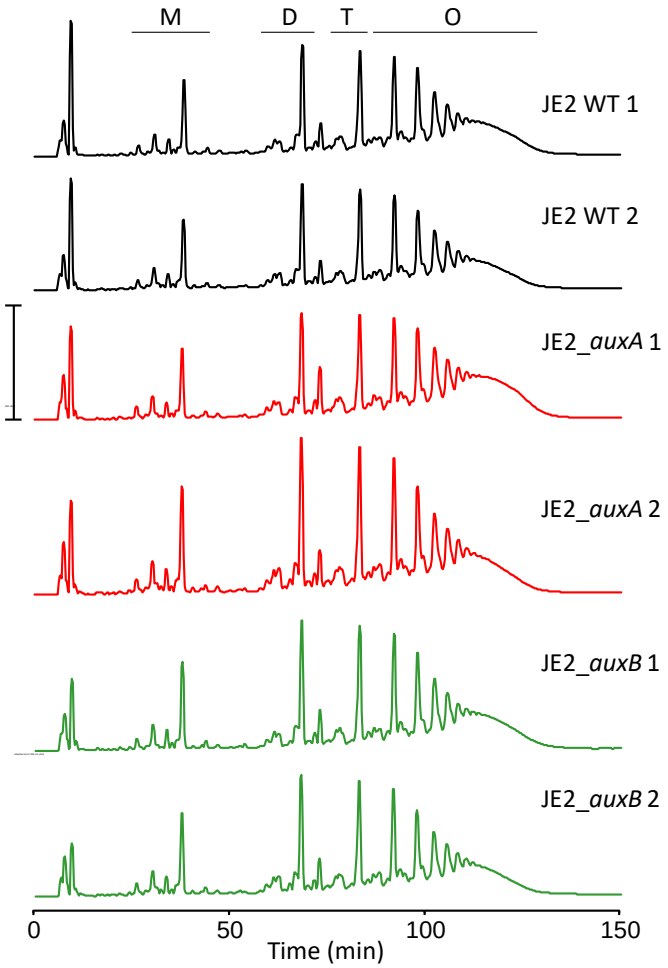

Figure S1. Peptidoglycan cross-linking analysis. *Muropeptide composition of WT and mutant strains obtained after digestion of peptidoglycan with cellosyl and separation of the resulting muropeptides by reverse-phase HPLC. Quantification of monomers (M), dimers (D), trimers (T), higher oligomers (O) is shown in Table S3.*

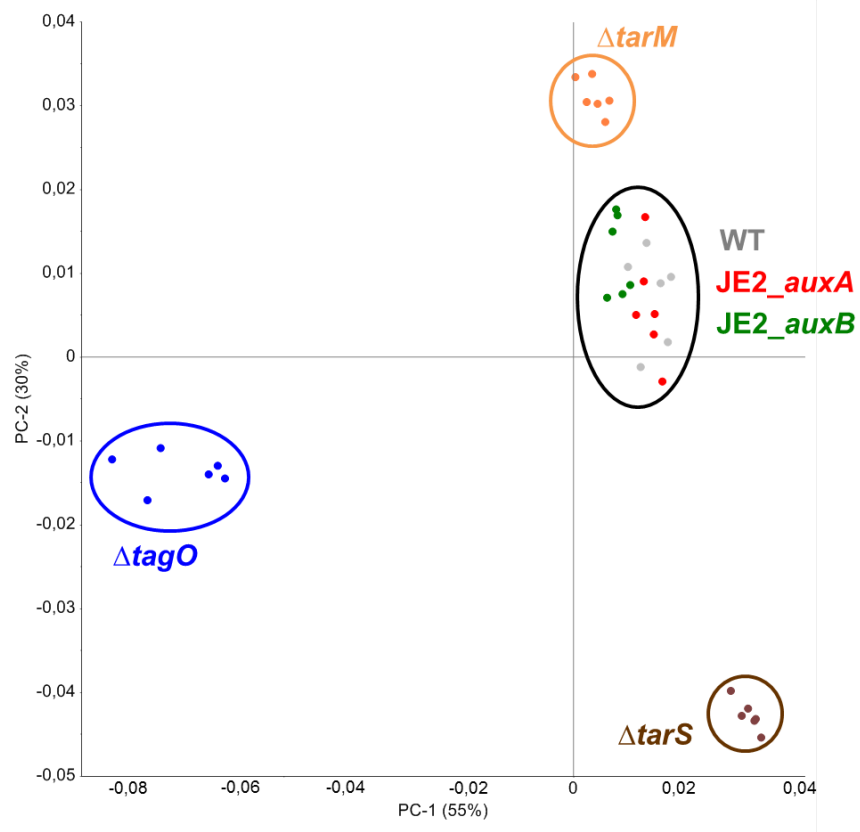

Figure S2: *Impact of transposon mutation of auxA, auxB on WTA structures detected by FTIR spectroscopy. PCA score of JE2 WT, auxA, auxB mutant, wild type (WT) as well as WTA mutants ΔtagO, ΔtarM and ΔtarS in the polysaccharide (1200–800cm^{-1}) spectral regions. Each data point represents one measurement derived from three independent experiments in duplicates per strain.*

1. Monk, I.R., et al., *Complete Bypass of Restriction Systems for Major Staphylococcus aureus Lineages.* mBio, 2015. **6**(3): p. e00308-15.
2. Kennedy, A.D., et al., *Epidemic community-associated methicillin-resistant Staphylococcus aureus: recent clonal expansion and diversification.* Proc Natl Acad Sci U S A, 2008. **105**(4): p. 1327-32.
3. Fey, P.D., et al., *A genetic resource for rapid and comprehensive phenotype screening of nonessential Staphylococcus aureus genes.* mBio, 2013. **4**(1): p. e00537-12.
4. Baba, T., et al., *Genome and virulence determinants of high virulence community-acquired MRSA.* Lancet, 2002. **359**(9320): p. 1819-27.
5. Gill, S.R., et al., *Insights on evolution of virulence and resistance from the complete genome analysis of an early methicillin-resistant Staphylococcus aureus strain and a biofilm-producing methicillin-resistant Staphylococcus epidermidis strain.* J Bacteriol, 2005. **187**(7): p. 2426-38.
6. Baba, T., et al., *Genome sequence of Staphylococcus aureus strain Newman and comparative analysis of staphylococcal genomes: polymorphism and evolution of two major pathogenicity islands.* J Bacteriol, 2008. **190**(1): p. 300-10.
7. Kurokawa, K., et al., *Glycoepitopes of staphylococcal wall teichoic acid govern complement-mediated opsonophagocytosis via human serum antibody and mannose-binding lectin.* J Biol Chem, 2013. **288**(43): p. 30956-68.

Manuscript 3:

Novel lipoteichoic acid stabilizing factors AuxA and AuxB interact with the divisome, DltD and LTA pathway members and are essential during D-serine stress.

Author list:

Kasper Mikkelsen[1], Ohood Alharbi[2], Guoqing Xia [2], Hanne Ingmer[1]

1. Department of Veterinary and Animal Sciences, University of Copenhagen, Denmark
2. Lydia Becker Institute of Immunology and Inflammation, Division of Infection, Immunity and Respiratory Medicine, School of Biological Sciences, Faculty of Biology, Medicine and Health, University of Manchester, Manchester Academic Health Science Centre, Manchester, M13 9PT, United Kingdom

Author contributions

KM made the experiments, except proteome analysis preparation which was done by OA. KM, GX and HI planned and analyzed the experiments and KM and HI wrote the manuscript.

Abstract

D-serine is a natural component that act as a neurotransmitter in the mammalian brain and is present in high concentrations in human urine. Being a non-uropathogenic bacterium, *Staphylococcus aureus* is sensitive to D-serine, and combinations of D-serine and β-lactam antimicrobials have shown promising synergistic effects against *S. aureus*. We here identify lipoteichoic acid pathway members YpfP and LtaA, and novel auxiliary factors AuxA and AuxB involved in lipoteichoic acid stability, as essential during D-serine stress. Growth of an *auxA* deletion mutant in presence of D-serine increased the abundance of protein export associated gene products, whereas a reduction was seen in the amount of the division proteins DivIB, FtsL and MurJ important for peptidoglycan synthesis at septum. Investigation of AuxA and AuxB interactions using the bacterial adenylate cyclase two-hybrid system demonstrated direct links with AuxA and AuxB to one another and to members of the lipoteichoic acid, peptidoglycan synthesis and cell division pathways. *aux* mutants have previously shown diminished autolysis, and transmission electron microscopy revealed an inhibition of cell separation upon D-serine treatment, which was detrimental to *ypfP*, *ltaA*, *auxA* and *auxB* mutants. We propose a model where incorporation of D-serine into the peptidoglycan stem peptides hampers autolysis and is detrimental when lipoteichoic acid structure and/or stability is compromised. Our results place AuxA and B as central players in coordinating cell division with peptidoglycan synthesis.

Introduction

D-serine, the enantiomer of the protein building block L-serine, acts as a neurotransmitter and co-activator of the N-methyl D-aspartate receptors in the mammalian brain and is the most prevalent D-amino acid in human blood serum and urine [1, 2]. D-serine has been reported to hold a bacteriostatic effect caused by inhibition of panthotenate and L-serine biosynthesis and by inhibition of type III secretion system in enterohaemorrhagic *Escherichia coli* [3, 4]. However, uropathogenic *Escherichia coli* is able to sense the high levels of D-serine in urine and turn on virulence to establish an infection [5, 6].

Staphylococcus saprophyticus is the second most common uropathogen and the only staphylococcal species commonly causing urinary tract infection (UTI) [7]. *S. saprophyticus* is distinguished from the staphylococcal pathogens *Staphylococcus aureus* and *Staphylococcus epidermidis* by a cell wall-anchored protein able to adhere to human bladder cells, by urease activity and the D-serine deaminase gene *dsdA* [8, 9]. D-serine deaminases degrade D-serine to pyruvate and ammonia, and the *dsdA* gene of *S. saprophyticus* have shown to enable *S. aureus* to grow in medium supplemented with 20 mg/ml D-serine [9]. The inability of *S. aureus* to metabolize D-serine has rendered it sensitive to this compound and UTIs caused by *S. aureus* is most commonly a result of a systemic infection seeding the kidneys [8].

The toxic effect of D-serine against *S. aureus* has been ascribed its ability to incorporate into the Gram-positive cell wall [10]. Peptidoglycan (PG) is the main component of *S. aureus* cell wall and is composed of linear glycan strands held together by short peptides. Each PG building block contain two sugar moieties linked to an L-Ala-*i*-Gln-L-Lys-D-Ala-D-Ala peptide stem. This is cross-linked by a pentaglycine cross-bridge between the third L-Lys of one stem with the fourth D-ala of another [11]. D-serine can be exchanged for the terminal D-ala residue of the PG stem peptide by the promiscuous carboxypeptidase activity of penicillin-binding protein 4 (PBP4) [12], and the modified stem peptide serves as a poor substrate for PBP transpeptidase activity[10]. Likewise, D-serine can be inserted into the pentaglycine cross-bridge at positions three and five by the activity of FmhA and position five by FmhC [13]. When incorporated into the fifth position in the cross-bridge, D-serine is a poor substrate for the cross-wall located D-Ala-gly endopeptidase

activity of LytN, important for the separation of the staphylococcal daughter cells [14]. The abilities of D-serine to inhibit both the separation of daughter cells and the transpeptidation step of PG synthesis have shown promising synergistic effects when combined with β-lactam antimicrobials, another group of PG transpeptidation inhibitors [10, 15].

In this study, we set out to find gene candidates able to increase sensitivity of *S. aureus* to D-serine by screening the Nebraska Transposon Mutant Library (NTML) [16] for lack of growth at 1/5 minimal inhibitory concentration (MIC). Surprisingly, the screen only revealed hits inactivating *auxA*, *auxB* and *ypfP*, consistent with *ypfP* inactivation previously being reported as conferring sensitivity towards glycine and D-serine [17]. YpfP is responsible for the synthesis of the glycolipid anchor diglycosyl-diacylglycerol (Glc_2DAG), which serves as the starting unit for lipoteichoic acid (LTA) synthesis. The Glc_2DAG anchor is synthesized in the cytoplasm by Ypfp from UDP-glucose and diacylglycerol (DAG) and flipped across the membrane by the LtaA flippase. From here the LTA synthase (LtaS) adds glycerol phosphate (GroP) units to the growing LTA polymer [18], which is heavily decorated with D-ala residues added to LTA via the *dltABCD* operon by DltD, which is shown to interact with both Ypfp, LtaA and LtaS [19].

AuxA and AuxB are membrane proteins with 10 and 3 transmembrane domains, respectively. Additionally, AuxA carries a 94 amino acid intracellular domain between helices 6 and 7 and AuxB has a 192 amino acid C-terminal extracellular domain. AuxA and AuxB have thus far been attributed a role in LTA stability, and mutants lacking either gene show increased sensitivity to β-lactam antimicrobials and *dlt* and LTA pathway inhibitors [20, 21] (manuscript 2), which are phenotypes shared by *ypfP* and *ltaA* mutants [22, 23]. Likewise, former screens have revealed increased sensitivity of *aux* and LTA pathway mutants towards daptomycin [24] and the cationic antimicrobial peptide polymyxin B [25].

Here we report the essentiality of *S. aureus* LTA associated genes *ypfP, ltaA, auxA* and *auxB* to withstand D-serine toxicity. Bacterial adenylate cyclase two-hybrid experiments revealed interactions of AuxA and AuxB with one another and with members of LTA synthesis, *dlt* pathway, cell division, and PG synthesis. D-serine showed an inhibitory effect on cell segregation, probably caused by D-serine containing PG stem peptides acting as a poor substrate for LytN

endopeptidase activity. Finally, we show that the cause of increased D-serine sensitivity of *auxA*, *auxB*, *ypfP* and *ltaA* mutants is related to cell splitting defects that hinder the cells ability to cope with additional D-serine-induced segregational stress, ultimately inhibiting cell division by trapping the cells inside their own cell wall.

Results and discussion

LTA pathway members are important for *S. aureus* D-serine tolerance. To identify genes necessary for *S. aureus* to withstand D-serine toxicity, we screened the NTML for lack of growth on TSA plates containing 1/5 of JE2 wild type (WT) D-serine MIC levels (25 mM). The only mutants displaying a 'no growth' phenotype were those with transposon inserts in the *auxA* (SAUSA300_0980), *auxB* (SAUSA300_1003) and *ypfP* (SAUSA300_0918) genes (onward referred to as JE2_*auxA*, JE2_*auxB* and JE2_*ypfp*, respectively). YpfP is a diacylglycerol glucosyltransferase responsible for the synthesis of the LTA Glc_2DAG anchor, while AuxA and AuxB are necessary for LTA stability (manuscript 2). The mutant lacking the LTA flippase, LtaA (JE2_*ltaA*) showed inhibited growth and was included for susceptibility testing. JE2_*ypfP* was the most sensitive of the mutants with a 32-fold increase in susceptibility towards D-serine compared to the WT. The JE2_*auxA,* JE2_*auxB,* and JE2_*ltaA* showed 16- to 8-fold differences in susceptibility compared to the WT (Table 1). Complementation of JE2_*auxA* and JE2_*auxB* returned susceptibility to that of the WT (JE2_*auxA*-C and JE2_*auxB*-C, respectively) (Table 1). Also D-alanylation of teichoic acids is important for cells to withstand D-serine toxicity as addition of the *dlt* pathway inhibitor, amsacrine reduced the MIC of WT cultures to the same level as JE2_*auxA* and JE2_*ltaA*. Thus, both LTA structure and alanylation is impacts D-serine susceptibility.

Previous studies have shown that the promiscuous carboxypeptidase activity of PBP4 can incorporate D-serine into the stem peptide of PG on the expense of D-alanine [12], and that the addition of L- or D-alanine rescues *S. aureus* from D-serine stress [10, 26]. Accordingly, L-alanine (1 or 10 mM) increased the D-serine MIC of JE2 WT by 2-fold, whereas addition of D-alanine increased the MIC by >4-fold (Table 1). L-alanine must enter the cell to be converted by the L-alanine racemase (*alr)* to D-alanine before being integrated into the cell wall. D-alanine is however readily available in the extracellular space where PBP4 can exchange it for D-serine in

the stem peptide directly. The ability of low concentrations of D-alanine to raise high D-serine MIC levels indicate that D-alanine is a better substrate for the PBP4 exchange reaction than D-serine. Also, addition of 10 mM D-ala-D-ala did not rescue the phenotype and had a synergistic effect with D-serine again supporting that D-serine incorporation and the competitive effect of D-alanine is taking place in the extracellular space (Table 1). Importantly, for the mutants with defects in LTA, the greatly impaired growth in the presence of D-serine was mitigated by D- and L-alanine with greatest effect of 10 mM D-alanine in the *auxA* mutant, increasing D-serine MIC by 16-fold. Thus, D-serine toxicity is closely related to LTA integrity.

Table 1. *D-serine MICs [mM] of WT, transposon inactivated mutants and complemented* aux *mutants, with or without addition of L/D-ala, D-ala-D-ala or amsacrine. ND, not determined.*

	[mM]	**WT (JE2)**	**JE2_*auxA***	**JE2_*auxB***	**JE2_*ltaA***	**JE2_*ypfP***	**JE2_*auxA*-C**	**JE2_*auxB*-C**
	0	**125**	7,8	15,6	7,8	3,9	125	125
L-ala	1	**250**	7,8	31,25	15,6	7,8	ND	ND
	10	**250**	15,6	62,5	62,5	15,6	ND	ND
D-ala	1	**250**	15,6	62,5	31,25	7,8	ND	ND
	10	**>500**	125	250	62,5	31,25	ND	ND
D-ala-D-ala	10	**62,5**	1,95	3,9	7,8	3,9	ND	ND
amsacrine	100 ug/ml	**7,8**	ND	ND	ND	ND	ND	ND

D-serine stress increases expression of export proteins in *auxA* mutant cells. To address how LTA associated proteins protect the *S. aureus* cells from D-serine stress, we compared protein abundance in an *auxA* deletion mutant (JE2Δ*auxA*) to that of the JE2 WT, when grown to mid-exponential phase in TSB with or without D-serine, at a concentration suitable for growth of both WT and mutant strains (1.5 mM) (Table 2 and Table 3). Changes in TSB medium were added as a control to distinguish between changes in protein abundance that are due to the *auxA* mutation (TSB), and changes caused by D-serine addition to the growth medium (D-ser).

The SecA2 protein was the most increased in abundance between the *auxA* mutant and WT when the cells were grown in presence of D-serine. SecA2 is a member of the accessory Sec protein export pathway, responsible for the export of the heavily glycosylated SraP adhesion protein [27]. This, together with increased protein levels of SAUSA300_1606 (important for protein secretion

during signal peptidase inhibition [28]), and SAUSA300_1334 (protein containing a signal peptidase type II domain) indicates that at least some protein export pathways are important to compensate the lack of AuxA during D-serine stress (Table 2).

Members of the guanine metabolic pathway (PurS, PurC and PurN) were likewise increased in the JE2Δ*auxA* strain upon D-serine treatment. This pathway have previously been reported to be important for high homogeneous oxacillin resistance through the activation of the stringent response [29, 30]. Influx into this pathway could stimulate the stringent response, which would result in slower growth and increased levels of e.g. PBP2a [31]. This could assist in the increased expression seen for PBP2a, although potentially resulting from the *auxA* mutation rather than D-serine treatment, as the changes with and without D-Serine are similar. Western blots were however unable to confirm elevated PBP2a levels in the JE2_*auxA* transposon mutant (manuscript 2). Other proteins increased in abundance include transcriptional regulators and members of amino acid metabolism (Table 2).

Table 2. *Increased protein abundance in JE2Δ*auxA *compared to WT, when grown in TSB with (D-ser) or without (TSB) presence of 1.5 mM D-serine. Proteins with a log2 difference of 1 or above of the JE2Δ*auxA *mutant compared to WT are shown for samples grown in TSB or D-serine individually.*

Accession Number	Gene name	Protein description	Fold change (log2)	
			TSB	**D-Ser**
SAUSA300_2584	*secA2*	preprotein translocase subunit secA	1,2	**2,5**
SAUSA300_0032	*mecA*	penicillin-binding protein 2a	2,5	**2,3**
SAUSA300_0683	-	transcriptional regulator, DeoR family; fructose operon transcriptional repressor	0,6	**2,1**
SAUSA300_2363	-	cation efflux family protein	-0,5	**1,9**
SAUSA300_2562	-	33AA peptide fragment	1,0	**1,5**
SAUSA300_2277	*hutI*	Imidazolonepropionase; Part of histidine degradation to glutamate	0,6	**1,4**
SAUSA300_0226	*fadB*	3-hydroxyacyl-CoA dehydrogenase	3,8	**1,4**
SAUSA300_1888	-	Trp repressor	1,6	**1,4**
SAUSA300_0266	-	Bacterial Pleckstrin Homology domain	0,6	**1,3**

SAUSA300_0194	-	sucrose-specific phosphotransferase system (PTS) transporter protein	-0,8	**1,2**
SAUSA300_1976	-	succinyl-diaminopimelate desuccinylase	-0,5	**1,2**
SAUSA300_0969	*purS*	phosphoribosylformylglycinamidine synthase	0,3	**1,2**
SAUSA300_1699	-	pseudouridine synthase;	-1,7	**1,2**
SAUSA300_0968	*purC*	phosphoribosylaminoimidazole-succinocarboxamide synthase; Acid-D-amino-acid ligases	0,1	**1,1**
SAUSA300_2168	-	AAA^{+} class of chaperone-like ATPases	0,4	**1,1**
SAUSA300_2149	*lacG*	6-phospho-beta-galactosidase; Glycosidase that hydrolyses O- and S-glycosyl compounds	0,3	**1,1**
SAUSA300_1606	-	Type IV secretion system pilin domain; required for protein secretion upon SPase inhibition	0,3	**1,1**
SAUSA300_2276	-	Peptidase, M20/M25/M40 family	-0,9	**1,1**
SAUSA300_2546	*betB*	betaine-aldehyde dehydrogenase Part of glycine, serine and threonine metabolism	0,8	**1**
SAUSA300_0636	*dhaK*	glycerone phosphotransferase	0,1	**1**
SAUSA300_0974	*purN*	phosphoribosylglycinamide formyltransferase	-0,1	**1**
SAUSA300_1679	*acsA*	acetyl-coenzyme A synthetase	-0,1	**1**
SAUSA300_0309	-	ABC transporter ATP-binding protein	0,7	**1**
SAUSA300_1288	*dapA*	4-hydroxy-tetrahydrodipicolinate synthase; Lysine biosynthesis	-0,7	**1**
SAUSA300_0394	-	FAD/NAD(P)-binding Rossmann fold Superfamily	0,1	**1**
SAUSA300_1334	-	Signal peptidase type II domain	-2,7	**1**

Transcriptional regulators and cell division proteins are decreased in expression in the *auxA* mutant during D-serine stress. The least abundant protein in the *auxA* mutant compared to WT after D-serine treatment was the AuxA protein, which serves as a good indicator of high data quality (Table 3). Among the significantly decreased gene products, several were transcriptional regulators, including SarV, SarX, PrsS and DeoR family regulatory proteins. SarV and SarX are both members of the the SarA protein family. SarV is reported to induce autolysin transcription and activity [32] and SarX negatively regulates cell surface-associated proteins and virulence factors,

in part by inhibiting the agr two-component system [33]. SarV increase autolytic activity both by an increase in autolysin transcription and reduced transcripts of autolytic inhibitors such as LrgB [32]. However, LrgB abundance is reduced in the *auxA* mutant upon D-serine treatment, why additional regulatory mechanisms must be in play. LrgB is an anti-holin protein that together with LrgA is thought to inhibit transport of cell wall hydrolases across the membrane by the CidAB holins [34]. Inactivating *lrgB* results in increased hydrolase activity [35], why the decrease in LrgB protein levels by D-serine treatment points to a reduction in hydrolase activity of the *auxA* deletion mutant. Although the SecA2 is the most augmented protein, several surface-associated and transport proteins are downregulated upon D-serine treatment in the *auxA* mutant. As the AuxA protein shares structural similarities to SecDF of *Thermus thermophiles* (manuscript 2), the *auxA* deletion might alter the activity of different protein export pathways, provided that it itself carries an assisting role in protein translocation.

PrsS is the *S. aureus* homologue of the *Bacillus subtilis* protease PrsW, which cleaves the anti-sigma factor RsiW to activate the σ^W response. PrsS phenocopies σ^S by increasing transcription of both cell wall acting genes (*mecA*, *hmrA*, *femB*) and genes essential for cell division (*ezrA*) [36]. The decrease in PrsS might serve to limit PG synthesis and cell division when the autolytic system is compromised.

Interestingly, the cell division proteins DivIC, FtsL and lipid II flippase MurJ all exhibited decreased abundance in the *auxA* mutant during D-serine stress. Together with DivIB, DivIC and FtsL recruits MurJ to the septum in later stages of cell division [37]. Lesser abundance of these proteins could be a sign of stalled septum formation and/or lowered PG cross-linking rates as a consequence of D-serine integration into PG stem peptides or cross-bridges. Furthermore, it may represent a coping strategy for the cells by lowering growth rates when hydrolase activity is low.

Table 3. *Decreased protein abundance in JE2Δ*auxA *compared to WT, when grown in TSB with (D-ser) or without (TSB) presence of 1.5 mM D-serine. Proteins with a log2 difference of 1 or above of the JE2Δ*auxA mutant compared to WT are shown for samples grown in TSB or D-serine individually.

Accession Number	Gene name	Protein description	Fold change (log 2)	
			TSB	**D-Ser**
SAUSA300_0980	*auxA*	Lipoteichoic acid associated gene	-3,9	**-5,1**

SAUSA300_ pUSA030001	*repA*	replication initiator protein	-2,4	**-2,3**
SAUSA300_1739	-	calcium-binding lipoprotein endonuclease	0,1	**-2,1**
SAUSA300_2218	*sarV*	HTH-type transcriptional regulator; Positive regulator of several autolysins under sarA and mgrA repression	0,0	**-2,1**
SAUSA300_2516	-	oxidoreductase, short chain dehydrogenase/reductase family	-1,1	**-2,1**
SAUSA300_1045	*uvrC*	Excinuclease ABC subunit C; Nucleotide excision repair	0,2	**-2,0**
SAUSA300_0031	*maoC*	(R)-specific enoyl-CoA hydratase	-0,3	**-2,0**
SAUSA300_2345	*nirD*	nitrite reductase small subunit (Nitrite to ammonia)	-0,3	**-2,0**
SAUSA300_2440	*fnbB*	fibronectin binding protein B	1,5	**-2,0**
SAUSA300_0654	*sarX*	HTH-type transcriptional regulator; negatively regulate cell surface-associated proteins / agr	0,9	**-2,0**
SAUSA300_2261	-	DeoR family regulatory protein	-1,0	**-2,0**
SAUSA300_0230	*prsS*	anti-sigma factor protease	-0,9	**-1,9**
SAUSA300_0145	-	phosphonate ABC transporter	-0,6	**-1,9**
SAUSA300_0257	*lrgB*	antiholin protein inhibiting murein hydrolase activity	1,4	**-1,8**
SAUSA300_1626	*rpmI*	50S ribosomal protein L35	-2,5	**-1,8**
SAUSA300_2070	-	L-threonylcarbamoyladenylate synthase	-0,8	**-1,7**
SAUSA300_2231	*fdhD*	Formate dehydrogenase family accessory protein	-0,7	**-1,6**
SAUSA300_0293	-	Antitoxin located in protein type VII secretion system	-0,4	**-1,6**
SAUSA300_0429	*ybjB*	PAP2 family protein; Type 2 phosphatidic acid phosphatase	-0,1	**-1,6**
SAUSA300_2155	*lacA*	Galactose-6-phosphate isomerase	-0,1	**-1,6**
SAUSA300_1680	*acuA*	Acetoin utilization protein; Acyltransferase	0,7	**-1,5**
SAUSA300_1267	*trpB*	Tryptophan synthase, beta chain	0,5	**-1,5**
SAUSA300_0671	-	ABC transporter; ATP-binding protein	0,5	**-1,5**
SAUSA300_1870	-	Aromatic acid exporter family	-0,8	**-1,5**
SAUSA300_0485	*divIC*	Cell division protein	-0,2	**-1,4**
SAUSA300_1074	*ftsL*	Cell division protein	-0,4	**-1,4**
SAUSA300_1700	*murJ*	Lipid II Flippase	0,2	**-1,4**
SAUSA300_1238	-	Homologue of HigB toxin	0,3	**-1,3**
SAUSA300_2398	-	ABC transport system permease protein	0,5	**-1,3**
SAUSA300_1701	-	NAD(FAD)-utilizing dehydrogenase	0,3	**-1,3**
SAUSA300_1695	-	Phosphotransferase family; aminoglycoside inactivation	0,6	**-1,3**

SAUSA300_0353	-	ABC-2 transporter family protein	0,0	**-1,3**
SAUSA300_1258	-	4-oxalocrotonate tautomerase; Xenobiotics biodegradation	1,2	**-1,3**
SAUSA300_2338	*nreB*	O_2-sensing histidine kinase	-1,0	**-1,3**
SAUSA300_0303	-	cystatin-like fold lipoprotein; Signal peptide for extracellular localization	0,2	**-1,2**
SAUSA300_1230	*efb*	fibrinogen-binding protein	0,1	**-1,2**
SAUSA300_0730	-	GGDEF domain protein; diguanylate cyclase activity	-0,3	**-1,2**
SAUSA300_1154	*cdsA*	phosphatidate cytidylyltransferase	0,8	**-1,2**
SAUSA300_1342	-	Hypothetical protein	-1,8	**-1,2**
SAUSA300_0850	*mnhF*	Na(+)/H(+) antiporter subunit F	0,0	**-1,2**
SAUSA300_2238	*ureA*	urease, gamma subunit	0,8	**-1,2**
SAUSA300_1017	*ctaM*	Required for menaquinol oxidase activity	0,7	**-1,1**
SAUSA300_0677	-	deoxyribodipyrimidine photolyase; single strand DNA repair	0,4	**-1,1**
SAUSA300_1934	-	phi77 ORF020-like protein; phage major tail protein	-0,9	**-1,1**
SAUSA300_1228	*thrB*	homoserine kinase; Glycine, serine and threonine metabolism	0,2	**-1,1**
SAUSA300_0136	*sasD*	cell wall surface anchor family protein; LPXTG cell wall anchor motif	0,3	**-1,1**
SAUSA300_2492	-	acetyltransferase family protein	0,5	**-1,1**
SAUSA300_2349	-	formate/nitrite transporter family protein	0,3	**-1,1**
SAUSA300_2475	-	acyl-CoA thioester hydrolase	-0,2	**-1,1**
SAUSA300_0216	*uhpT*	Organophosphate:Pi antiporter (OPA) family; hexose phosphate transport protein	0,4	**-1,1**
SAUSA300_2367	*hlgB*	gamma-hemolysin component B; Pore-forming toxin	-0,1	**-1,0**
SAUSA300_1089	*lspA*	lipoprotein signal peptidase; Type II protein export peptidase	0,4	**-1,0**
SAUSA300_2233	-	BioY family protein; biotin transport system substrate-specific component	0,4	**-1,0**
SAUSA300_1524	-	DeoR family transcriptional regulator	-0,5	**-1,0**
SAUSA300_2295	-	Surface located protein	0,7	**-1,0**

AuxA and AuxB interact to form a putative hetero-multimeric complex associated with the LTA pathway. Lipoteichoic acids are important for cell division [38] and interactions between members of the LTA pathway and cell division proteins have been described [19]. As *auxA* and *auxB* mutants share several phenotypes with *ltaA* and *ypfP* LTA pathway mutants (manuscript 2), we reasoned that AuxA and AuxB proteins would interact with members of the LTA pathway and

possibly with members of the cell division machinery. Utilizing the bacterial adenylate cyclase two-hybrid (BACTH) system, we constructed N- or C-terminal fusions of AuxA or AuxB to the T25 or T18 fragment of the *Bordetella pertussis* adenylate cyclase. We co-transformed AuxA and AuxB constructs with constructs of members of the LTA or cell division pathways and spotted these on plates containing X-gal and IPTG to screen for blue color development, indicative of positive interactions between the transformed constructs (Figure 1). As *auxA* and *auxB* mutants share multiple phenotypes [21, 22], we expected the two proteins to interact. Accordingly, AuxA and AuxB formed strong interactions with and amongst themselves, indicating that AuxA and AuxB form a hetero-multimeric complex. AuxB also binds the immediate downstream gene product (SAUSA300_1004), which may represent an additional member to the complex. Additionally, the Aux proteins form strong interactions with LtaA, LtaS and YpfP, and with the final protein in the D-alanylation pathway, DltD, supporting the premise that AuxA and AuxB are LTA associated proteins that provide stability to LTA pathway members and/or the growing polymer and its modifications (manuscript 2).

Aux proteins interact with members of the divisome and PG synthesis. When examining binding to cell division proteins, we found interactions of both Aux proteins with DivIB, DivIC and FtsL. These three proteins form a septum synthesis initiator complex, which recruit the lipid II flippase MurJ to start septal formation [37]. The binding of the Aux proteins to the DivIB-DivIC-FtsL complex along with MurJ, could assist the flipping activity of MurJ or stabilize the complex during septum formation. The fact that DivIC, FtsL and MurJ all are downregulated during D-serine treatment in cells lacking AuxA could indicate a reduced need for septal PG synthesis during D-serine stress without AuxA present. Interestingly, both Aux proteins bind EzrA while AuxB additionally binds GpsB. EzrA depletion causes delocalization of GpsB and PBP2 from the septum, and EzrA is thought to recruit DivIB-DivIC-FtsL, PBP1, PBP2 and GpsB to mid-cell to initiate septal growth [39]. Upon arrival to midcell, GpsB interacts with FtsZ to create bundles that stimulate FtsZ GTP hydrolysis and treadmilling [40]. The Aux complex may play an important role in stabilizing the divisome via EzrA and GpsB interactions. Aux binding to the cell division inhibitor SosA was shown to inhibit growth upon over-expression [41], supporting the importance of the Aux complex in *S. aureus* divisome stability.

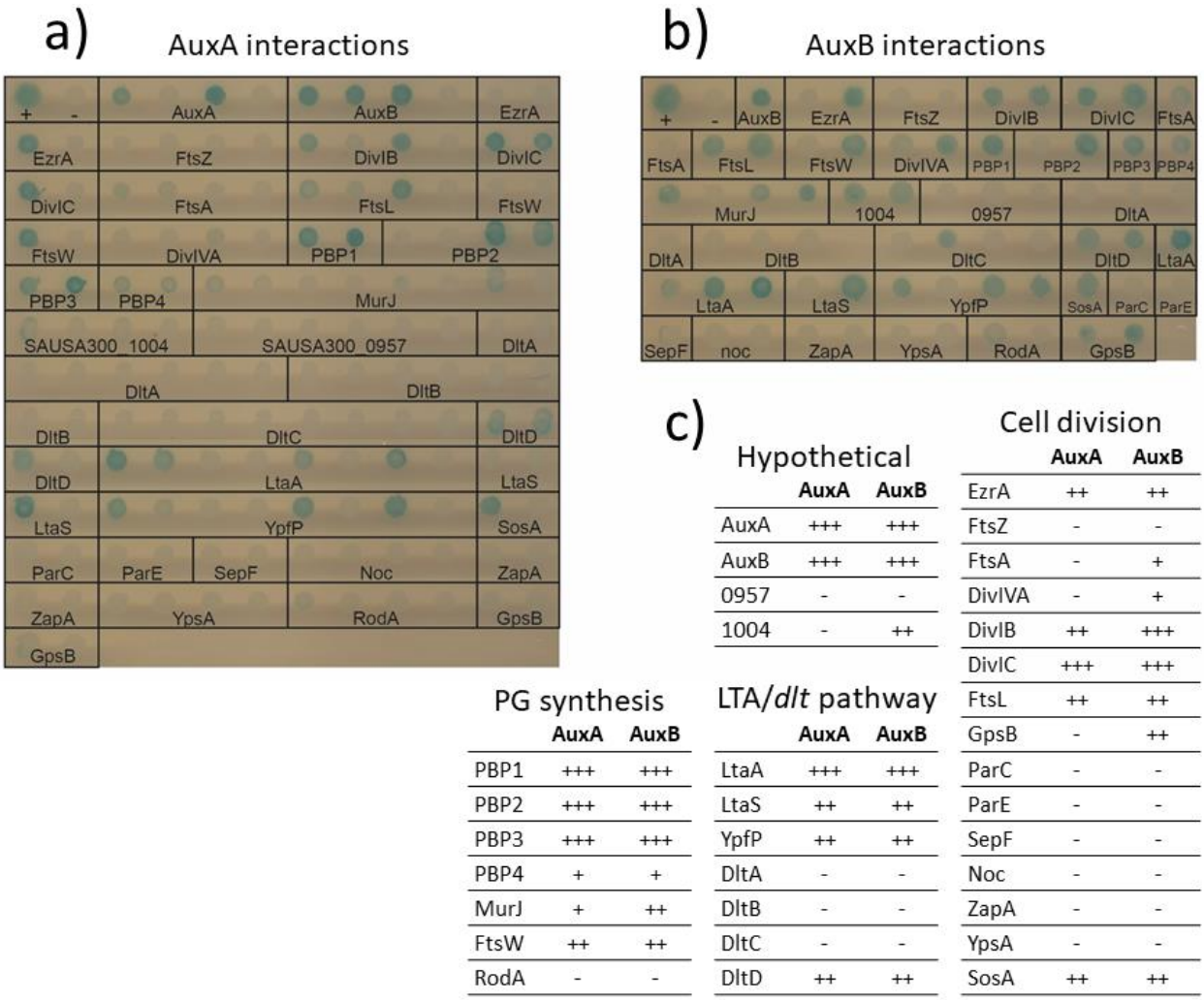

Hypothetical

	AuxA	AuxB
AuxA	+++	+++
AuxB	+++	+++
0957	-	-
1004	-	++

Cell division

	AuxA	AuxB
EzrA	++	++
FtsZ	-	-
FtsA	-	+
DivIVA	-	+
DivIB	++	+++
DivIC	+++	+++
FtsL	++	++
GpsB	-	++
ParC	-	-
ParE	-	-
SepF	-	-
Noc	-	-
ZapA	-	-
YpsA	-	-
SosA	++	++

PG synthesis

	AuxA	AuxB
PBP1	+++	+++
PBP2	+++	+++
PBP3	+++	+++
PBP4	+	+
MurJ	+	++
FtsW	++	++
RodA	-	-

LTA/*dlt* pathway

	AuxA	AuxB
LtaA	+++	+++
LtaS	++	++
YpfP	++	++
DltA	-	-
DltB	-	-
DltC	-	-
DltD	++	++

Figure 1. BACTH interaction network of Aux proteins. *Interactions between T18- or T25-fused AuxA* ***(a)*** *or AuxB* ***(b)*** *constructs and constructs with members of PG synthesis, cell division and LTA/dlt pathways.* ***(c)*** *The interactions are scored based on color development on plates containing X-gal. +++, more than positive control; ++, same as positive control; +, less than positive control; -, no color development. Plasmid constructs were made with N- and C-terminal fusions to the T18 and T25 fragments of the BACTH system why multiple interactions between two proteins are shown.*

When lipid II is flipped across the septal membrane, its glycan moieties are connected to a growing glycan chain of connected lipid II molecules by the transglycosylation activities of PBP2, and the shape, elongation, division and sporulation (SEDS) protein, FtsW [42, 43]. The growing glycan strands are then integrated into the growing PG network via cross-linking of the lipid II stem peptides by transpeptidase activity of the PBPs [44]. Both Aux proteins strongly bound PBP1, PBP2 and PBP3 and FtsW. FtsW and PBP1 form a complex which arrives to the division site prior to MurJ recruitment, and is suspected to stabilize the early divisome [42]. Interestingly, the

Aux proteins only bound PBP3 and not RodA, the SEDS protein forming a complex with PBP3 and being responsible for sidewall PG synthesis at mid-cell during septation [42]. Based on the interactions found via the BACTH system, the AuxA and AuxB proteins could form a hetero-multimeric complex that, through interactions with members of the LTA, cell division and PG synthesis pathways, supports and stabilizes LTA polymerization and cell division. The highly similar interaction patterns shared between the Aux proteins and LTA pathway members [19], suggests the Aux proteins are LTA associated.

***auxA*, *auxB*, *ypfP,* and *ltaA* mutants display cell separation inhibition amplified by D-serine exposure.** To gain a deeper insight into the consequences of D-serine treatment, we looked at mid-exponential cultures grown for an additional two hours in presence or absence of WT MIC (125 mM) D-serine, using transmission electron microscopy (TEM) (Figure 2a). Grown in TSB, none of the mutants showed multiple cell division septa or new septa non-orthogonal to previous division sites as previously reported in other strain backgrounds [17, 23]. However, JE2_*auxA*, _*auxB*, and _*ypfP* showed an increase in the number of cells with complete septa, indicating an impaired separation after the division ended. JE2_*ltaA* showed an increase in cell numbers with partial septal formation (Figure 2b).

D-serine treated WT cells showed a similar increase in the number of cells having trouble separating after ended cell division, similarly to the mutants grown without D-serine. This phenotype was more pronounced in all four mutants showing lysed cells and newly divided cells sticking together creating misshaped daughter cells. Some cells succeeded to separate while still attached to their sister cell via old layers of PG. When held back long enough, the cell wall started to rupture as the cells grew without separating from the daughter cells (most obvious in the JE2_*ypfp* mutant) (Figure 2a). The phenotypes of JE2_*auxA*, _*auxB*, and _*ypfP* indicate that the mutations impact the autolytic activity needed for cell separation after completion of the septum, which correlates with the reduced triton X-100 mediated lysis in mutant compared to WT cells (manuscript 2).

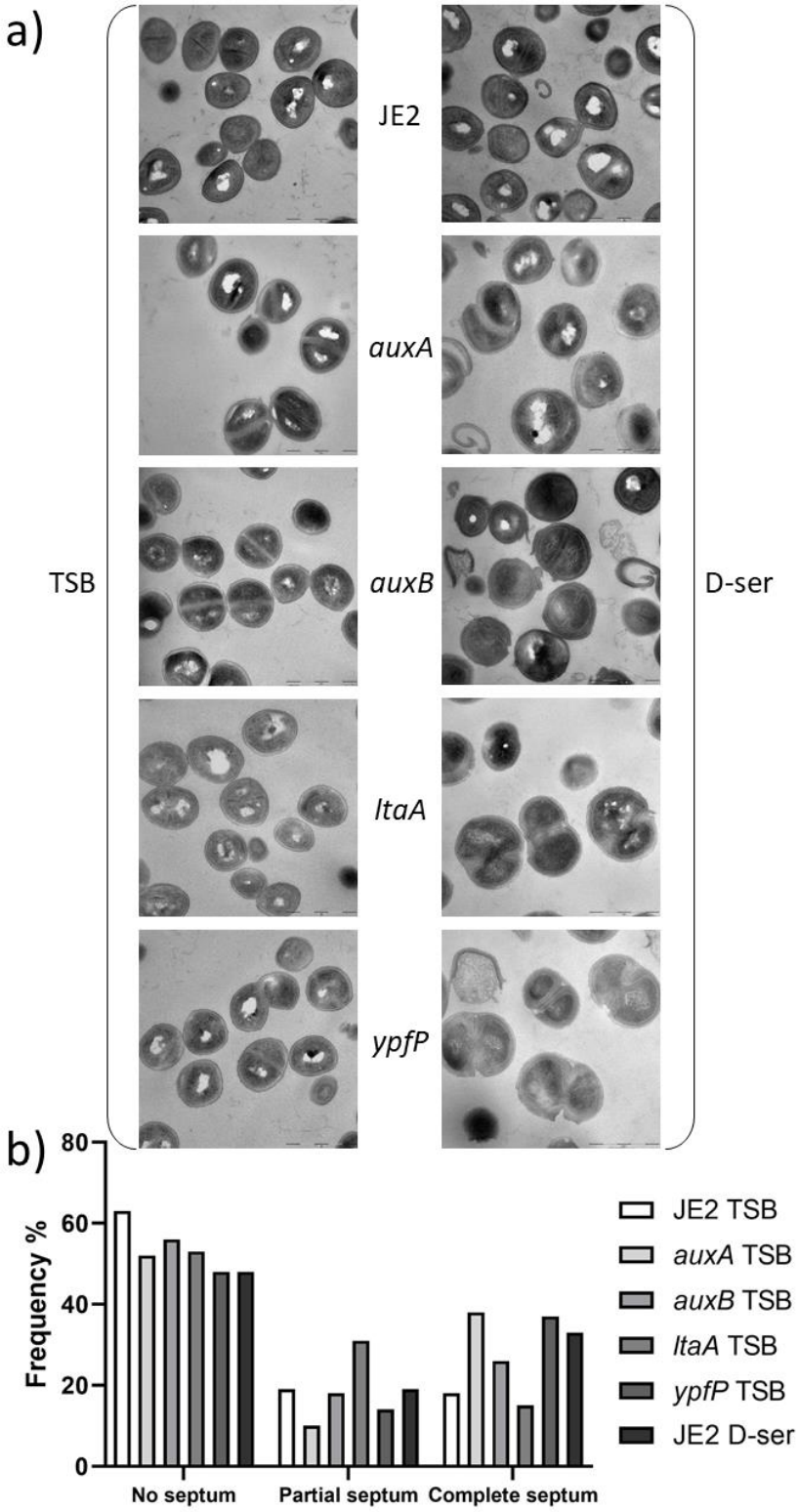

Figure 2. D-serine inhibit cell segregation. *(a) Transmission electron microscopy images of WT and transposon inactivated mutant cultures grown in presence or absence of 125 mM D-serine for two hours after reaching mid-exponential phase. (b) Cell cycle stage frequency plot (n = >120). Mutant cells treated with D-serine were too indistinguishable to report.*

Impact of *auxA* and *auxB* on autolysis. In order to test if changes in abundance/activity of autolytic enzymes were altered in JE2_*auxA* and _*auxB*, we examined mid-exponential whole cell lysates using standard zymography on gels containing JE2 WT heat-killed cell lysates (to visualize Atl amidase and Sle1 bands) or *Micrococcus luteus* purified cell wall (to visualize Atl glucosaminidase bands) (Figure 3). In TSB, a slight increase in intensity in Atl amidase (AM) and glucosaminidase (GL) bands was witnessed for both JE2_*auxA* (Figure 3a) and JE2_*auxB* (Figure 3b) compared to JE2 WT, whereas no obvious differences were seen for Sle1. If treated with the PBP2/PBP3 inhibitor oxacillin at sub-MIC, the increase in Atl AM and GL band intensity of the *aux* mutants compared to WT were more pronounced. Taken that the *aux* mutants show decreased lysis upon triton X-100 stimulation, the increase in Atl band intensity could act to compensate for the reduced lysis profiles. Presence of sub-MIC oxacillin decreased JE2_*auxA* and JE2_*auxB* triton X-100 induced lysis profiles (manuscript 2), while clearly increasing intensity of Atl bands (Figure 3). This could indicate inhibitory conditions present in JE2_*aux* whole cells that are lacking in the zymogram conditions containing heat-killed JE2 WT cells or *Micrococcus luteus* purified cell wall. These inhibitory conditions may be caused by decreased LTA stability (manuscript 2) leading to inhibition and/or mislocalization of the autolytic machinery.

Recently, it has been shown that FmhA and FmhC incorporates D-serine residues into the cross-bridge between PG peptide stems, and that D-serine in the fifth position in the bridge prevents LytN activity [13]. LytN contains a YSIRK/GS-type signal peptide that secretes it into the cross-wall between dividing cells [45], where it cleaves the peptide bond between the fifth Gly residue of the pentaglycine cross-bridge and the D-Ala of the stem peptide [14]. We predict that substitution of D-alanine of the stem peptide with D-serine also decreases LytN activity and propose that this reduction may be responsible for the observed phenotypes. Future experiments will be aimed at addressing this notion.

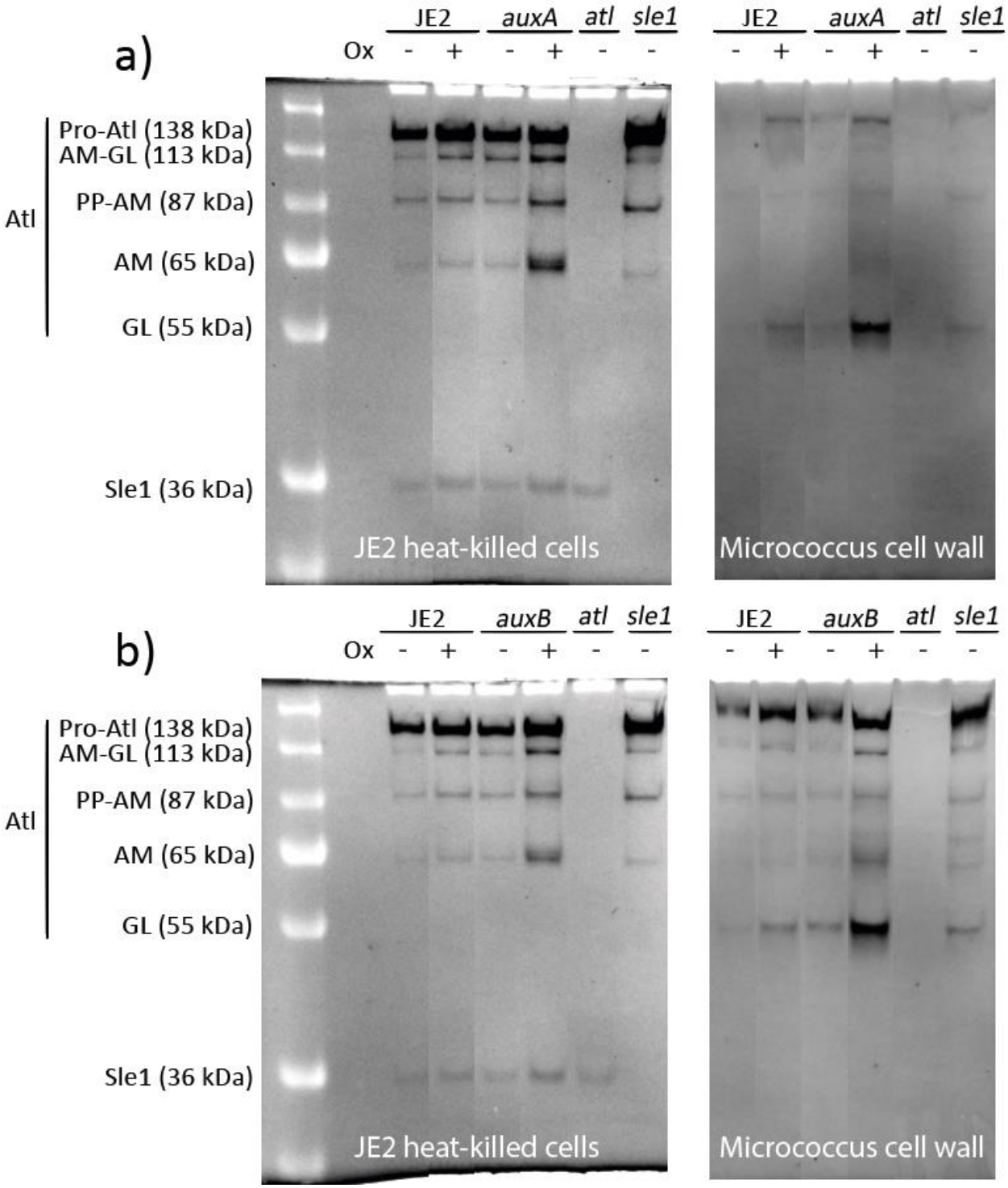

Figure 3. Increased Atl band intensity of aux mutants. *Zymogram of JE2 WT, JE2_*auxA ***(a)****, and JE2_*auxB ***(b)*** *whole cell lysates grown to mid-exponential phase with or without presence of 0.1 µg/ml oxacillin was normalized and loaded onto SDS gels containing heat-killed JE2 WT cells or* Micrococcus luteus *purified cell wall.* atl *and* sle1 *transposon inactivated mutants were added as negative controls. Inverted images are shown.*

Teichoic acids have been proposed to be involved in the localization of the autolytic enzymes. LytM domains, of which Sle1 [46, 47] holds three and LytN one [14], are shown to bind the disaccharide repeat units of PG, whilst being repelled by wall teichoic acids [47] and LTA in *Lactococcus lactis* [48]. The major autolysin Atl is directed to the cell division site by binding of repeat domains to LTA [49]. The LTA is thought to act in close proximity to the membrane [50], which could guide the LytM containing protein LytN away from the membrane and into the less dense central cavity between two dividing daughter cells [51]. Disturbance of LTA structure and/or modifications would likely cause cell separation problems through inhibition or mislocalization of the cross-wall located LytN and/or the excreted Sle1 and Atl autolysins.

The LTA polymer is negatively charged due to the phosphate containing backbone [18]. Removal of the D-alanine modifications that neutralize the negative polymer, through inactivation of the *dlt* pathway, is reported to decrease autolytic activity [52]. This correlates with a 16-fold decrease in D-serine MIC when the DltB inhibitor amsacrine is added to the growth medium (Table 1). Inactivation of *ypfP* or *ltaA* will abrogate or diminish availability of the Glc_2DAG anchor to the LTA synthase [53]. This has shown to create extended LTA polymers loosely attached to the membrane [54] that, when left uncoated due to amsacrine treatment, is detrimental to the cell [23]. Amsacrine is as well synthetically lethal against JE2_*auxA* and _*auxB* [22], without these mutants having extended LTA polymers (manuscript 2). However, the release of LTA polymers from the membrane seen in these mutants might be what causes the autolytic inhibitory effect of these mutants (manuscript 2).

Based on structure predictions, AuxA resembles SecDF from *Thermus thermophilus* (manuscript 2). SecDF is an accessory component of the Sec protein export pathway [55], and it is tempting to speculate an additional role besides LTA stability in protein secretion. The upregulation of SecA2 in the AuxA deletion mutant during growth both with and without D-serine imply that protein export could be altered by the lack of AuxA. The accessory protein export pathway that SecA2 is a member of transports the serine-rich surface protein SraP, which anchor to the cell wall from where it can provide adhesion to human plates [56]. SraP is predicted to be 227 kDa, and alterations in the presence of a protein of this size could provide some structural rearrangements of the cell wall, with unknown consequences. The increase in SecA2 could as

well be to compensate for altered activity of other protein export pathways, and it is tempting to speculate that transport of autolytic enzymes could be either directly or indirectly affected by the *auxA* deletion.

The ability of D-alanine to buffer D-serine stress (Table 1), indicate that D-serine exchange with D-ala of the PG stem peptide due to the promiscuous activity of PBP4 [12], rather than integrate into the pentaglycine cross-bridge. Addition of glycine as well put stress to both wild type [26] and *auxA, auxB, ltaA,* and *ypfP* mutant cells ([17] and own observations), by exchanging D-alanine in the PG stem peptide [26]. As the addition of glycine would not affect the pentaglycine cross-bridge composition (Gly exchanged for Gly), the integration of glycine (and likely D-serine) into the fourth position of the PG stem, rather than changes in the cross-bridge, is what would inhibit LytN endopeptidase activity. Sle1 and Atl hold N-acetylmuramoyl-L-alanine amidase and N-acetylglucosaminidase (Atl only) activities, why these enzymes would not be directly affected by D-serine or glycine incorporation into the PG stem, but might be inhibited or mislocated by altered LTA structures of the *aux, ltaA* and *ypfP* mutations.

We have here presented data to support a role for D-serine as a compound that inhibit cells from segregating after ended cell division. Mutations in genes synthesizing or flipping the LTA anchor or stabilizing the LTA polymer and/or its synthesis machinery, all show cell segregation defects, which become fatal upon D-serine treatment. The Aux proteins form a hetero-multimeric complex that interact directly with LTA pathway members and DltD, which is shown to provide stability to the LTA polymer (manuscript 2). The cell divisional proteins EzrA, SosA, and GpsB along with the DivIB-DivIC-FtsL division complex that recruit MurJ to the division septum, as well interact with the Aux complex. As JE2_*auxA* cells are unable to spilt upon D-serine stress, septal growth becomes undesirable, which could be why the *auxA* mutant downregulates DivIB, FtsL and MurJ. Likewise, the interactions of the Aux complex members to the PG synthesis machinery could provide a regulative function, leaving the PBPs of *aux* mutants active when slow synthesis rates are needed. The regulative function could as well be of the autolysins to initiate hydrolase activity when cell division has ended, and daughter cells are to split.

We here propose a model by which the autolytic defect of mutants of the LTA pathway (*ltaA* and *ypfP*) or Aux complex (*auxA* and *auxB*) fail to cope with the additional autolytic inhibition provided by D-serine stress (Figure 4). In wild type cells, LTA is anchored to the membrane by Glc_2DAG and is coated with sugar and D-alanine moieties that neutralize the polymer, keeping the autolysins active (Figure 3a). When the cell is challenged by D-serine, this is integrated into the fourth position of the PG stem peptide, inhibiting the activity of the cross-wall located LytN endopeptidase (Figure 3b). If the cell is further challenged by an inactivation of either *ltaA, ypfP, auxA* or *auxB*, LTA will detach from the membrane and add to the inhibitory effect, which might include inhibition of Sle1 and Atl outside the cross-wall. Detached LTA polymers might as well lead to mislocalization of LytN, Sle1 and Atl. In JE2_*ypfP* and JE2_*ltaA* the polymers are known to be longer and more negative, whereas JE2_*auxA* and JE2_*auxB* have WT length polymers. The inactivation of *auxA* and *auxB* might as well influence protein export and with that, influence presence of important players needed in the cross-wall for proper cell segregation (Figure 3b).

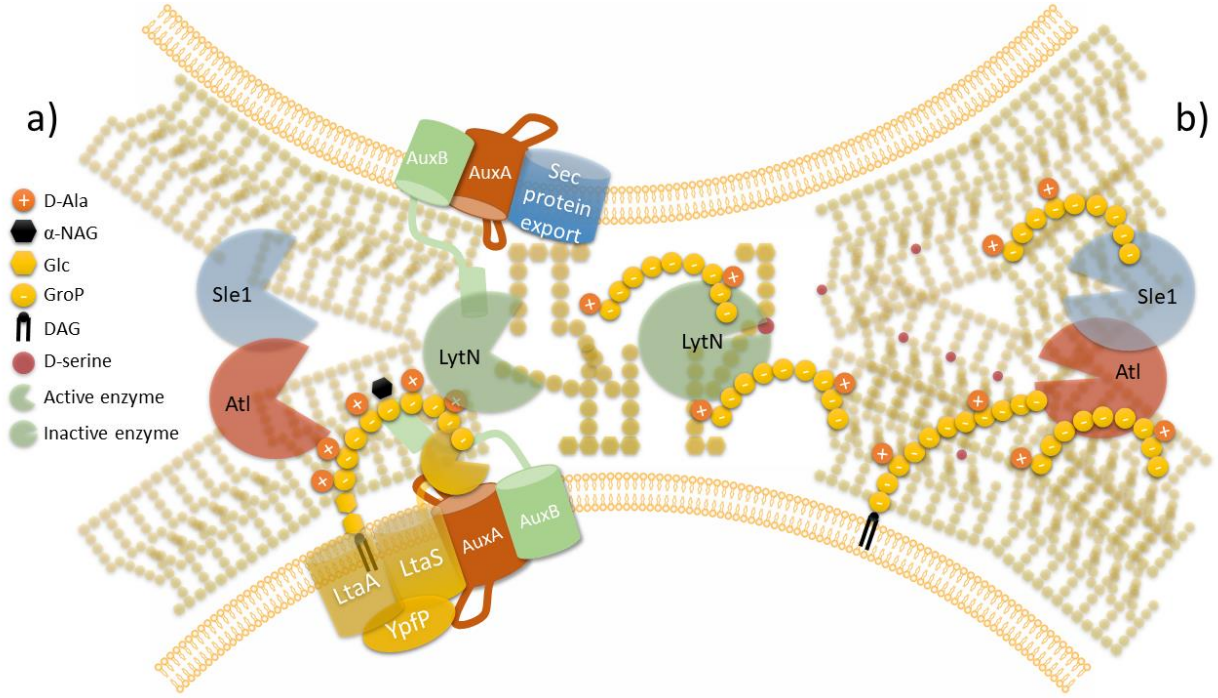

Figure 4. Proposed model for the D-serine effect and the role of LTA associated genes in D-serine tolerance. *During non-stressful conditions* ***(a)****, the LTA polymer is attached to a Glc_2DAG anchor and decorated with D-alanine and α-N-acetylglucosamine moieties. This allows for stable cell divisional autolytic activity by Sle1 and Atl outside the cross-wall and LytN inside. Upon D-serine stress* ***(b)****, LytN activity is inhibited by the exchange of D-alanine for D-serine in the fourth position of the PG stem peptide. Mutants with altered LTA stability release LTA into the exterior, which bind and further inhibit autolytic activity, leaving the cells unable to segregate.*

Acknowledgements

We would like to thank Professor Yin Chen for the great help with the proteomics assay and data analysis.

We would like to thank Angelika Gründling and Charlotte Millership for the kind gesture of shipping BACTH constructs ANG1284 to ANG1325.

HI was supported by grants from Danmarks Fri Forskningsfond (7017-00079B).

Materials and methods

Bacterial strains and plasmids. Bacterial strains used:

Table 4. *Strains used in this study*

Name	Characteristics	Reference
E. coli IM08B	Lab strain used for cloning	[57]
E. coli BTH101	Adenylate cyclase deficient (*cya*) reporter strain	Euromedex
JE2	USA300 CA-MRSA isolate and parent strain of the Nebraska Transposon Mutant Library	[58]
JE2_*auxA*	NE1044 NTML mutant (SAUSA300_0980)	[59]
JE2_*auxB*	NE1420 NTML mutant (SAUSA300_1003)	
JE2_*ltaA*	NE462 NTML mutant (SAUSA300_0917)	
JE2_*ypfP*	NE1663 NTML mutant (SAUSA300_0918)	
JE2_*atl*	NE460 NTML mutant (SAUSA300_0955)	
JE2_*sle1*	NE1688 NTML mutant (SAUSA300_0438)	
JE2Δ*auxA*	Clean deletion of *auxA* in JE2	Manuscript 2
JE2_*auxA-C*	JE2_*auxA* complemented with chromosomal *auxA* integration	This study
JE2_*auxB-C*	JE2_*auxB* complemented with chromosomal *auxB* integration	This study
	pUT18C-auxA in IM08B; T18 fused to N-terminus of AuxA	This study
	pUT18-auxA in IM08B; T18 fused to C-terminus of AuxA	This study
	pKT25-auxA in IM08B; T25 fused to N-terminus of AuxA	This study
	pKNT25-auxA in IM08B; T25 fused to C-terminus of AuxA	This study
	pUT18C-auxB in IM08B; T18 fused to N-terminus of AuxB	This study
	pKT25-auxB in IM08B; T25 fused to N-terminus of AuxB	This study
	pUT18C-murJ in IM08B; T18 fused to N-terminus of MurJ	This study

	pUT18-murJ in IM08B; T18 fused to C-terminus of MurJ	This study
	pKT25-murJ in IM08B; T25 fused to N-terminus of MurJ	This study
	pKNT25-murJ in IM08B; T25 fused to C-terminus of MurJ	This study
	pUT18C-1004 in IM08B; T18 fused to N-terminus of SAUSA300_1004 gene product	This study
	pKT25-1004 in IM08B; T25 fused to N-terminus of SAUSA300_1004 gene product	This study
	pUT18C-0957 in IM08B; T18 fused to N-terminus of SAUSA300_0957 gene product	This study
	pKT25-0957 in IM08B; T25 fused to N-terminus of SAUSA300_0957 gene product	This study
	pKNT25-0957 in IM08B; T25 fused to C-terminus of SAUSA300_0957 gene product	This study
ANG1284	pKT25-dltA in XL1 Blue; T25 fused to N-terminus of DltA;	[19]
ANG1285	pKT25-dltB in XL1 Blue; T25 fused to N-terminus of DltB;	
ANG1286	pKT25-dltC in XL1 Blue; T25 fused to N-terminus of DltC;	
ANG1287	pKT25-dltD in XL1 Blue; T25 fused to N-terminus of DltD;	
ANG1289	pKT25-ltaA in XL1 Blue; T25 fused to N-terminus of LtaA;	
ANG1290	pKT25-ltaS in XL1 Blue; T25 fused to N-terminus of LtaS;	
ANG1291	pKT25-ypfP in XL1 Blue; T25 fused to N-terminus of YpfP;	
ANG1301	pKNT25-dltA in XL1 Blue; T25 fused to C-terminus of DltA;	
ANG1302	pKNT25-dltB in XL1 Blue; T25 fused to C-terminus of DltB;	
ANG1303	pKNT25-dltC in XL1 Blue; T25 fused to C-terminus of DltC;	
ANG1304	pKNT25-dltD in XL1 Blue; T25 fused to C-terminus of DltD;	
ANG1306	pKNT25-ltaA in XL1 Blue; T25 fused to C-terminus of LtaA;	
ANG1307	pKNT25-ltaS in XL1 Blue; T25 fused to C-terminus of LtaS;	
ANG1308	pKNT25-ypfP in XL1 Blue; T25 fused to C-terminus of YpfP;	
ANG1311	pUT18-dltA in XL1 Blue; T18 fused to C-terminus of DltA;	

ANG1312	pUT18-dltB in XL1 Blue; T18 fused to C-terminus of DltB;	
ANG1313	pUT18-dltC in XL1 Blue; T18 fused to C-terminus of DltC;	
ANG1314	pUT18-dltD in XL1 Blue; T18 fused to C-terminus of DltD;	
ANG1316	pUT18-ltaA in XL1 Blue; T18 fused to C-terminus of LtaA;	
ANG1317	pUT18-ltaS in XL1 Blue; T18 fused to C-terminus of LtaS;	
ANG1318	pUT18-ypfP in XL1 Blue; T18 fused to C-terminus of YpfP;	
ANG1319	pUT18C-dltA in XL1 Blue; T18 fused to N-terminus of DltA;	
ANG1320	pUT18C-dltB in XL1 Blue; T18 fused to N-terminus of DltB;	
ANG1321	pUT18C-dltC in XL1 Blue; T18 fused to N-terminus of DltC;	
ANG1322	pUT18C-dltD in XL1 Blue; T18 fused to N-terminus of DltD;	
ANG1324	pUT18C-ltaA in XL1 Blue; T18 fused to N-terminus of LtaA;	
ANG1325	pUT18C-ltaS in XL1 Blue; T18 fused to N-terminus of LtaS;	

Primers used in this study

***Table 5**. Primers used in this study*

Name	**Sequence**
BACTH_BamHI_auxA_F	CGGGATCCCTCTTTTCTTAGGAAACACGCCG
BACTH_KpnI_auxA_R	GGGGTACCCGTGGTCGCTCTCGTAATTGTAACG
BACTH_BamHI_auxB_F	CGGGATCCCACTGGAGAACAATTTACTCAAATTAAACG
BACTH_KpnI_auxB_R	GGGGTACCCGTTCTTGCTCTTTTTTGTCCTTAACTTC
BACTH_BamHI_0957_F	CGGGATCCCAGTAGAAAAACATACGAAAAGATTGC
BACTH_KpnI_0957_R	GGGGTACCCGTAGTGCTTCTTTTCTAATAATTGCTG
BACTH_BamHI_1004_F	CGGGATCCCAATAGAAAACCTGAATTAATCATGGCTTG
BACTH_KpnI_1004_R	GGGGTACCCGATGATAAATATACTCATCGTCCTTATGTG
BACTH_BamHI_MurJ_F	GATACAGGATCCCAGTGAAAGTAAAGAAATGGTGCG
BACTH_KpnI_MurJ_R	GATACAGGTACCCGTCGTAAAAACCTAACTCTACGTC
pKT+pUT_seq	cactcattaggcaccccagg
pUT18C_seqR	gtaagcggatgccgggagc

pKT25C_seqR	cttcgctattacgccagctg
pKT25N_seqR	gagcagattgtactgagagtgc
auxA_comp_F	GATACAGGATCCGTGTATCTTGGATATCTTGTTTTGTTTG
auxA_comp_R	GATACACCCGGGTTATGGTCGCTCTCGTAATTGTAAC
auxB_comp_F	GATACAGGATCCAGACGACCATCGTTTTTATCCGAC
auxB_comp_R	GATACACCCGGGTTATTCTTGCTCTTTTTTGTCCTTAACTTC

Culture conditions and antimicrobials. Strains were cultured in tryptic soy broth (TSB), Luria-Bertani broth (LB), tryptic soy agar (TSA), or Luria-Bertani agar (LA) (Thermo Fisher Scientific). X-gal solution was from while antibiotics (kanamycin, ampicillin, and tetracycline), Isopropyl β-D-1-thiogalactopyranoside (IPTG), Amino acids (D-serine, D-alanine, L-alanine and D-Ala-D-Ala), and DltB inhibitor amsacrine was purchased from Merck KGaA.

Screening of transposon mutant library. Material from the frozen Nebraska Transposon Mutant Library was transferred with a Deutz 96 cryo-replicator from the 96 wells microtiter plates onto TSA plates containing 1/5 of JE2 WT D-serine minimal inhibitory concentration (MIC) (25 mM). The plates were incubated at 37°C for 24 hours and visually inspected for lack of growth of individual mutants.

Complementation of JE2_*auxA* and JE2_*auxB*. Primer pairs auxA_comp_F/R and auxB_comp_F/R were used to amplify *auxA* and *auxB* genes plus promoter sequences, respectively, before being sub-cloned into pJC1306 [60], using BamHI and SmaI restriction enzymes (Thermo Fisher Scientific). The pJC1306_auxA and pJC1306_auxA plasmids were passed through *E. coli* IM08, before 2 µg of plasmid was transformed into the restriction deficient RN9011, (carrying a plasmid with the SaPI1 integrase) grown at 37 °C for 1 hour and plated on TSA plates containing 10 µg/ml tetracycline. The SaPI1 attachment site integrated plasmids was then moved into JE2_*auxA* and JE2_*auxB* strains by generalized transduction and confirmed by paired-end sequencing using the NextSeq 550 system (Illumina) at Statens Serum Institut (SSI) .

D-serine susceptibility tests. We used the broth microdilution method to assess MIC for D-serine. D-serine was dissolved in TSB and serial two-fold dilutions added to a 96-well round bottom microtiter plate (Corning). A bacterial culture was adjusted with saline to a McFarland standard

of 0.5, diluted 10-fold and 5 µl was transferred to individual wells of the microtiter plate. The plate was incubated at 37°C overnight and the MICs were recorded as the lowest concentration with no growth.

Proteomics preparation and bioinformatics. Overnight cultures of JE2 wt and JE2Δ*auxA* were diluted to OD_{600} 0.05 in fresh 50 ml TSB media with or without 1.5 mM of D-serine and grown at 37°C to OD_{600} 0.8-0.9. Samples were centrifuged for 15 min at 4000 rpm and supernatants withdrawn and filtered (0.2 µm) twice prior to freezing. Pellet fractions were centrifuged 2 min at 4000 rpm and snap-frozen in liquid nitrogen. Exoprotein was extracted from the supernatant fractions via trichloroacetic acid precipitation according to a modification of the method detailed in Lidbury *et al.* [61] using 1x Bolt LDS sample buffer and 1x NuPAGE Sample Reducing Agent (Invitrogen). Total protein was extracted from the pellet fractions through heat lysis in 1x Bolt LDS sample buffer and 1x NuPAGE Sample Reducing Agent. Briefly, samples were heated in boiled water for five minutes, then sonicated for five minutes. These steps were repeated prior to a final 5 minute heating step. All protein samples were loaded onto 4-12% NuPAGE Bis-Tris gels (Invitrogen) and subjected to in-gel tryptic digestion following reduction and alkylation with Tris-2-carboxyethylphosphine (TCEP) and iodoacetamide (IAA). Extracted peptides were analysed using an Orbitrap Fusion Ultimate 3000 RSLCNano System (Thermo Scientific) in electrospray ionization mode at the Warwick Proteomics Research Technology Platform. Data analyses were carried out using Perseus software package using default settings.

Bacterial adenylate cyclase two hybrid (BACTH) interaction studies. Plasmids were constructed by amplifying *auxA, auxB, murJ, SAUSA300_0957*, and *SAUSA300_1004* genes from *S. aureus* JE2 chromosomal DNA, using respective BACTH primers (Table 5), and sub-cloned into pUT18C, pUT18, pKT25 and pKNT25 for *auxA, murJ,* and *_0957*, and pUT18C and pKT25 for *auxB* and *_1004* (AuxB and 1004 are predicted to position their C-terminus extracellularly, why T18 and T25 fusions will only work as N-terminal fusions) using BamHI and KpnI restriction sites. pUT and pK(N)T plasmids were transformed into IM08B *E. coli* cells and selected on ampicillin (Amp) (100 µg/ml) and kanamycin (Kan) (50 µg/ml), respectively. pUT18C/pUT18 and pKT25/pKNT25 constructs were transformed into chemically competent BTH101 *E. coli* on Amp (100 µg/ml) + Kan (50 µg/ml) LA plates and transformants spotted onto LA supplemented with Amp (100

µg/ml), Kan (50 µg/ml), X-gal (40 µg/ml) and IPTG (0.5 mM). Pictures were taken after 48 hours at 30 °C.

Transmission electron microscopy (TEM). Overnight cultures of JE2 WT, JE2_*auxA*, JE2_*auxB*, JE2_*ltaA*, and JE2_*ypfP* were diluted to OD_{600} 0.05 in TSB and grown for two hours at 37 °C to mid-exponential phase. Cultures were split in two and continued to grow for an additional two hours, one in presence of 125 mM D-serine and one in TSB only. Cells were collected from 0.5 ml (TSB) or 1 ml (D-serine) cultures by centrifugation at 8,000 x g, and pellets suspended in fixation solution (2.5% glutaraldehyde in 0.1M cacodylate buffer [pH 7.4]) and stored overnight at 4 °C. The fixed cells were treated with 2% osmium tetroxide, followed by 0.25% uranyl acetate treatment for contrast enhancement. The cells were then dehydrated in increasing concentrations of ethanol followed by pure propylene oxide, and embedded in Epon resin. Thin sections of bacteria were stained with lead citrate and observed in a Philips CM100 BioTWIN transmission electron microscope connected to an Olympus Veleta camera. Sample processing and microscopy were performed at the Core Facility for Integrated Microscopy (CFIM), Faculty of Health and Medical Sciences, University of Copenhagen.

Zymographic analysis. Overnight cultures of JE2 WT, JE2_*auxA*, JE2_*auxB*, JE2_*atl*, and JE2_*sle1* were diluted to OD_{600} 0.05 in TSB and grown at 37 °C to mid-exponential phase with or without presence of 0.1 µg/ml oxacillin. Cultures were centrifuged (6,000 rpm, 5 min) and pellet washed once and normalized according to OD_{600} in phosphate-buffered saline (PBS). Cells were opened by bead beating (6.0 m/sec, 45 sec, 3 times) using a FastPrep-24 homogenizer (MP Biomedicals), centrifuged (12,000 rpm, 5 min), and supernatants were loaded onto an SDS-PAGE gel using a 10% resolving gel containing 1% heat-killed JE2 WT cells or purified *Micrococcus luteus* cell wall. After electrophoresis, gels were washed in deionized water (15 min, 3x) and left in renaturing buffer (50 mM Tris-HCl [pH 7.5], 0.1% Triton X-100, 10 mM CaCl2, 10 mM $MgCl_2$) for 24 hours at 37°C with gentle agitation. The gels were rinsed in water prior to imaging.

References

1. Wolosker, H., et al., *D-amino acids in the brain: D-serine in neurotransmission and neurodegeneration.* FEBS J, 2008. **275**(14): p. 3514-26.
2. Bruckner, H. and A. Schieber, *Determination of amino acid enantiomers in human urine and blood serum by gas chromatography-mass spectrometry.* Biomed Chromatogr, 2001. **15**(3): p. 166-72.
3. Cosloy, S.D. and E. McFall, *Metabolism of D-serine in Escherichia coli K-12: mechanism of growth inhibition.* J Bacteriol, 1973. **114**(2): p. 685-94.
4. Connolly, J.P., et al., *The host metabolite D-serine contributes to bacterial niche specificity through gene selection.* ISME J, 2015. **9**(4): p. 1039-51.
5. Haugen, B.J., et al., *In vivo gene expression analysis identifies genes required for enhanced colonization of the mouse urinary tract by uropathogenic Escherichia coli strain CFT073 dsdA.* Infect Immun, 2007. **75**(1): p. 278-89.
6. Roesch, P.L., et al., *Uropathogenic Escherichia coli use d-serine deaminase to modulate infection of the murine urinary tract.* Mol Microbiol, 2003. **49**(1): p. 55-67.
7. Nicolle, L.E., *Uncomplicated urinary tract infection in adults including uncomplicated pyelonephritis.* Urol Clin North Am, 2008. **35**(1): p. 1-12, v.
8. Kuroda, M., et al., *Whole genome sequence of Staphylococcus saprophyticus reveals the pathogenesis of uncomplicated urinary tract infection.* Proc Natl Acad Sci U S A, 2005. **102**(37): p. 13272-7.
9. Sakinc, T., et al., *The uropathogenic species Staphylococcus saprophyticus tolerates a high concentration of D-serine.* FEMS Microbiol Lett, 2009. **299**(1): p. 60-4.
10. De Jonge, B.L., D. Gage, and N. Xu, *The carboxyl terminus of peptidoglycan stem peptides is a determinant for methicillin resistance in Staphylococcus aureus.* Antimicrob Agents Chemother, 2002. **46**(10): p. 3151-5.
11. Vollmer, W., D. Blanot, and M.A. de Pedro, *Peptidoglycan structure and architecture.* FEMS Microbiol Rev, 2008. **32**(2): p. 149-67.
12. Qiao, Y., et al., *Detection of lipid-linked peptidoglycan precursors by exploiting an unexpected transpeptidase reaction.* J Am Chem Soc, 2014. **136**(42): p. 14678-81.
13. Willing, S., et al., *FmhA and FmhC of Staphylococcus aureus incorporate serine residues into peptidoglycan cross-bridges.* J Biol Chem, 2020. **295**(39): p. 13664-13676.
14. Frankel, M.B., et al., *LytN, a murein hydrolase in the cross-wall compartment of Staphylococcus aureus, is involved in proper bacterial growth and envelope assembly.* J Biol Chem, 2011. **286**(37): p. 32593-605.
15. Wang, Q., et al., *In vitro and in vivo activity of d-serine in combination with beta-lactam antibiotics against methicillin-resistant Staphylococcus aureus.* Acta Pharm Sin B, 2019. **9**(3): p. 496-504.
16. Bae, T., et al., *Generating a collection of insertion mutations in the Staphylococcus aureus genome using bursa aurealis.* Methods Mol Biol, 2008. **416**: p. 103-16.
17. Kiriukhin, M.Y., et al., *Biosynthesis of the glycolipid anchor in lipoteichoic acid of Staphylococcus aureus RN4220: role of YpfP, the diglucosyldiacylglycerol synthase.* J Bacteriol, 2001. **183**(11): p. 3506-14.
18. Percy, M.G. and A. Grundling, *Lipoteichoic acid synthesis and function in gram-positive bacteria.* Annu Rev Microbiol, 2014. **68**: p. 81-100.
19. Reichmann, N.T., et al., *Differential localization of LTA synthesis proteins and their interaction with the cell division machinery in Staphylococcus aureus.* Mol Microbiol, 2014. **92**(2): p. 273-86.
20. Pasquina, L., et al., *A synthetic lethal approach for compound and target identification in Staphylococcus aureus.* Nat Chem Biol, 2016. **12**(1): p. 40-5.

21. Rajagopal, M., et al., *Multidrug Intrinsic Resistance Factors in Staphylococcus aureus Identified by Profiling Fitness within High-Diversity Transposon Libraries.* mBio, 2016. **7**(4).
22. Matano, L.M., et al., *Accelerating the discovery of antibacterial compounds using pathway-directed whole cell screening.* Bioorg Med Chem, 2016. **24**(24): p. 6307-6314.
23. Hesser, A.R., et al., *The length of lipoteichoic acid polymers controls Staphylococcus aureus cell size and envelope integrity.* J Bacteriol, 2020.
24. Coe, K.A., et al., *Multi-strain Tn-Seq reveals common daptomycin resistance determinants in Staphylococcus aureus.* PLoS Pathog, 2019. **15**(11): p. e1007862.
25. Vestergaard, M., et al., *Inhibition of the ATP Synthase Eliminates the Intrinsic Resistance of Staphylococcus aureus towards Polymyxins.* mBio, 2017. **8**(5).
26. de Jonge, B.L., et al., *Effect of exogenous glycine on peptidoglycan composition and resistance in a methicillin-resistant Staphylococcus aureus strain.* Antimicrob Agents Chemother, 1996. **40**(6): p. 1498-503.
27. Siboo, I.R., et al., *Characterization of the accessory Sec system of Staphylococcus aureus.* J Bacteriol, 2008. **190**(18): p. 6188-96.
28. Schallenberger, M.A., et al., *Type I signal peptidase and protein secretion in Staphylococcus aureus.* J Bacteriol, 2012. **194**(10): p. 2677-86.
29. Dordel, J., et al., *Novel determinants of antibiotic resistance: identification of mutated loci in highly methicillin-resistant subpopulations of methicillin-resistant Staphylococcus aureus.* mBio, 2014. **5**(2): p. e01000.
30. Pardos de la Gandara, M., et al., *Genetic Determinants of High-Level Oxacillin Resistance in Methicillin-Resistant Staphylococcus aureus.* Antimicrob Agents Chemother, 2018. **62**(6).
31. Aedo, S. and A. Tomasz, *Role of the Stringent Stress Response in the Antibiotic Resistance Phenotype of Methicillin-Resistant Staphylococcus aureus.* Antimicrob Agents Chemother, 2016. **60**(4): p. 2311-7.
32. Manna, A.C., et al., *Identification of sarV (SA2062), a new transcriptional regulator, is repressed by SarA and MgrA (SA0641) and involved in the regulation of autolysis in Staphylococcus aureus.* J Bacteriol, 2004. **186**(16): p. 5267-80.
33. Manna, A.C. and A.L. Cheung, *Expression of SarX, a negative regulator of agr and exoprotein synthesis, is activated by MgrA in Staphylococcus aureus.* J Bacteriol, 2006. **188**(12): p. 4288-99.
34. Rice, K.C., et al., *The Staphylococcus aureus cidAB operon: evaluation of its role in regulation of murein hydrolase activity and penicillin tolerance.* J Bacteriol, 2003. **185**(8): p. 2635-43.
35. Groicher, K.H., et al., *The Staphylococcus aureus lrgAB operon modulates murein hydrolase activity and penicillin tolerance.* J Bacteriol, 2000. **182**(7): p. 1794-801.
36. Krute, C.N., et al., *The membrane protein PrsS mimics sigmaS in protecting Staphylococcus aureus against cell wall-targeting antibiotics and DNA-damaging agents.* Microbiology (Reading), 2015. **161**(Pt 5): p. 1136-1148.
37. Monteiro, J.M., et al., *Peptidoglycan synthesis drives an FtsZ-treadmilling-independent step of cytokinesis.* Nature, 2018. **554**(7693): p. 528-532.
38. Rajagopal, M. and S. Walker, *Envelope Structures of Gram-Positive Bacteria.* Curr Top Microbiol Immunol, 2017. **404**: p. 1-44.
39. Steele, V.R., et al., *Multiple essential roles for EzrA in cell division of Staphylococcus aureus.* Mol Microbiol, 2011. **80**(2): p. 542-55.
40. Eswara, P.J., et al., *An essential Staphylococcus aureus cell division protein directly regulates FtsZ dynamics.* Elife, 2018. **7**.
41. Bojer, M.S., et al., *SosA inhibits cell division in Staphylococcus aureus in response to DNA damage.* Mol Microbiol, 2019. **112**(4): p. 1116-1130.

42. Reichmann, N.T., et al., *SEDS-bPBP pairs direct lateral and septal peptidoglycan synthesis in Staphylococcus aureus.* Nat Microbiol, 2019. **4**(8): p. 1368-1377.
43. Taguchi, A., et al., *FtsW is a peptidoglycan polymerase that is functional only in complex with its cognate penicillin-binding protein.* Nat Microbiol, 2019. **4**(4): p. 587-594.
44. Pinho, M.G. and J. Errington, *Recruitment of penicillin-binding protein PBP2 to the division site of Staphylococcus aureus is dependent on its transpeptidation substrates.* Mol Microbiol, 2005. **55**(3): p. 799-807.
45. DeDent, A., et al., *Signal peptides direct surface proteins to two distinct envelope locations of Staphylococcus aureus.* EMBO J, 2008. **27**(20): p. 2656-68.
46. Kajimura, J., et al., *Identification and molecular characterization of an N-acetylmuramyl-L-alanine amidase Sle1 involved in cell separation of Staphylococcus aureus.* Mol Microbiol, 2005. **58**(4): p. 1087-101.
47. Frankel, M.B. and O. Schneewind, *Determinants of murein hydrolase targeting to cross-wall of Staphylococcus aureus peptidoglycan.* J Biol Chem, 2012. **287**(13): p. 10460-71.
48. Steen, A., et al., *Cell wall attachment of a widely distributed peptidoglycan binding domain is hindered by cell wall constituents.* J Biol Chem, 2003. **278**(26): p. 23874-81.
49. Zoll, S., et al., *Ligand-binding properties and conformational dynamics of autolysin repeat domains in staphylococcal cell wall recognition.* J Bacteriol, 2012. **194**(15): p. 3789-802.
50. Reichmann, N.T. and A. Grundling, *Location, synthesis and function of glycolipids and polyglycerolphosphate lipoteichoic acid in Gram-positive bacteria of the phylum Firmicutes.* FEMS Microbiol Lett, 2011. **319**(2): p. 97-105.
51. Matias, V.R. and T.J. Beveridge, *Native cell wall organization shown by cryo-electron microscopy confirms the existence of a periplasmic space in Staphylococcus aureus.* J Bacteriol, 2006. **188**(3): p. 1011-21.
52. Peschel, A., et al., *The D-alanine residues of Staphylococcus aureus teichoic acids alter the susceptibility to vancomycin and the activity of autolytic enzymes.* Antimicrob Agents Chemother, 2000. **44**(10): p. 2845-7.
53. Hesser, A.R., et al., *Lipoteichoic acid polymer length is determined by competition between free starter units.* Proc Natl Acad Sci U S A, 2020. **117**(47): p. 29669-29676.
54. Grundling, A. and O. Schneewind, *Genes required for glycolipid synthesis and lipoteichoic acid anchoring in Staphylococcus aureus.* J Bacteriol, 2007. **189**(6): p. 2521-30.
55. Schneewind, O. and D. Missiakas, *Sec-secretion and sortase-mediated anchoring of proteins in Gram-positive bacteria.* Biochim Biophys Acta, 2014. **1843**(8): p. 1687-97.
56. Siboo, I.R., H.F. Chambers, and P.M. Sullam, *Role of SraP, a Serine-Rich Surface Protein of Staphylococcus aureus, in binding to human platelets.* Infect Immun, 2005. **73**(4): p. 2273-80.
57. Monk, I.R., et al., *Complete Bypass of Restriction Systems for Major Staphylococcus aureus Lineages.* mBio, 2015. **6**(3): p. e00308-15.
58. Kennedy, A.D., et al., *Epidemic community-associated methicillin-resistant Staphylococcus aureus: recent clonal expansion and diversification.* Proc Natl Acad Sci U S A, 2008. **105**(4): p. 1327-32.
59. Fey, P.D., et al., *A genetic resource for rapid and comprehensive phenotype screening of nonessential Staphylococcus aureus genes.* mBio, 2013. **4**(1): p. e00537-12.
60. Chen, J., et al., *Single-copy vectors for integration at the SaPI1 attachment site for Staphylococcus aureus.* Plasmid, 2014. **76**: p. 1-7.
61. Lidbury, I.D., et al., *Comparative genomic, proteomic and exoproteomic analyses of three Pseudomonas strains reveals novel insights into the phosphorus scavenging capabilities of soil bacteria.* Environ Microbiol, 2016. **18**(10): p. 3535-3549.

Manuscript 4:

The CRISPR-Cas type III-A system in the emerging *Staphylococcus aureus* MRSA clone ST630 is highly excisable and provides immunity against phage attack

Author list:

Kasper Mikkelsen[1]*, Janine Zara Bowring[1]*, Yong Kai Ng[1,2], Qiuchun Li[3], Raphael N. Sieber[2], Paal Skytt Andersen[1,2], Nina Molin Høyland-Kroghsbo[1,4], Hanne Ingmer[1]

* These authors contributed equally to this work

1. Department of Veterinary and Animal Sciences, University of Copenhagen, Denmark
2. Department of Bacteria, Parasites and Fungi, Statens Serum Institut, Copenhagen, Denmark
3. Jiangsu Key Lab of Zoonosis/Jiangsu Co-Innovation Center for Prevention and Control of Important Animal Infectious Diseases and Zoonoses, Yangzhou University, China
4. Department of Plant and Environmental Science, University of Copenhagen, Denmark

Author contributions

KM and JZB performed the wet lab experiments. YKN screened the SSI collection for *cas* genes, analyzed positive hits through CRISPRCasFinder. KM extracted CRISPR array sequences and QL did phylogenic CRISPR array representation. KM found spacer targets and did graphic illustrations. PSA and RNS contributed with strains, complete genome sequencing, and fruitful discussions. KM, YKN, NMHK and HI wrote the manuscript.

Abstract

In prokaryotes, clustered regularly interspaced short palindromic repeats (CRISPR) loci along with their CRISPR-associated (*cas*) genes provide protection against invading mobile genetic elements such as bacteriophages and plasmids. Defense is mediated by the acquisition of 'spacer' sequences from the invading element and protection is provided by Cas nucleases that, guided by processed transcripts of the spacer region, degrade target DNA or RNA. Despite this seemingly important biological activity not all bacteria harbor CRISPR-Cas and for some bacterial species it is only present in a small fraction of strains. One example is *Staphylococcus aureus*, a human pathogen that can cause a variety of infections ranging from mild skin lesions to life-threatening conditions such as bacteremia and endocarditis. Here we analyzed genome sequences of 1504 *S. aureus* strains, all isolated in Denmark, for the presence of CRISPR-*cas* and found that 3.6% of the strains harbor the type III-A CRISPR-Cas system, characterized by a Cas nuclease complex targeting both DNA and RNA. We identified 38 different CRISPR spacers, of which 50% target published phage or plasmid sequences. Importantly, all strains carrying CRISPR-Cas are methicillin-resistant *S. aureus* (MRSA) with the CRISPR locus located within the small staphylococcal chromosomal cassette (SCCMec) type V(5C2&5) that confers resistance to β-lactam antibiotics. We found that the SCC*mec* excises from the chromosome at high frequencies to form a circular element carrying the CRISPR-Cas locus, but was not transferrable by phage φ11 mediated transduction. The CRISPR-Cas system of the clinical isolate 110900 was active against phage infection, however, could be bypassed by phage mutations. Our results show that primary targets of CRISPR-Cas in *S. aureus* are mobile genetic elements and that CRISPR-Cas may be transferred together with the SCC*mec* cassette, making the recipient a phage-resistant MRSA strain.

Relevance

Phage therapy is emerging as one solution to the global threat of antibiotic resistant pathogens. In Denmark, emerging clinical isolates of *S. aureus,* MRSA encode methicillin resistance by the

SCCMec element type V that also contains a type III-A CRISPR-Cas system providing resistance to lytic phages. We show that the entire module is highly excisable with the possibility of subsequent transfer. We speculate that such transfer will pose a challenge to both treatment with antibiotics and future phage therapy efforts.

Introduction

Clustered regularly interspaced short palindromic repeats (CRISPR) and the CRISPR-associated (Cas) genes are microbial adaptive immune systems that protect against invading genetic elements such as plasmids and bacteriophages. They are present in most archaeal genomes and in roughly half of bacterial genomes [1]. The CRISPR arrays store the genetic memory of prior encounters with foreign genetic elements as spacers, separated by repeats. There are three stages to CRISPR-Cas immunity; adaptation, CRISPR RNA (crRNA) biogenesis, and interference [2]. During adaptation, CRISPR-Cas immune complexes acquire a fragment of foreign DNA and inserts it into the CRISPR array after the upstream CRISPR leader region as a new spacer [3]. During the crRNA biogenesis stage, the CRISPR array is expressed as a long pre-CRISPR RNA. The CRISPR repeats fold into hairpin loops and serve as rulers for Cas proteins to cut the transcript into mature crRNAs. During the interference stage, each of the mature crRNAs guide Cas protein complexes to recognize complementary foreign genetic sequences, termed protospacers. Upon crRNA binding of a protospacer, Cas nucleases cleave and destroy the foreign genetic element [2].

CRISPR-Cas systems are divided into two classes. Class 1 systems have multiple Cas proteins forming an effector complex with the crRNA and function in unity to bind and cleave the target. The class 2 systems use a single multi-domain effector Cas protein to bind crRNA and inactivate the target [4]. CRISPR-Cas systems primarily target foreign DNA, however, the class 1 type III-A system both degrade DNA and RNA. This system is dependent on transcription of the target sequence, and holds specific RNase activity against the targeted transcript [5]. The system as well contains non-specific RNase activity by the Csm6 protein to limit phage replication by shutting down cell growth [6]. The RNase activity of Csm6 is turned on by the binding of cyclic

oligoadenylates (cOA), a product of Cas10 palm domain activation upon complex binding to the target transcript [7]. Additionally, Cas10 holds single-stranded DNase activity, which leads to degradation of the foreign DNA. The transcriptional requirement of the type III-A system allows for the integration of temperate phages into the bacterial genome under conditions where prophage protospacers are transcriptionally repressed [8]. Maintenance of the targeted prophage in the genome depends on activity of prophage-internal promoters and spacer-target mismatches [9].

Not all bacteria harbor CRISPR-Cas immune systems, and they may rely on other defense mechanisms to protect themselves against invading phages and plasmids [10-12]. Furthermore, for some bacterial species it is only a subset of strains that harbor CRISPR-Cas systems. One example is *Staphylococcus aureus*. An opportunistic, human pathogen that naturally colonize both humans and animals but also give rise to serious, life-threatening infections. Strains of *S. aureus* are subdivided based on multilocus sequence types and on composition of the *spa* gene and they are categorized as being either hospital-, community- or livestock-associated [13, 14]. When treating staphylococcal infections, methicillin-resistant *S. aureus* (MRSA), is an increasing challenge as the staphylococcal chromosomal cassette (SCC) that carries the methicillin resistance gene, *mecA*, is becoming widespread among *S. aureus* strains [15]. In *S. aureus*, the first CRISPR-Cas element was reported for the livestock-associated MRSA strain 08BA02176, with the sequence type ST398 and spa type t034 [16]. It was isolated from a human infection in Canada and carried an intact CRISPR-Cas locus with 15 spacers located upstream of the cas genes and 3 spacers downstream. Interestingly, the CRISPR-Cas element was located within the SCCMec cassette that was designated type V based on the presence of a single cassette chromosome recombinase CcrC among other features [14, 16]. In another study, 5 clinical isolates of MRSA were demonstrated to carry a type III-A CRISPR-Cas system all of which were located in the SCCMec type V cassette [17]. Importantly, this study showed transcription dependent activity of the CRISPR-Cas system during plasmid invasion and that Cas10, Csm2, Csm3, Csm4 and Cas6 are required for CRISPR-Cas interference.

Recently, *S. aureus* strains belonging to the ST1850 and ST2250 were categorized as being part of a new species namely *S. argenteus* [18]. In this species, there are several examples of type III-

A CRISPR-Cas systems present in strains lacking the SCCMec cassette [17, 19] and interestingly in one of the strains the CRISPR-Cas system is inserted in *orfX,* the gene that commonly is the integration site of SCCMec cassette [19]. CRISPR-Cas systems also appear in a small percentage of strains belonging to other Staphylococcal species including *S. epidermidis, S. lugdunensis, S. capitis* and *S. warneri* [20, 21]. Analysis of these CRISPR-positive staphylococci suggest that there may have been recent exchange of CRISPR-Cas systems between CoNS and *S. aureus* as indicated by two reports of MRSA strains carrying composite SCCmec elements that include both CRISPR-Cas genes and genes with extensive homology to CoNS [22, 23]. Further, the strain JS395 carried spacers matching those of both *S. capitis* and *S. schleferi* as well as the MRSA strain, 08BA02176 [23].

We report the prevalence of CRISPR-Cas systems in clinical isolates of *S. aureus* in Denmark and show that the Type III-A CRISPR-Cas is present in more than half of the isolated emerging clone ST630. We further confirm that the CRISPR system is associated with the SCCmec cassette and show that the SCCmec cassette is able to circularize at high frequencies. Our data suggest that sweeps of selective pressure, i.e. methicillin usage, could select for acquisition of CRISPR-Cas in a species with otherwise low CRISPR-Cas prevalence.

Results

CRISPR-Cas in Danish clinical *S. aureus* isolates. To conduct an extensive analysis of the prevalence in CRISPR-Cas systems in *S. aureus*, we analyzed 1504 clinical *S. aureus* isolates sequenced at Statens Serum Institut (SSI) between 27th of October 2017 and 12th of March 2019. We screened the isolates for the presence of the ubiquitous Cas1 and Cas2 [4], and typed the CRISPR systems by running positive hits through the CRISPRCasFinder database [24]. Of the initial 1504 isolates, 54 contained a complete CRISPR-Cas system, equivalent of 3.6%, all belonging to the Type III-A system (Table 1). We found the highest prevalence of CRISPR-Cas systems in ST types 2250 and 1850. However, these isolates were annotated incorrectly and are actually *S. argenteus* [18], and one ST5 isolate showed to be *S. epidermidis*. Excluding these isolates, the prevalence of *S. aureus* CRISPR-positive (CRISPR+) strains was reduced to 2.8%, with all isolates being MRSAs. The most prevalent CRISPR+ *S. aureus* clone is the ST630 with more than half of the isolates carrying CRISPR, followed by ST1 (7.1%), ST5 (3.8%) and ST130 (2.4%). As ST630 is an emerging clone in both Denmark and China [25, 26], we decided to include additional ST630 isolates sequenced after 12th of March 2019. We likewise excluded a few isolates due to CRISPR array sequencing issues (Table 1).

***Table 1**. Methicillin-resistant S. aureus that contains the CRISPR-Cas type III-A system (CRISPR+).*

***S. aureus* ST Type**	**CRISPR+ isolates**	**CRISPR+ within ST Type (%)**	**isolates included in study**
1	13	7.1	12
5	5	3.8	4
130	2	2.4	0
630	22	55	52
1850	1	100	0
2250	10	83	0
3208	1	100	1
Total	**54**		**69**

Spacer patterns of the *S. aureus* III-A CRISPR-Cas system. CRISPR adaptation allows acquisition of new spacers targeting a foreign threat [27]. The sequence upstream of the CRISPR array is known as the leader sequence that directs insertion of new spacers and repeats (Figure 1a) [28]. The canonical insertion site is located in the 5' end of the CRISPR array, between the leader

sequence and the first repeat, making the previous spacer number one become spacer number two etc. [3].

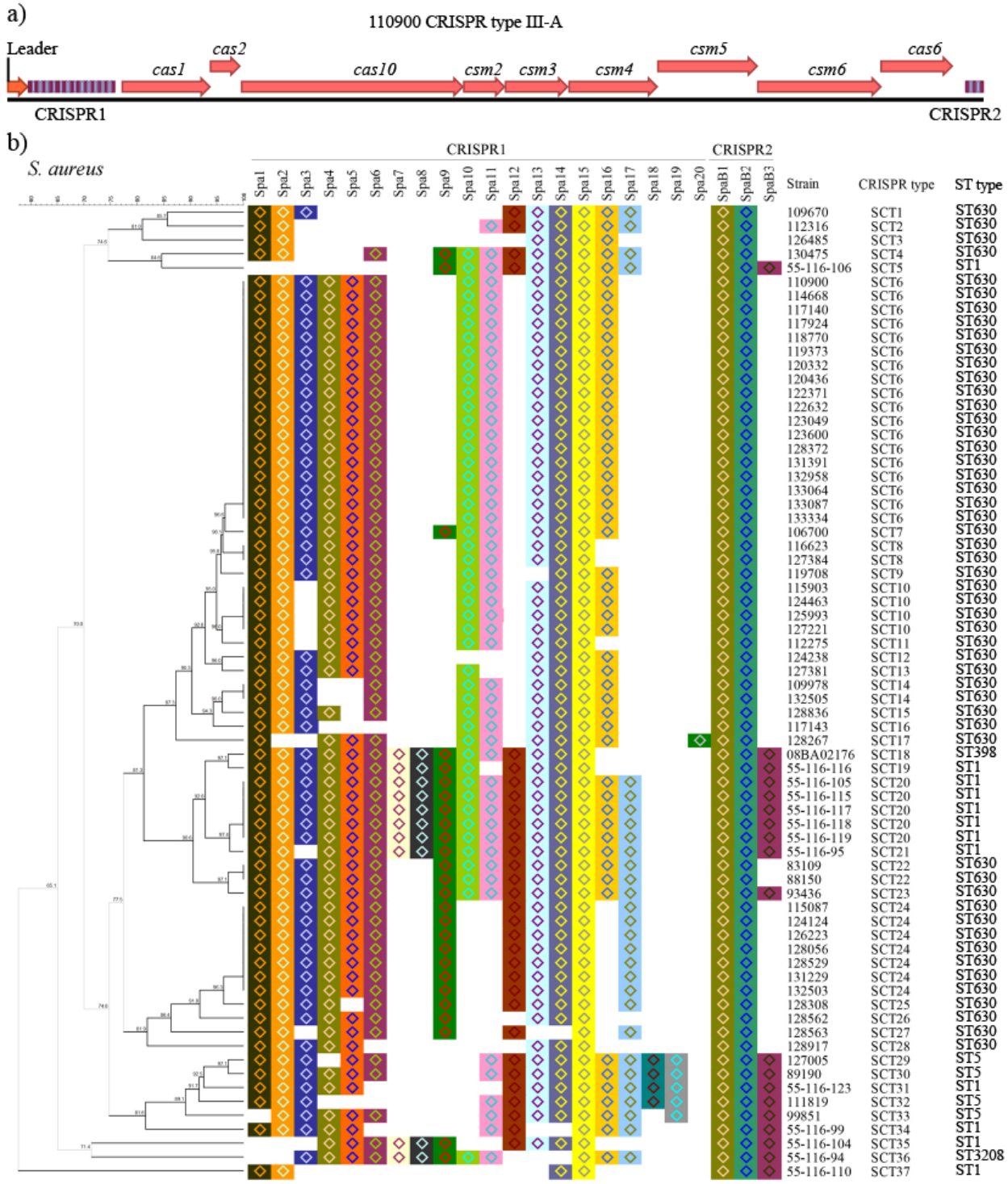

Figure 1. Phylogenic CRISPR array representation of 70 CRISPR-positive S. aureus strains. *Graphic representation of the type III-A CRISPR system of ST630 110900* ***(a)*** *and of spacer content in CRISPR1 and CRISPR2 for 37 S. aureus CRISPR types (SCT) in 69 Danish clinical isolates and 1 reference strain (08BA02176)* ***(b)****. The name above the colored spacers represents the spacers. The presence and absence of a spacer was indicated as 1 and 0, respectively, in BionNumericus 7.5 software (Applied Maths, Belgium). A dendrogram of 70 strains was constructed using the method with arithmetic means (UPGMA). N.B. The figure represent presence of spacers and not their exact location in the array.*

The distribution of spacers shows that they are quite conserved within *S. aureus*, indicating that adaptation is rare in these isolates. In the CRISPR1 locus, the last three spacers are highly conserved, with all CRISPR1 loci ending with the exact same spacer (Spa15; Figure 1b). The CRISPR1 leader-end spacers are likewise highly conserved and only a few isolates containing new spacers in front of these. Considering that adaptation of new spacers into the CRISPR locus occurs in the leader-end, the lack of diversity in the beginning of the loci is surprising. The spacer variability between isolates seems to be limited to the center of the array, why an alternative integration into the center of the array is plausible, a phenomenon termed ectopic spacer integration. Ectopic spacer integration has been described in the CRISPR type II-A system, where mutations in the five last nucleotides of the leader sequence (termed leader anchoring sequence (LAS)) altered the preferred adaptation site [29]. However, all *S. aureus* isolates contained identical leader sequences, suggesting that they all harbor the same LAS mutation or that other factors account for the ectopic spacer integration.

The CRISPR2 array seem to be less active as it only contains two or three spacers that are conserved within ST types, where ST630 carries two spacers (except 93436 that carries three) and ST1, ST5 and ST3208 have an additional spacer in the 3' end (Figure 1b).

Conservation of Danish *S. aureus* spacers among staphylococcal species. To see the distribution of the staphylococcal CRISPR type III-A system, we conducted a blastn search based on the *cas* genes of ST630 110900 against the entire NCBI database. *S. aureus* strains share the same CRISPR type III-A system as *S. capitis*, *S. schleiferi* and *S. pseudintermedius* covering all 9 *cas* genes with > 99.5% identity. *S. argenteus* share 94% identity to the *S. aureus cas* genes followed by *S. epidermidis* (89% identity) and *S. lugdunensis* (76% identity).

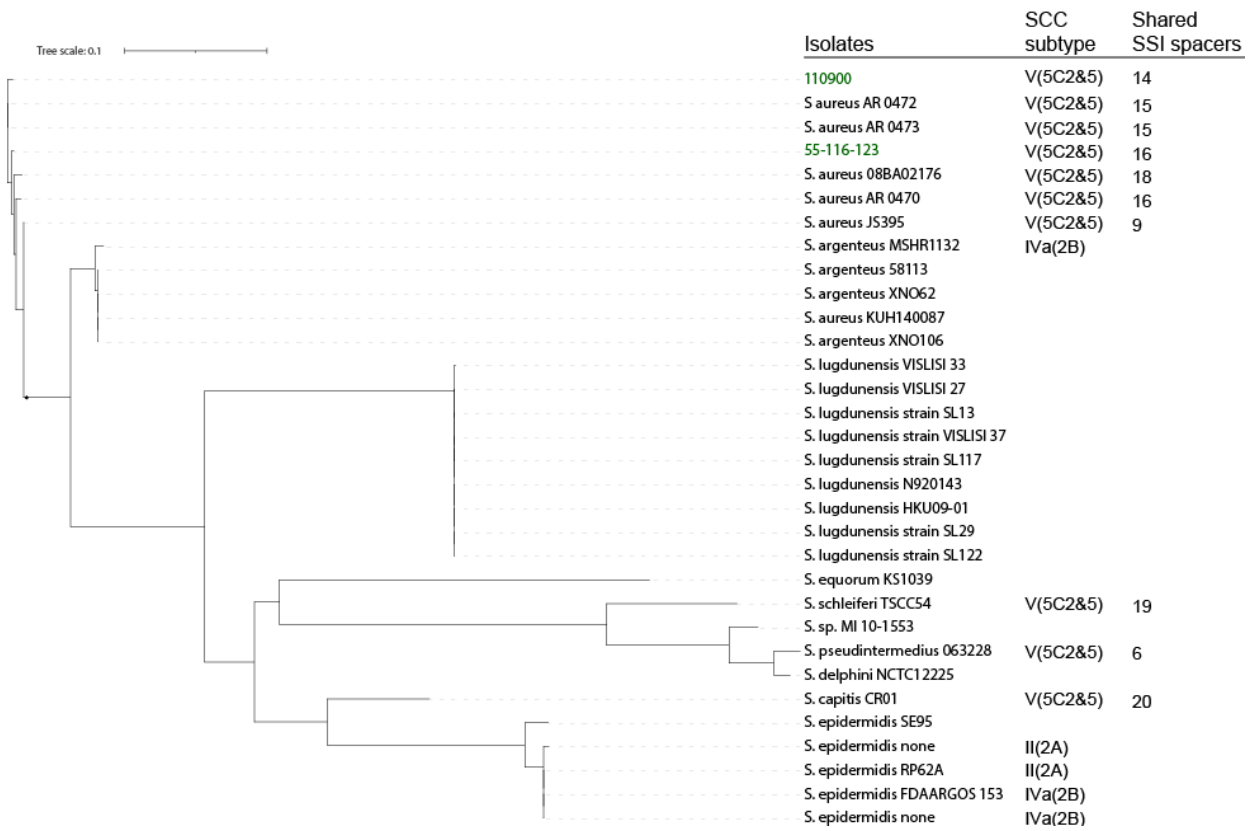

Figure 2. The Danish CRISPR+ isolates share spacer content with other staphylococcal species. *Phylogenetic SNP tree of CRISPR type III-A containing isolates. Danish ST630 (110900) and ST1 (55-116-123) isolates are colored green. The SCC subtype and number of shared spacers are noted, blank = no SCC*mec*/shared spacers.*

We constructed a phylogenetic tree based on a core with 867 SNPs containing the strains carrying the staphylococcal type III-A *cas* genes (Figure 2), and noted the number of spacers shared with the Danish ST630 isolates along with their SCC subtype. Besides sharing a highly conserved *cas* locus, the *S. capitis*, *S. schleiferi* and *S. pseudintermedius* strains share an almost identical SCC*mec* type V(5C2&5) with the Danish isolates, with a 99% identity from the *ccrc1-8* to the DR2, which includes both recombinase genes, the *mecA* gene and the entire CRISPR-Cas system (including possible differences in spacer content) (Figure 4a). Interestingly, the sharing of spacers seem to be exclusive to isolates carrying the SCC*mec* type V(5C2&5), which is highly indicative of a concurrent spread of the CRISPR-Cas type III-A and this particular SCC type (Figure 2).

Spacers target staphylococcal phages and plasmids. CRISPR arrays show a history of past infections, as new spacers can be incorporated when the bacterial cell is under attack by invading mobile genetic elements (MGE) such as bacteriophages or plasmids [3]. When blasting the NCBI

database against spacers found in the Danish clinical isolates, we found hits to MGEs in 7 of 23 spacers (Table 2). Five of the seven spacers target staphylococcal phages while the remaining two target plasmids, in line with a study showing the vast majority of CRISPR protospacers in the NCBI database originates from MGEs [30]. Several isolates contain multiple spacers that target the same phage (Spa11 and Spa20; Table 2 and Figure 1b), which could point towards primed spacer adaptation, a mechanism enhancing acquisition of additional spacers if one spacer is already targeting an invading MGE [31]. The remaining 16 spacers most likely target yet un-discovered or un-sequenced MGEs [3].

The dependency on protospacer transcription of the type III-A system has shown to direct acquisition of new spacers homologous to the template strand of transcribed genomic areas [17]. The majority of the Danish *S. aureus* protospacers are located within open reading frames (ORFs), with others covering the ribosome binding site (RBS) and start codon.

Table 2. Spacer targets. *Homology of spacers from CRISPR arrays 1 and 2 were blasted against the NCBI database using the blastn algorithm.*

Spacer	Description	Identity	Gene target	Accession	Comments
Spa6	Staphylococcus phage phiIPLA-RODI	33/35	Hypothetical protein	KP027446.1	Homologous to template strand
	Staphylococcus phage K	32/35		KF766114.1	
Spa11	Staphylococcus phage phiIPLA-C1C	33/36	TreK hypothetical protein	KP027447.1	Homologous to template strand
	Staphylococcus phage phiIBB-SEP1	33/36		NC_041928.1	
Spa13	Staphylococcus phage GRCS	33/36	DNA encapsidation/ packaging protein	NC_023550.1	Homologous to template strand
	Staphylococcus phage BP39	32/36		KM366100.1	
Spa14	Staphylococcus sp. CDC3 plasmid SAP020A	32/34	Hypothetical protein	GQ900386.1	Homologous to template strand
Spa15	Staphylococcus epidermidis strain NCCP 16828 plasmid	30/36	Intergenic region	CP043848.1	Promoter region of ParA family protein & replication initiator protein A RepA

Spa20	Staphylococcus phage Terranova	31/35	Hypothetical protein	MH542234.1	Targets in the cross-section between 2 genes in same operon. Covers 2nd gene RBS
	Staphylococcus phage phiIBB-SEP1	31/35		NC_041928.1	
	Staphylococcus phage Twillingate	30/35		MH321491.1	
	Staphylococcus phage phiIPLA-C1C	30/35		KP027447.1	
SpaB2	Uncultured Caudovirales phage clone 7F_7	33/37	DNA-directed RNA polymerase subunit alpha	MF417907.1	Homologous to template strand
	Staphylococcus phage IME1365_01	33/37		KY653129.1	

The ST630 Type III-A CRISPR system is active against phage infection. The Spa6 spacer targets the lytic Myoviridae family phage phiIPLA-RODI (Table 2), a spacer the ST630 Danish clinical isolate 110900 holds. We wanted to test if the strain 110900 was resistant to infection by phiIPLA-RODI in a liquid infection assay and included a ST630 CRISPR-negative (CRISPR÷) isolate (125231) closely related to 110900 as a control. At a very low multiplicity of infection (MOI) of 10^{-7} the 110900 strain survived the infection whereas the CRISPR÷ 125231 strain was killed (Figure 3). At a of MOI^{-6}, some technical replicates could cope with the phage infection and declined in optical density (OD_{600}) whereas others survived, resulting in the large standard deviations seen in Figure 2. This phenomenon may be caused by mutations in the phage protospacer, making the phage able to overcome CRISPR immunity. At increasing MOIs, the ability of the CRISPR-Cas system in the 110900 strain to withstand the phage decreased. However, the bacterial killing, as measured by a decline in OD_{600}, occured later in the 110900 isolate compared to the CRISPR÷ 125231. Thus, these results indicate that the CRISPR-Cas system is active against phage infection in the ST630 isolates and the efficacy is depending on the MOI.

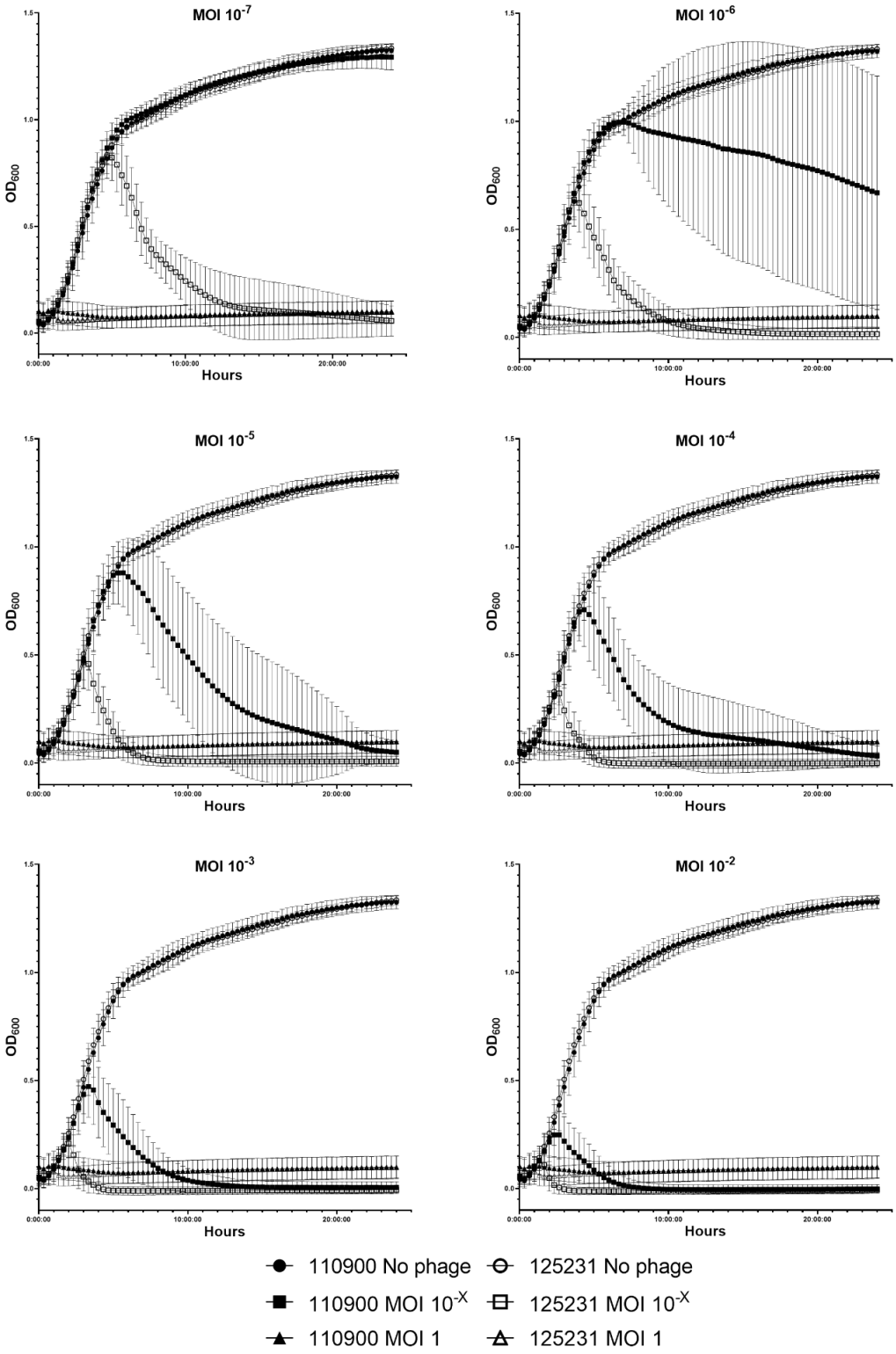

Figure 3. Danish ST630 isolate 110900 carries CRISPR-Cas immune activity against liquid infections. *Starting cultures (OD_{600} 0.05) of 110900 (CRISPR+) or 125231 (CRISPR÷) cultures were challenged by increasing MOIs of phage phiIPLA-RODI in TSB medium (n=3, 5 technical replicates).*

Co-localization and mobility of CRISPR along with SCC*mec* type V(5C2&5). Thus far, the CRISPR-Cas type III-A system in *S. aureus* has been reported to be located within the SCC*mec* type V(5C2&5) [17]. All the Danish *S. aureus* CRISPR-positive clinical isolates carry the type III-A CRISPR system in the SCCmec type V(5C2&5) around 3-5 kb downstream of the *ccrC1*-allele-2 within the SCC*mec* joining region 1 (J1 region) [32]. The J1 region is a primed location of integration known to carry resistance genes in the form of integrated plasmids and transposons [33]. In addition to the CRISPR system, the J1 region holds a transposon with the enterotoxin H gene followed by a sulfite/sulfate resistance cassette in ST1 isolates, a sulfite/sulfate resistance cassette in ST5 and a kdp operon and arsenite/arsenate resistance cassette in ST630 (Figure 4a).

As distantly related staphylococcal species share a highly similar SCC*mec* type V(5C2&5) containing the CRISPR-Cas type III-A system (Figure 2), we examined if SCC*mec* excision from the ST630 isolate 110900 was a possible mechanism of transfer. When integrated into the chromosome, the SCC*mec* is flanked by direct repeats (DR) (Figure 4a and c), which can recombine to form a circle [34]. Two circularized fragments will contain the CRISPR-Cas system along with the *mecA* gene; a 38 kb fragment via recombination of DR1/DR2 (SCC*mec*-CRISPR) and the entire 59 kb SCC*mec*, including the kdp and ars operons, via recombination of the extremity DR1/DR1 (Figure 4a). We designed primers facing across the junction of the circular SCC*mec* and compared quantities of excised circularized PCR products with that of a chromosomal PCR product located 1kb upstream of the SCC*mec* into the *adsA* gene. The entire SCC*mec* showed a very high frequency of excision of 10^{-1} relative to the chromosomal copy number, when grown in tryptic soy broth (TSB) (Figure 4b). This corresponds to one excised SCC*mec* fragment for every ten chromosomal copies under non-stressful conditions. We saw no differences if we added either sub-MIC of the cell wall targeting antimicrobial oxacillin or the DNA damaging agent mitomycin C. The excision frequency of the SCC-CRISPR fragment was approximately 10^{-7} with and without addition of antibiotics, which makes it a six orders of magnitude excision frequency difference between the two circular fragments. This difference may be caused by the three-nucleotide difference between DR1 and DR2 (Figure 4c).

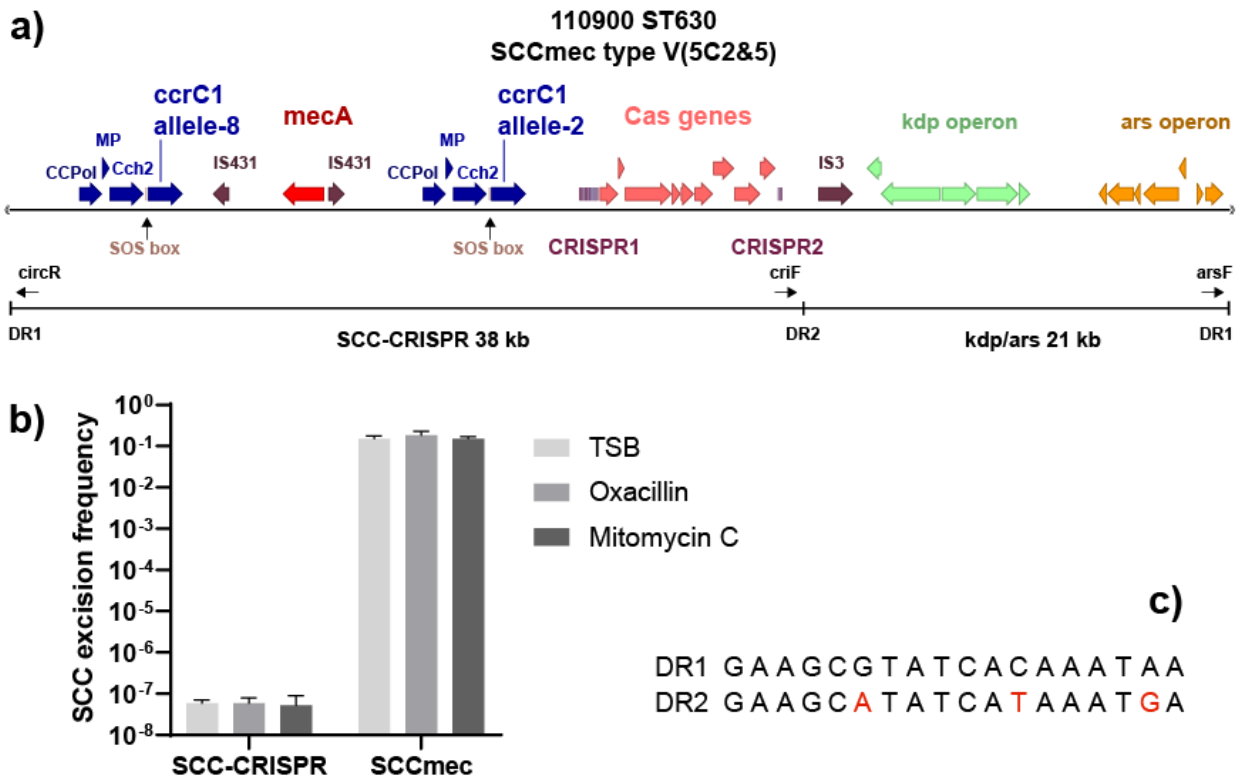

Figure 4. SCCmec excision happens at high frequencies. (a) *Graphic illustration of the SCCmec type V(5C2&5) of the Danish ST630 1109000 isolate. Fragments and primers used in (b) and location of direct repeats (DR) (c) are shown underneath the SCCmec.* ***(b)*** *SCCmec excision frequencies of the SCC-CRISPR fragment or the entire SCCmec compared to chromosomal DNA quantities (n=3). Primer pairs criF/circR and arsF/circR was used for SCC-CRISPR and SCCmec, respectively.* ***(c)*** *Alignment of DR1 and DR2, with mismatches highlighted in red in the DR2 sequence.*

Transfer mechanisms of the circularized SCC*mec*. The high frequency of SCC*mec* circularization might serve as an efficient way of distributing collective β-lactam resistance and CRISPR immunity to other isolates. The CRISPR-Cas system itself has been shown to be mobile via phage mediated transduction [35], and CRISPR spacers have likewise shown to enhance transduction events of circular plasmids [36]. The SCCmec itself has as well been shown to be moved by phage transduction, even though loss of parts of the SCC*mec* was detected [37]. We tested if transduction is the mechanism of SCC*mec* type V(5C2&5) transfer by using standard laboratory transducing phage φ11. However, despite multiple attempts, φ11 does not seem able to transfer DNA fragments of 59kb in size. This indicates that other routes of transfer, such as transformation or conjugation, could be involved in the dissemination of the CRISPR-Cas containing SCC*mec* type V(5C2&5) MGE.

Discussion

Here, we show that the emerging Danish *S. aureus* clone ST630 along with ST1, ST5, and ST3208 contain the CRISPR-Cas type III-A system, which resides within the SCC*mec* typeV(5C2&5). The conservation of spacers was quite high among the isolates, and mainly differed at the center of the array. This was not due to changes in the leader sequences leading to ectopic spacer integration, as seen for the type II-A CRISPR system of *Streptococcus pyogenes* [29]. Spacer adaptation via Cas1 and Cas2 has never experimentally been shown to expand the CRISPR array in the type III-A system [6], why this system could rely on other methods to acquire new spacers. CRISPR spacers are shown to recombine with their cognate protospacer of their foreign invader to act as a form of specialized transduction [36]. In this manner, the type III-A locus would be able to acquire new sets of spacers at different locations. The slow rate of adaptation might save the cell from autoimmunity. An amino acid substitution in the type II-A Cas9, enhanced the CRISPR immune response by 100-fold and showed the phenotype to be due to an increase in spacer acquisition rates [38]. However, this as well increased autoimmunity events, why a slow spacer adaptation machinery might serve to guard the cell from self-targeting.

The homology of spacers between staphylococcal species (Figure 2) and isolates from around the world [Li, Y, Mikkelsen, K *et al.*, submitted manuscript] confirm the picture of a slow or inactive adaptation machinery in the type III-A CRISPR-Cas system carried by these isolates. The interference machinery of the 110900 ST630 isolate showed activity against infection with the lytic IPLA-RODI phage, however, growth profiles at a MOI of 10^{-6} indicates that the phage mutates to escape type III-A immunity (Figure 3). However, the type III-A system is not dependent on PAM or seed regions, why escape from this system has been shown to result in large deletions of the invading MGE that include the protospacer region [39]. Tolerance to protospacer point mutations have likewise shown to be high in the type III-A system [39], why it will be interesting to sequence the escaped phage particles to see if the robustness of the system is preserved in the ST630 110900 isolate. This will further enlighten if the decline in OD_{600}, seen for MOIs of 10^{-5} and above, are due to a higher frequency of phage escape mutations, or due to limited activity of the type III-A system that is unable to keep up with the increasing phage numbers.

In addition to pointing to low adaptation frequencies, the homology of spacers between species is indicative of a horizontal transfer mechanism across species level. Specifically, as the CRISPR-Cas Type III-A is located within the SCC*mec* typeV(5C2&5) in all the Danish isolates, and the highly homologous SCC*mec* typeV(5C2&5) cassettes carrying the type III-A CRISPR system are found in both *S. capitis*, *S. schleiferi* and *S. pseudintermedius*, it strongly suggests that the SCC*mec* is involved in interspecies CRISPR-Cas transfer. This adds to the perception that the SCC*mec* is of coagulase-negative *S. epidermidis* origin, in which the emergence of CRISPR-Cas systems was reported prior to *S. aureus* [40]. The excision frequency of the typeV(5C2&5) SCC*mec* have previously shown to be induced by addition of the DNA damaging agent Mitomycin C leading to induction of the SOS response in *S. haemolyticus* [34]. Although we did not see this inducible effect of Mitomycin C, the excision rates in general were higher than reported in *S. haemolyticus*, why the expression of the *ccrC1* recombinase genes could be left unregulated, even though the SOS box, to which LexA binds, is preserved in the *S. aureus* SCC*mec* typeV(5C2&5). Another reason for the high apparent circularization rates could be the potential ability of SCC*mec* to replicate once excised and circularized [41]. Recently, the three genes immediately upstream of the two *ccrC1* genes were characterized as A-family DNA polymerases (CCPol), primases (MP) and 3'-to-5' helicases (Cch2) (Figure 4a) [42]. This strongly indicate that the SCC*mec* can replicate once excised and suggests, combined with the high excision rates for the entire SCC*mec* element shown here, that the SCC*mec* typeV(5C2&5) is a beneficial location for the dispersion of CRISPR-Cas.

The transfer of CRISPR-Cas systems between strains has previously been shown via transduction by a φTE phage able to transfer DNA fragments of around 100 kb [35]. Transfer of the SCC*mec* cassette has as well shown to be possible via transduction, even though at low frequencies and occasionally associated with deletions or truncations in the SCC*mec* [37]. We tried to transduce the SCC*mec* cassette through transduction with φ11, but did not succeed in getting any lysogenized colonies able to grow on plates containing β-lactam antibiotics, which suggests that other methods of transfer are more likely. Conjugative plasmids have been shown to be able to capture the SCC*mec* via homologous recombination of the IS431 insertion sequences present in

all SCC*mec* types [43], and transformation of the excised and circularized SCC*mec* inside biofilm environments was recently been suggested as another mechanism of transfer [44].

The integration of the CRISPR-Cas type III-A into the SCCmec and the high excision rates seen in this study indicate that circularization of the SCC*mec* element might serve to select for, and spread, methicillin resistance and adaptive immunity in one.

Materials and Methods

Isolate collection and classification. All primary samples are recovered from Danish patients who were admitted due to a healthcare-associated infection between 27/10/2017 and 12/3/2019. They were subjected to whole-genome sequencing and analysed as described below. All isolates were typed at Statens Serum Institut as part of the national MRSA surveillance program. Isolates that contain a *cas1* and *cas2* genes were selected for further exploration.

Whole-genome sequencing and analysis. All isolates were whole-genome sequenced on an Illumina MiSeq with 2 x 251 bp paired-end reads. Isolates were assembled using SKESA or SPAdes. CRISPRCasFinder was used to identify isolates that contain the *cas1* and *cas2* genes. Spacers corresponding with each CRISPR positive isolates were extracted, aligned using Clustal Omega and clustered by hierarchical clustering with Ward's method based on 2 indel difference calculated by ape version 5.0. A maximum-likelihood phylogenetic tree was calculated using IQ-TREE with default settings running with bootstrap of 100 from single nucleotide polymorphism (SNPs) called and filtered by NASP version 1.0. Visualisation of the spacers were done using CRISPRStudio version 1.0 and BionNumericus 7.5 software (Applied Maths, Belgium). A dendrogram of 70 strains was constructed using the method with arithmetic means (UPGMA).

Identification of spacer targets. The spacer groups were blasted against the entire NCBI database using the blastn algorithm on January 7, 2021. Bacterial isolates carrying the CRISPR-Cas system and CRISPR arrays were discarded as protospacer hits. Hits representative of the targeted protospacer was included in Table 2.

Liquid infection assay. ST630 isolates CRISPR-positive 110900 and CRISPR-negative 125231 were grown overnight and diluted to OD600 0.15. The strains were then transferred into honeycomb

bioscreen plates (95025BIO) in 125 µL aliquots and 125 µL of various phage IPLA-RODI lysate dilutions in phage buffer, equivalent to MOIs 1 – 10-7, were added. The OD600 of each well was measured in a Bioscreen C instrument (Oy Growth Curves Ab Ltd) with measurements every 20 mins for 24 hours, at 30°C, with shaking. Shaking was paused 5 secs before each reading. For each experiment, 5 technical replicates of each condition were included and 3 biological replicates were performed in total. Positive bacterial growth controls including 125 µL bacterial culture and 125 µL phage buffer without phage, as well as negative controls of TSB and phage buffer (125 µL:125 µL) were included in each run. Results were plotted in an XY graph (GraphPad Prism 9) as mean +/- standard deviation.

SCC*mec* excision frequency assay. ST630 isolate 110900 was grown overnight and diluted to OD_{600} 0.05. Cultures were grown for two hours at 37 °C, where the cultures were left untreated or treated with antibiotics (oxacillin or mitomycin C, 0.5 µg/ml). After 1 hour additional incubation at 37 °C, 1 ml of culture was withdrawn and chromosomal DNA extracted using the DNeasy blood and tissue kit (Qiagen). Concentrations were normalized and diluted 1:5, before being used in RT-PCR reactions. RT-PCR reactions were set up using the FastStart Essential DNA Green Master kit (Roche), using four different primer pairs; criF/circR (SCC-CRISPR excisition), arsF/circR (SCC*mec* excision), adsAF/adsAR (chromosomal reference), tpiF/tpiR (normalization). Reactions were run on a LightCycler® 96 instrument (Roche) and data was analyzed using the $2^{-\Delta\Delta Ct}$ method. The PCR products using the same primer sets were verified by sanger sequencing (Eurofins).

circR	CCGCTCCTTTTATATTATGCAC
criF	GGTTTTTAGCAAAATCACTGATAGG
arsF	CCGCATCATTAACCGATACG
adsAF	GCGAAACAACCAGTGCCAAG
adsAR	CAGCAGTTCCTTCCAATGCG
tpiF	TAAAGAAGGAAAAGCACAAGG
tpiR	TTCAGAATGACCGATAACAAC

SCC*mec* transduction experiment. ST630 isolate 110900 was grown overnight and diluted to OD_{600} 0.05. For initial phage infection of strain 110900, 200 mL cultures were grown at 37 °C until OD_{600} 0.15 and the cells collected, before resuspension in 1:1 TSB:phage buffer, at half volume (100 mL). The cultures were infected with φ11 at various MOIs, at 30°C for 4 hours. If visual lysis of the culture was not complete, the culture was further incubated at room temperature overnight. Once visual lysis was complete, the lysates were filtered to remove any remaining bacterial cells (0.22 µm filters, Millipore stericup, PES).

Lysates were precipitated to increase the concentration of phage particles and any potential CRIPSR/SCC*mec* transductant particles. Lysates were incubated with DNase (2.5 U ml^{-1}) and RNase (1 µg ml^{-1}) at 37°C for 1 hour. $NaCl_2$ was added (58.4 g L^{-1}) and lysates incubated on ice with shaking for 1 hour. Lysates were centrifuged at 11 000 x g for 10 mins at 4°C and the supernatant collected. PEG 8000 was added at 10% w/v and the lysates incubated on ice at 4°C overnight. The lysates were centrifuged at 11 000 x g for 10 mins at 4°C and the supernatant discarded. Phage precipitants were resuspended in 1.6 mL phage buffer, and quantified by titration methods.

Transduction assays were attempted using recipient strains RN4220, 8325-4 φ11, and Newman. Briefly, overnight cultures of recipients were diluted to OD_{600} 0.05 and grown to OD_{600} 1.4, before 1 mL recipient, 100 µL of phage lysate and 4.4 mM $CaCl_2$ were incubated at 37°C for 20 mins. The mixture was plated out in 3 mL TSA top agar (50% agar) on TSA with oxacillin (0.4 µg mL^{-1}) and sodium citrate (17 mM). Plates were incubated at 37°C for 24 hours and checked for colonies, if no colonies were seen the plates were incubated for an additional 24 hours and checked again.

Acknowledgements

NMHK was supported by Lundbeck grant R264-2017-3936. HI was supported by grants from Danmarks Fri Forskningsfond (7017-00079B).

We thank Vi Phuong Thi Nguyen and Gitte Petersen for technical assistance in purifying *S. aureus* chromosomal DNA.

References

1. Bhaya, D., M. Davison, and R. Barrangou, *CRISPR-Cas systems in bacteria and archaea: versatile small RNAs for adaptive defense and regulation.* Annu Rev Genet, 2011. **45**: p. 273-97.
2. Hille, F., et al., *The Biology of CRISPR-Cas: Backward and Forward.* Cell, 2018. **172**(6): p. 1239-1259.
3. McGinn, J. and L.A. Marraffini, *Molecular mechanisms of CRISPR-Cas spacer acquisition.* Nat Rev Microbiol, 2019. **17**(1): p. 7-12.
4. Makarova, K.S., et al., *Evolutionary classification of CRISPR-Cas systems: a burst of class 2 and derived variants.* Nat Rev Microbiol, 2020. **18**(2): p. 67-83.
5. Jiang, W., P. Samai, and L.A. Marraffini, *Degradation of Phage Transcripts by CRISPR-Associated RNases Enables Type III CRISPR-Cas Immunity.* Cell, 2016. **164**(4): p. 710-21.
6. Pyenson, N.C. and L.A. Marraffini, *Type III CRISPR-Cas systems: when DNA cleavage just isn't enough.* Curr Opin Microbiol, 2017. **37**: p. 150-154.
7. Niewoehner, O., et al., *Type III CRISPR-Cas systems produce cyclic oligoadenylate second messengers.* Nature, 2017. **548**(7669): p. 543-548.
8. Goldberg, G.W., et al., *Conditional tolerance of temperate phages via transcription-dependent CRISPR-Cas targeting.* Nature, 2014. **514**(7524): p. 633-7.
9. Goldberg, G.W., et al., *Incomplete prophage tolerance by type III-A CRISPR-Cas systems reduces the fitness of lysogenic hosts.* Nat Commun, 2018. **9**(1): p. 61.
10. Ofir, G., et al., *DISARM is a widespread bacterial defence system with broad anti-phage activities.* Nat Microbiol, 2018. **3**(1): p. 90-98.
11. Labrie, S.J., J.E. Samson, and S. Moineau, *Bacteriophage resistance mechanisms.* Nat Rev Microbiol, 2010. **8**(5): p. 317-27.
12. Hampton, H.G., B.N.J. Watson, and P.C. Fineran, *The arms race between bacteria and their phage foes.* Nature, 2020. **577**(7790): p. 327-336.
13. Enright, M.C., et al., *Multilocus sequence typing for characterization of methicillin-resistant and methicillin-susceptible clones of Staphylococcus aureus.* J Clin Microbiol, 2000. **38**(3): p. 1008-15.
14. Lakhundi, S. and K. Zhang, *Methicillin-Resistant Staphylococcus aureus: Molecular Characterization, Evolution, and Epidemiology.* Clin Microbiol Rev, 2018. **31**(4).
15. Kock, R., et al., *Methicillin-resistant Staphylococcus aureus (MRSA): burden of disease and control challenges in Europe.* Euro Surveill, 2010. **15**(41): p. 19688.
16. Golding, G.R., et al., *Livestock-associated methicillin-resistant Staphylococcus aureus sequence type 398 in humans, Canada.* Emerg Infect Dis, 2010. **16**(4): p. 587-94.
17. Cao, L., et al., *Identification and functional study of type III-A CRISPR-Cas systems in clinical isolates of Staphylococcus aureus.* Int J Med Microbiol, 2016. **306**(8): p. 686-696.
18. Tong, S.Y.C., et al., *Novel staphylococcal species that form part of a Staphylococcus aureus-related complex: the non-pigmented Staphylococcus argenteus sp. nov. and the non-human primate-associated Staphylococcus schweitzeri sp. nov.* Int J Syst Evol Microbiol, 2015. **65**(Pt 1): p. 15-22.
19. Aung, M.S., et al., *Molecular characterization of Staphylococcus argenteus in Myanmar: identification of novel genotypes/clusters in staphylocoagulase, protein A, alpha-haemolysin and other virulence factors.* J Med Microbiol, 2019. **68**(1): p. 95-104.
20. Li, Q., et al., *Characterization of CRISPR-Cas system in clinical Staphylococcus epidermidis strains revealed its potential association with bacterial infection sites.* Microbiol Res, 2016. **193**: p. 103-110.
21. Rossi, C.C., et al., *CRISPR-Cas Systems Features and the Gene-Reservoir Role of Coagulase-Negative Staphylococci.* Front Microbiol, 2017. **8**: p. 1545.

22. Kinnevey, P.M., et al., *Emergence of sequence type 779 methicillin-resistant Staphylococcus aureus harboring a novel pseudo staphylococcal cassette chromosome mec (SCCmec)-SCC-SCCCRISPR composite element in Irish hospitals.* Antimicrob Agents Chemother, 2013. **57**(1): p. 524-31.
23. Larsen, J., et al., *Staphylococcus aureus CC395 harbours a novel composite staphylococcal cassette chromosome mec element.* J Antimicrob Chemother, 2017. **72**(4): p. 1002-1005.
24. Couvin, D., et al., *CRISPRCasFinder, an update of CRISRFinder, includes a portable version, enhanced performance and integrates search for Cas proteins.* Nucleic Acids Res, 2018. **46**(W1): p. W246-W251.
25. Dai, Y., et al., *Decreasing methicillin-resistant Staphylococcus aureus (MRSA) infections is attributable to the disappearance of predominant MRSA ST239 clones, Shanghai, 2008-2017.* Emerg Microbes Infect, 2019. **8**(1): p. 471-478.
26. Sieber, R.N., et al., *Complete Genome Sequences of Methicillin-Resistant Staphylococcus aureus Strains 110900 and 128254, Two Representatives of the CRISPR-Cas-Carrying Sequence Type 630/spa Type t4549 Lineage.* Microbiol Resour Announc, 2020. **9**(41).
27. Barrangou, R., et al., *CRISPR provides acquired resistance against viruses in prokaryotes.* Science, 2007. **315**(5819): p. 1709-12.
28. Jansen, R., et al., *Identification of genes that are associated with DNA repeats in prokaryotes.* Mol Microbiol, 2002. **43**(6): p. 1565-75.
29. McGinn, J. and L.A. Marraffini, *CRISPR-Cas Systems Optimize Their Immune Response by Specifying the Site of Spacer Integration.* Mol Cell, 2016. **64**(3): p. 616-623.
30. Shmakov, S.A., et al., *The CRISPR Spacer Space Is Dominated by Sequences from Species-Specific Mobilomes.* mBio, 2017. **8**(5).
31. Fineran, P.C., et al., *Degenerate target sites mediate rapid primed CRISPR adaptation.* Proc Natl Acad Sci U S A, 2014. **111**(16): p. E1629-38.
32. International Working Group on the Classification of Staphylococcal Cassette Chromosome, E., *Classification of staphylococcal cassette chromosome mec (SCCmec): guidelines for reporting novel SCCmec elements.* Antimicrob Agents Chemother, 2009. **53**(12): p. 4961-7.
33. Ito, T., et al., *Staphylococcal Cassette Chromosome mec (SCCmec) analysis of MRSA.* Methods Mol Biol, 2014. **1085**: p. 131-48.
34. Liu, P., et al., *Antibiotics trigger initiation of SCCmec transfer by inducing SOS responses.* Nucleic Acids Res, 2017. **45**(7): p. 3944-3952.
35. Watson, B.N.J., R.H.J. Staals, and P.C. Fineran, *CRISPR-Cas-Mediated Phage Resistance Enhances Horizontal Gene Transfer by Transduction.* mBio, 2018. **9**(1).
36. Varble, A., et al., *Recombination between phages and CRISPR-cas loci facilitates horizontal gene transfer in staphylococci.* Nat Microbiol, 2019. **4**(6): p. 956-963.
37. Scharn, C.R., F.C. Tenover, and R.V. Goering, *Transduction of staphylococcal cassette chromosome mec elements between strains of Staphylococcus aureus.* Antimicrob Agents Chemother, 2013. **57**(11): p. 5233-8.
38. Heler, R., et al., *Mutations in Cas9 Enhance the Rate of Acquisition of Viral Spacer Sequences during the CRISPR-Cas Immune Response.* Mol Cell, 2017. **65**(1): p. 168-175.
39. Pyenson, N.C., et al., *Broad Targeting Specificity during Bacterial Type III CRISPR-Cas Immunity Constrains Viral Escape.* Cell Host Microbe, 2017. **22**(3): p. 343-353 e3.
40. Otto, M., *Coagulase-negative staphylococci as reservoirs of genes facilitating MRSA infection: Staphylococcal commensal species such as Staphylococcus epidermidis are being recognized as important sources of genes promoting MRSA colonization and virulence.* Bioessays, 2013. **35**(1): p. 4-11.

41. Mir-Sanchis, I., et al., *Staphylococcal SCCmec elements encode an active MCM-like helicase and thus may be replicative.* Nat Struct Mol Biol, 2016. **23**(10): p. 891-898.
42. Bebel, A., et al., *A novel DNA primase-helicase pair encoded by SCCmec elements.* Elife, 2020. **9**.
43. Ray, M.D., S. Boundy, and G.L. Archer, *Transfer of the methicillin resistance genomic island among staphylococci by conjugation.* Mol Microbiol, 2016. **100**(4): p. 675-85.
44. Maree, M., et al., *MRSA emerges through natural transformation.* bioRxiv, 2020: p. 2020.12.08.415893.

Discussion

Staphylococcus aureus is naturally susceptible to almost any antimicrobial drug ever developed [1]. However, since the introduction of the first antimicrobial agents, it has evolved into one of six "ESKAPE" pathogens that are responsible for the majority of nosocomial infections and able to escape the biocidal action of antibiotics and pass in on to other bacteria [2]. This evolutionary ability of *S. aureus* to gain resistance, has made it important to get insight into resistance mechanisms to be able to predict resistance and find new drug targets.

In manuscript 1, we looked through the genomes of 100 MRSA isolates, to find acquired "non-obvious" resistance mechanisms that contribute to the maintenance of high level resistance phenotypes. We managed to verify the method, as we found hits to known resistance genes and chromosomal mutations against agents showing binary MIC profiles. As the majority of the MRSA isolates were susceptible to vancomycin, daptomycin, and linezolid we were only able to find candidates involved in β-lactam resistance, which displayed more scattered MIC profiles. The top hits were found in CC22 isolates, to genes inside the J1 region of the type IVh SSC*mec* and within prophages. A study investigating *S. aureus* isolates from bloodstream infections found CC22 to be a highly overrepresented clonal complex with nearly all isolates carrying the SCC*mec* type IVh [3]. The study further revealed a gain in prophage content in the CC22 isolates over time. Even though we did not see a change in susceptibility of SCC*mec* IVh J1 deletion mutants or C22 phage lysogens, the success of CC22 isolates to establish bloodstream infections imply that these MGEs are important for *S. aureus* resilience and virulence. It may not be the J1 region of IVh SCC*mec* that assist the high β-lactam phenotype of the CC22 isolates, but rather the entire SCC*mec* that provides high β-lactam protection. It might be that the SCC*mec* IVh excise from the chromosome at high rates, followed by SCC*mec* replication [4]. This would result in more copies of the *mecA* resistance gene, which has been shown to drastically increase resistance levels [5]. The hits to prophage genes were present in the same isolates that carried the SCC*mec* IVh, why the prophages probably rather serve as a virulence reservoir [6] to supplement SCC*mec* IVh-driven resistance to establish a successful infection. These isolates as well contain the *sraP* gene that is

important in the binding of human platelets [7] and by that would contribute to successful bloodstream infections.

In manuscripts 2 and 3, we took another approach to find resistance determinants, as we screened the NTML against sub-MIC β-lactam antimicrobials and D-serine, respectively. In both screens, we found mutants of *SAUSA300_0980* and *SAUSA300_1003* (which we named *auxA* and *auxB*, respectively) to be unable to grow at sub-MIC conditions and found the phenotypes to be complement-able and reproducible across strain backgrounds. Previous screens have shown that inactivation of these novel auxiliary factors renders *S. aureus* more susceptible to oxacillin, vancomycin, and daptomycin [8], polymyxin B [9] and the *dlt* pathway inhibitor amsacrine [10]. Additionally, *auxA* mutants display decreased levels of biofilm associated eDNA [11], which has shown to be influenced by the autolytic activity of both Atl and Sle1 [12, 13]. This thereby supports the attenuated autolytic activity of the *aux* mutants we report in the two manuscripts. In manuscript 2, we hypothesize that this attenuated autolytic activity could be due to instability of the LTA polymer. Contrary to mutants of LTA anchor synthesis or flipping that release extended LTA polymers into the growth medium, the *aux* mutants release LTA polymers of wild type length. The Aux proteins must thereby provide stability to the LTA polymer without influencing the accessibility of the Glc_2DAG anchor to the LTA synthase.

In manuscript 3, we further introduce LytN activity as possibly being influenced, both by D-serine integration into the stem peptide, but also by the *aux* mutations. Homologs of LytN, AuxA, and AuxB (as well as SAUSA300_1004) are only found in staphylococcal species ([14] and own observations), stressing that these proteins carry a unique role in staphylococcal cell segregation and division. We propose a model by which the inhibition of autolytic activity and its possible mislocalization by unstable/released LTA polymers is what renders *aux*, and LTA pathway mutants sensitive to D-serine. *S. aureus* separates in a combined enzymatic and mechanistic manner, where LytN degrade the complete cross-wall from within, whereas Atl and Sle1 hydrolyse peptidoglycan from the outside until the cells rapidly split in less than 2 milliseconds by the tension created by the growing daughter cells [15-17]. The regulation of LytN is crucial as overexpression leads to cell lysis, and deletion of LytN result in defects in the splitting of cross-wall peptidoglycan and changes in the general structure of the peptidoglycan in the bacterial

envelope [14, 18]. The localization of LytN to the central cavity between the two OWZs of the daughter cells [19] is very likely to be important for proper cell splitting even though the LysM domain is not absolutely critical for its function [18]. LytN localization might be "pushed" away from the membrane by LTA polymers and WTA intermediates [20], enabling LytN only to access PG further away from the membrane (Figure 1). As teichoic acid polymers are essential for directing Atl and Sle1 to the outer cell division site, either by attracting (Atl repeat units to LTA [21]) or repelling (LysM domains away from WTA and LTA [18]) forces, the integrity and stability of these polymers must be essential to maintain cell wall homoeostasis.

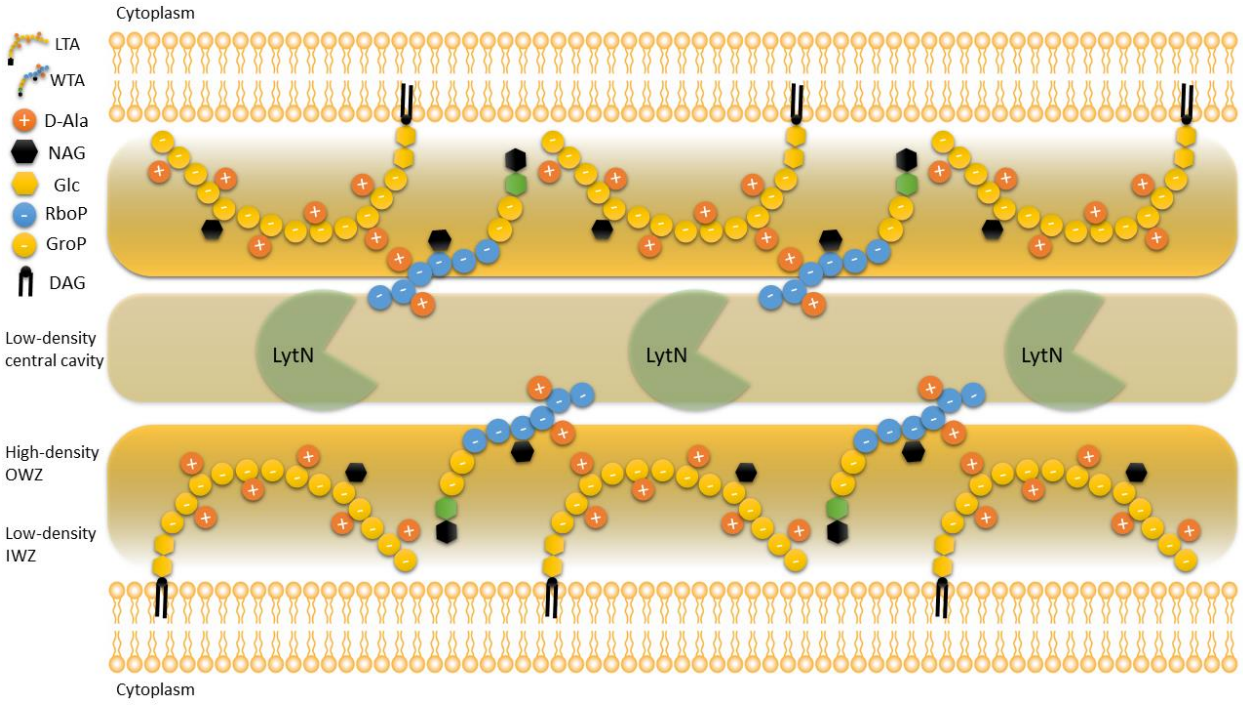

Figure 1. Localization of LytN to the central cavity of the septal cross-wall. *Within the septal cross-wall, LytN might be directed to its right location in the Low-density central cavity by repelling forces from LTA polymers and WTA polymer intermediates.*

Susceptibility testing of the D-serine/D-alanine/glycine importer *cycA* mutant present in the NTML did not raise D-serine MIC (data not shown), which supports that D-serine harms the cell by extracellular mechanisms. Mutants of *lytN*, *atl* and *sle1* are also present in the NTML, and since none of these mutants displayed growth defects in the screen at 25 mM D-serine, the *aux* and LTA pathway mutants must carry additional roles than merely regulate autolytic activity. We found that AuxAB interact with several cell division proteins, DltD, LTA pathway members and peptidoglycan synthesis proteins. This interaction network is highly similar to that of LtaA, YpfP

and LtaS [22]. Cell division defects combined with attenuated autolysis are most likely what renders both LTA pathway and *aux* mutants sensitive to both β-lactams and D-serine. Both Aux proteins as well bind the cell division inhibitor SosA [23], which supports the idea of an important role in cell division for the Aux protein complex. It will be interesting to test if the direct interaction reported in manuscript 3 to e.g. EzrA or DivIC, alters the localization of these important cell division proteins in an *aux* mutant background.

Mutations inactivating the c-di-AMP phosphodiesterase enzyme GdpP, have shown to enable growth of otherwise inviable LTA-deficient strains [24]. In manuscript 2, we saw similar inactivating mutations of *gdpP* to compensate for the *auxA* and *auxB* mutations when challenged by the β-lactam antimicrobial cefotaxime, which again support the overlap with the LTA pathway of these mutants. GdpP degrades c-di-AMP inside the cell, and inactivation of this enzyme increases intracellular levels of this secondary messenger, which indirectly affects cell envelope integrity by controlling osmolyte transport and decrease cell size [25]. While preparing cells with sodium dodecyl sulfate (SDS) for zymographic analysis, we detected that the *auxA* and *auxB* mutants began to lyse (data not shown), indicating that the general cell wall and/or membrane integrity in these mutants is compromised. Increasing levels of c-di-AMP is an easy way for the cell to regain its lost integrity.

The c-di-AMP regulatory network overlaps with that of the stringent response through direct interactions of c-di-AMP and (p)ppGpp messenger molecules with a member of each other's pathway [26]. In manuscript 3, members of the guanine metabolic pathway were increased in abundance in the *auxA* deletion mutant after D-serine stress, which is an important pathway for the synthesis of the stringent response messenger (p)ppGpp. Activation of the stringent response, by the addition of sub-MIC levels of the isoleucyl-tRNA synthase inhibitor mupirocin, increases PBP2a expression and β-lactam resistance [27]. This phenotype is lost in the *auxA* and *auxB* mutant backgrounds (data not shown), which could imply that the stringent response signal goes through the Aux proteins or that the PBP2a enzyme is inactive if AuxAB is missing. The increase in mupirocin-induced β-lactam resistance and PBP2a activity is dependent on PBP2 transglycosylase activity [27, 28]. As we have shown that both AuxA and AuxB interact with PBP2

(manuscript 3), AuxAB might be important for proper PBP2 transglycosylase activity during β-lactam stress.

The largest increase in protein abundance of the *auxA* mutant compared to WT cells during D-serine stress was member of the accessory Sec protein export parthway, SecA2. This pathway is responsible for the export of the SraP protein that binds human platelets [7]. We additionally came across the SraP protein in manuscript 1, where it was present in the bloodstream infection-related CC22 isolates with high β-lactam MICs. AuxA show structural similarity to the Sec pathway accessory factor SecDF (manuscript 2), and *auxA* mutants have shown attenuated virulence in a mouse model and reduced the microbial burden of infected mouse hearts [29]. These results support the idea of the Aux protein complex to assist the accessory Sec protein pathway in exporting SraP across the membrane to help establish bloodstream infections by platelet adhesion. It will be exciting to see if AuxAB interact with members of the accessory Sec protein export pathway, and which role a large cell wall anchored protein like SraP play in *S. aureus'* fight against β-lactam antibiotics. As the *aux* mutants both show attenuated virulence and β-lactam resistance, inhibitors targeting the Aux protein complex can become an important weapon in the war against methicillin-resistant *Staphylococcus aureus*.

In *S. aureus*, additional resistance mechanisms can be co-localized together with β-lactam resistance inside the staphylococcal chromosome cassette. **In manuscript 4,** we looked into the CRISPR-Cas type III-A system of the emerging Danish clone ST630. We found that the CRISPR arrays are quite conserved, hinting at an inefficient spacer adaptation mechanism. Recent studies have shown that enhanced spacer adaptation leads to self-targeting [30], and that type II-A CRISPR-Cas systems use a single-guide RNA to autoregulate Cas9 effector activity to avoid autoimmunity [31]. It would be interesting to screen for similar mechanisms in *S. aureus* CRISPR-Cas type III-A systems, to test if there is a need for autoregulation of this system.

The variance within the CRISPR1 array was limited to the center positions, contradictory to the general understanding of CRISPR-Cas spacer adaptation as happening by an extension of the array at the leader-end [32]. We searched for changes in the leader sequences, which have shown to cause ectopic spacer integration, but found all isolates to carry identical leader sequences.

This could be due to a common ancestor having acquired leader sequence mutations and then evolved the CRISPR array subsequently, or it may be due to alternative paths of expanding the CRISPR locus. One could be by recombination events of the CRISPR array spacer with its cognate MGE protospacer that have shown to act as a form of specialized transduction [33]. Alternatively, transposons have shown to carry CRISPR arrays and non-effector *cas* genes, which might assist in both expanding the CRISPR array and facilitate its spread via plasmids and phages [34].

We tested if the entire SCC*mec*, and thereby the integrated CRISPR-Cas type III-A system, of the 110900 ST630 isolate was transferable by transduction with phage φ11. Despite several attempts we did not succeed in getting any transductants. This suggest that phage φ11 is not involved in the joint spread of CRISPR and methicillin resistance. However, staphylococcal conjugative plasmids have successfully shown to capture a 30 kb SCC*mec* fragment via homologous recombination between cognate IS431 MGEs of the plasmid and SCC*mec* [35]. The type V(5C2&5) SCC*mec* carried by the ST630 isolates is 59 kb, and it is uncertain whether a fragment twice the size would be able to integrate to the same extend. Looking at excision rates of the SCC*mec* we found that the 38 kb SCC-CRISPR fragment were able to excise though at very low frequencies, why transfer of this element onto a conjugative plasmid rather than the entire SCC*mec* would be unlikely. The high excision frequencies we found for the complete ST630 carried SCC*mec* type V(5C2&5) might be why this is a successful emerging clone in Denmark and China. It carries two recombinase genes, *ccrC1-8* and *ccrC1-2*, responsible for excision and two sets of DNA polymerase, primase and helicase genes, implying that this cassette is replicative [4] and could result in both elevated β-lactam resistance and spread of CRISPR-Cas-mediated phage immunity. It would be interesting to test if the presence of CRISPR-Cas has an influence on the high excision frequencies, and if reverting the three-nucleotide difference between DR1 and DR2 would increase frequencies of the SCC-CRISPR fragment.

Recent work suggest that the spread of circular SCC*mec* fragments is driven by transformation inside bacterial biofilm [36]. As *cas* gene expression is reported to be induced by quorum sensing in *Pseudomonas aeruginosa* [37], it is tempting to speculate that both CRISPR-Cas activity and dissemination mainly operate in high cell density environments. We found that the type III-A system was only able to fully survive phage attack when the phage was outnumbered $1:10^7$. This

indicate that only large numbers of bacteria can overcome phage attack, why biofilm might be the only setting enabling *S. aureus* to survive phage infections via CRISPR-Cas immunity. Future efforts will be put into the idea of SCC*mec*-mediated CRISPR-Cas transfer inside biofilm communities and further investigate the connection between β-lactam resistance and CRISPR-Cas immunity.

Conclusion

The findings presented in this thesis cover multiple approaches to find solutions to resistance mechanisms of the opportunistic pathogen *Staphylococcus aureus*. By screening a transposon mutant library, we discovered and characterized two novel auxiliary factors that we named *auxA* and *auxB*, which can be used as targets for future drug solutions against β-lactam methicillin-resistant *Staphylococcus aureus*. AuxA and AuxB are membrane-embedded proteins that form a multimeric complex which interacts with members of the peptidoglycan synthesis machinery, the divisome, and members of the lipoteichoic acid pathway. They are involved in the stability of the LTA polymer and *aux* mutants show attenuated autolytic activity, which becomes detrimental when challenged by D-serine. The AuxA protein structure resembles the SecDF accessory factor of the Sec protein translocation machinery, and additional roles within protein transport and cell division seem plausible. Data presented here strongly suggest that inhibitors of these auxiliary factors could re-potentiate β-lactams and be an important weapon against MRSA infections.

We also describe another approach to find resistance mechanism determinants by mapping methicillin-resistant *Staphylococcus aureus* genomes to susceptibility data. By this measure, we re-discovered known resistance mechanisms and found new candidates that could assist a high-level β-lactam resistance profile. These candidates were the mobile genetic elements SCC*mec* type IVh and inherent prophages of the highly β-lactam resistant clonal complex 22 MRSAs, that might contribute to high resistance levels and virulence, respectively.

Finally, we describe the CRISPR-Cas type III-A system of the emerging Danish ST630 clone. The CRISPR-Cas system resides within the SCC*mec* type V(5C2&5) and holds a quite conserved array of spacers targeting staphylococcal plasmids and phages. The CRISPR-Cas system was active

against phages infection and we found the SCC*mec* carrying the CRISPR-Cas system to be highly excisable, but unable to be transferred by phage mediated transduction.

The outcomes presented in this thesis provides novel insights into staphylococcal mechanisms that could be exploited to combat this multi-resistant pathogen.

References

1. Chambers, H.F. and F.R. Deleo, *Waves of resistance: Staphylococcus aureus in the antibiotic era.* Nat Rev Microbiol, 2009. **7**(9): p. 629-41.
2. Pendleton, J.N., S.P. Gorman, and B.F. Gilmore, *Clinical relevance of the ESKAPE pathogens.* Expert Rev Anti Infect Ther, 2013. **11**(3): p. 297-308.
3. Jamrozy, D., et al., *Evolution of mobile genetic element composition in an epidemic methicillin-resistant Staphylococcus aureus: temporal changes correlated with frequent loss and gain events.* BMC Genomics, 2017. **18**(1): p. 684.
4. Bebel, A., et al., *A novel DNA primase-helicase pair encoded by SCCmec elements.* Elife, 2020. **9**.
5. Gallagher, L.A., et al., *Tandem Amplification of the Staphylococcal Cassette Chromosome mec Element Can Drive High-Level Methicillin Resistance in Methicillin-Resistant Staphylococcus aureus.* Antimicrob Agents Chemother, 2017. **61**(9).
6. Bondy-Denomy, J. and A.R. Davidson, *When a virus is not a parasite: the beneficial effects of prophages on bacterial fitness.* J Microbiol, 2014. **52**(3): p. 235-42.
7. Siboo, I.R., H.F. Chambers, and P.M. Sullam, *Role of SraP, a Serine-Rich Surface Protein of Staphylococcus aureus, in binding to human platelets.* Infect Immun, 2005. **73**(4): p. 2273-80.
8. Rajagopal, M., et al., *Multidrug Intrinsic Resistance Factors in Staphylococcus aureus Identified by Profiling Fitness within High-Diversity Transposon Libraries.* mBio, 2016. **7**(4).
9. Vestergaard, M., et al., *Inhibition of the ATP Synthase Eliminates the Intrinsic Resistance of Staphylococcus aureus towards Polymyxins.* mBio, 2017. **8**(5).
10. Pasquina, L., et al., *A synthetic lethal approach for compound and target identification in Staphylococcus aureus.* Nat Chem Biol, 2016. **12**(1): p. 40-5.
11. DeFrancesco, A.S., et al., *Genome-wide screen for genes involved in eDNA release during biofilm formation by Staphylococcus aureus.* Proc Natl Acad Sci U S A, 2017. **114**(29): p. E5969-E5978.
12. Bose, J.L., et al., *Contribution of the Staphylococcus aureus Atl AM and GL murein hydrolase activities in cell division, autolysis, and biofilm formation.* PLoS One, 2012. **7**(7): p. e42244.
13. Liu, Q., et al., *The ATP-Dependent Protease ClpP Inhibits Biofilm Formation by Regulating Agr and Cell Wall Hydrolase Sle1 in Staphylococcus aureus.* Front Cell Infect Microbiol, 2017. **7**: p. 181.
14. Frankel, M.B., et al., *LytN, a murein hydrolase in the cross-wall compartment of Staphylococcus aureus, is involved in proper bacterial growth and envelope assembly.* J Biol Chem, 2011. **286**(37): p. 32593-605.
15. Giesbrecht, P., et al., *Staphylococcal cell wall: morphogenesis and fatal variations in the presence of penicillin.* Microbiol Mol Biol Rev, 1998. **62**(4): p. 1371-414.
16. Monteiro, J.M., et al., *Cell shape dynamics during the staphylococcal cell cycle.* Nat Commun, 2015. **6**: p. 8055.

17. Zhou, X., et al., *Bacterial division. Mechanical crack propagation drives millisecond daughter cell separation in Staphylococcus aureus.* Science, 2015. **348**(6234): p. 574-8.
18. Frankel, M.B. and O. Schneewind, *Determinants of murein hydrolase targeting to cross-wall of Staphylococcus aureus peptidoglycan.* J Biol Chem, 2012. **287**(13): p. 10460-71.
19. Matias, V.R. and T.J. Beveridge, *Native cell wall organization shown by cryo-electron microscopy confirms the existence of a periplasmic space in Staphylococcus aureus.* J Bacteriol, 2006. **188**(3): p. 1011-21.
20. Atilano, M.L., et al., *Teichoic acids are temporal and spatial regulators of peptidoglycan cross-linking in Staphylococcus aureus.* Proc Natl Acad Sci U S A, 2010. **107**(44): p. 18991-6.
21. Zoll, S., et al., *Ligand-binding properties and conformational dynamics of autolysin repeat domains in staphylococcal cell wall recognition.* J Bacteriol, 2012. **194**(15): p. 3789-802.
22. Reichmann, N.T., et al., *Differential localization of LTA synthesis proteins and their interaction with the cell division machinery in Staphylococcus aureus.* Mol Microbiol, 2014. **92**(2): p. 273-86.
23. Bojer, M.S., et al., *SosA inhibits cell division in Staphylococcus aureus in response to DNA damage.* Mol Microbiol, 2019. **112**(4): p. 1116-1130.
24. Corrigan, R.M., et al., *c-di-AMP is a new second messenger in Staphylococcus aureus with a role in controlling cell size and envelope stress.* PLoS Pathog, 2011. **7**(9): p. e1002217.
25. Commichau, F.M., et al., *A Delicate Connection: c-di-AMP Affects Cell Integrity by Controlling Osmolyte Transport.* Trends Microbiol, 2018. **26**(3): p. 175-185.
26. Corrigan, R.M., et al., *Cross-talk between two nucleotide-signaling pathways in Staphylococcus aureus.* J Biol Chem, 2015. **290**(9): p. 5826-39.
27. Aedo, S. and A. Tomasz, *Role of the Stringent Stress Response in the Antibiotic Resistance Phenotype of Methicillin-Resistant Staphylococcus aureus.* Antimicrob Agents Chemother, 2016. **60**(4): p. 2311-7.
28. Pinho, M.G., H. de Lencastre, and A. Tomasz, *An acquired and a native penicillin-binding protein cooperate in building the cell wall of drug-resistant staphylococci.* Proc Natl Acad Sci U S A, 2001. **98**(19): p. 10886-91.
29. Paudel, A., et al., *Large-Scale Screening and Identification of Novel Pathogenic Staphylococcus aureus Genes Using a Silkworm Infection Model.* J Infect Dis, 2020. **221**(11): p. 1795-1804.
30. Heler, R., et al., *Mutations in Cas9 Enhance the Rate of Acquisition of Viral Spacer Sequences during the CRISPR-Cas Immune Response.* Mol Cell, 2017. **65**(1): p. 168-175.
31. Workman, R.E., et al., *A natural single-guide RNA repurposes Cas9 to autoregulate CRISPR-Cas expression.* Cell, 2021.
32. McGinn, J. and L.A. Marraffini, *Molecular mechanisms of CRISPR-Cas spacer acquisition.* Nat Rev Microbiol, 2019. **17**(1): p. 7-12.
33. Varble, A., et al., *Recombination between phages and CRISPR-cas loci facilitates horizontal gene transfer in staphylococci.* Nat Microbiol, 2019. **4**(6): p. 956-963.
34. Peters, J.E., et al., *Recruitment of CRISPR-Cas systems by Tn7-like transposons.* Proc Natl Acad Sci U S A, 2017. **114**(35): p. E7358-E7366.
35. Ray, M.D., S. Boundy, and G.L. Archer, *Transfer of the methicillin resistance genomic island among staphylococci by conjugation.* Mol Microbiol, 2016. **100**(4): p. 675-85.
36. Maree, M., et al., *MRSA emerges through natural transformation.* bioRxiv, 2020: p. 2020.12.08.415893.
37. Hoyland-Kroghsbo, N.M., et al., *Quorum sensing controls the Pseudomonas aeruginosa CRISPR-Cas adaptive immune system.* Proc Natl Acad Sci U S A, 2017. **114**(1): p. 131-135.